NCHRP

REPORT 533

Handbook for Predicting Stream Meander Migration

TRANSPORTATION RESEARCH BOARD
OF THE NATIONAL ACADEMIES

NCHRP REPORT 533

Handbook for Predicting Stream Meander Migration

P. F. Lagasse
W. J. Spitz
L. W. Zevenbergen

AND

D. W. Zachmann
Owen Ayres & Associates, Inc.
Fort Collins, CO

TRANSPORTATION RESEARCH BOARD

NATIONAL COOPERATIVE HIGHWAY RESEARCH PROGRAM

Systematic, well-designed research provides the most effective approach to the solution of many problems facing highway administrators and engineers. Often, highway problems are of local interest and can best be studied by highway departments individually or in cooperation with their state universities and others. However, the accelerating growth of highway transportation develops increasingly complex problems of wide interest to highway authorities. These problems are best studied through a coordinated program of cooperative research.

In recognition of these needs, the highway administrators of the American Association of State Highway and Transportation Officials initiated in 1962 an objective national highway research program employing modern scientific techniques. This program is supported on a continuing basis by funds from participating member states of the Association and it receives the full cooperation and support of the Federal Highway Administration, United States Department of Transportation.

The Transportation Research Board of the National Academies was requested by the Association to administer the research program because of the Board's recognized objectivity and understanding of modern research practices. The Board is uniquely suited for this purpose as it maintains an extensive committee structure from which authorities on any highway transportation subject may be drawn; it possesses avenues of communications and cooperation with federal, state and local governmental agencies, universities, and industry; its relationship to the National Research Council is an insurance of objectivity; it maintains a full-time research correlation staff of specialists in highway transportation matters to bring the findings of research directly to those who are in a position to use them.

The program is developed on the basis of research needs identified by chief administrators of the highway and transportation departments and by committees of AASHTO. Each year, specific areas of research needs to be included in the program are proposed to the National Research Council and the Board by the American Association of State Highway and Transportation Officials. Research projects to fulfill these needs are defined by the Board, and qualified research agencies are selected from those that have submitted proposals. Administration and surveillance of research contracts are the responsibilities of the National Research Council and the Transportation Research Board.

The needs for highway research are many, and the National Cooperative Highway Research Program can make significant contributions to the solution of highway transportation problems of mutual concern to many responsible groups. The program, however, is intended to complement rather than to substitute for or duplicate other highway research programs.

Note: The Transportation Research Board of the National Academies, the National Research Council, the Federal Highway Administration, the American Association of State Highway and Transportation Officials, and the individual states participating in the National Cooperative Highway Research Program do not endorse products or manufacturers. Trade or manufacturers' names appear herein solely because they are considered essential to the object of this report.

NOTICE

The project that is the subject of this report was a part of the National Cooperative Highway Research Program conducted by the Transportation Research Board with the approval of the Governing Board of the National Research Council. Such approval reflects the Governing Board's judgment that the program concerned is of national importance and appropriate with respect to both the purposes and resources of the National Research Council.

The members of the technical committee selected to monitor this project and to review this report were chosen for recognized scholarly competence and with due consideration for the balance of disciplines appropriate to the project. The opinions and conclusions expressed or implied are those of the research agency that performed the research, and, while they have been accepted as appropriate by the technical committee, they are not necessarily those of the Transportation Research Board, the National Research Council, the American Association of State Highway and Transportation Officials, or the Federal Highway Administration, U.S. Department of Transportation.

Each report is reviewed and accepted for publication by the technical committee according to procedures established and monitored by the Transportation Research Board Executive Committee and the Governing Board of the National Research Council.

THE NATIONAL ACADEMIES
Advisers to the Nation on Science, Engineering, and Medicine

The **National Academy of Sciences** is a private, nonprofit, self-perpetuating society of distinguished scholars engaged in scientific and engineering research, dedicated to the furtherance of science and technology and to their use for the general welfare. On the authority of the charter granted to it by the Congress in 1863, the Academy has a mandate that requires it to advise the federal government on scientific and technical matters. Dr. Bruce M. Alberts is president of the National Academy of Sciences.

The **National Academy of Engineering** was established in 1964, under the charter of the National Academy of Sciences, as a parallel organization of outstanding engineers. It is autonomous in its administration and in the selection of its members, sharing with the National Academy of Sciences the responsibility for advising the federal government. The National Academy of Engineering also sponsors engineering programs aimed at meeting national needs, encourages education and research, and recognizes the superior achievements of engineers. Dr. William A. Wulf is president of the National Academy of Engineering.

The **Institute of Medicine** was established in 1970 by the National Academy of Sciences to secure the services of eminent members of appropriate professions in the examination of policy matters pertaining to the health of the public. The Institute acts under the responsibility given to the National Academy of Sciences by its congressional charter to be an adviser to the federal government and, on its own initiative, to identify issues of medical care, research, and education. Dr. Harvey V. Fineberg is president of the Institute of Medicine.

The **National Research Council** was organized by the National Academy of Sciences in 1916 to associate the broad community of science and technology with the Academy's purposes of furthering knowledge and advising the federal government. Functioning in accordance with general policies determined by the Academy, the Council has become the principal operating agency of both the National Academy of Sciences and the National Academy of Engineering in providing services to the government, the public, and the scientific and engineering communities. The Council is administered jointly by both the Academies and the Institute of Medicine. Dr. Bruce M. Alberts and Dr. William A. Wulf are chair and vice chair, respectively, of the National Research Council.

The **Transportation Research Board** is a division of the National Research Council, which serves the National Academy of Sciences and the National Academy of Engineering. The Board's mission is to promote innovation and progress in transportation through research. In an objective and interdisciplinary setting, the Board facilitates the sharing of information on transportation practice and policy by researchers and practitioners; stimulates research and offers research management services that promote technical excellence; provides expert advice on transportation policy and programs; and disseminates research results broadly and encourages their implementation. The Board's varied activities annually engage more than 5,000 engineers, scientists, and other transportation researchers and practitioners from the public and private sectors and academia, all of whom contribute their expertise in the public interest. The program is supported by state transportation departments, federal agencies including the component administrations of the U.S. Department of Transportation, and other organizations and individuals interested in the development of transportation. **www.TRB.org**

www.national-academies.org

FOREWORD

By Timothy G. Hess
Staff Officer
Transportation Research
Board

This report presents the findings of research to develop a practical methodology for predicting the rate and extent of channel migration in proximity to transportation facilities. The report presents, in the form of a handbook, an empirical methodology developed for predicting stream meander migration. The methodology presented in the handbook will assist practicing engineers in evaluating bridges and other structures and in determining the need for countermeasures to address the potential impacts of channel meander migration over the life of the facility. This report will be particularly useful to structural, hydraulic, and highway engineers responsible for the design and construction of bridges or other structures in proximity to naturally meandering stream channels.

Rivers prone to channel migration may be spanned by structures or paralleled by fixed highway alignments and appurtenances. Channel migration is a major consideration in designing bridge crossings and other transportation facilities. Channel migration is typically an incremental process. On meandering streams, the problem at a bridge site may become apparent two or three decades after the bridge is constructed. Channel migration is often evident throughout large sections of a drainage basin and is not localized in the vicinity of a bridge. It is a natural phenomenon that occurs in the absence of specific disturbances, but it may be exacerbated by such basin-wide factors as land use changes, gravel mining, dam construction, and removal of vegetation. Remedial action, such as constructing guide banks or installing bank protection, becomes increasingly expensive or difficult as the channel migrates. Given the expense of countermeasures and difficulty in accurately predicting channel migration, there was a need for a methodology to evaluate the potential for channel movement and to predict future channel migration.

Under NCHRP Project 24-16, Ayres Associates developed a methodology for predicting the rate and extent of stream meander migration. After conducting an extensive literature review, the research team developed a screening and classification system for meandering streams. Using photogrammetric principles, the research team also developed map and aerial photo comparison techniques. A stream meander prediction methodology was then developed, and limitations and sources of error were identified. Finally, the results of the research were incorporated into a handbook for use by practitioners. *NCHRP Report 533: Handbook for Predicting Stream Meander Migration* describes the application of the prediction methodology and provides illustrated examples for applying the methodology as well as a CD-ROM (*CRP-CD-48*) that contains an ArcView-based data logger and channel migration predictor.

The contractor's final report for NCHRP Project 24-16 is available as *NCHRP Web Document 67* and can be accessed by clicking on "NCHRP Web Docs" at www4.trb.org/trb/onlinepubs.nsf. A companion product to *NCHRP Web Document 67* is

CRP-CD-49, a four-set CD-ROM that contains all meander site data acquired for this research. The database includes 141 meander sites containing 1,503 meander bends on 89 rivers in the United States and will be of particular interest to those conducting research in the area of stream meander migration.

CONTENTS

CHAPTER **1**

INTRODUCTION AND APPLICATIONS

1.1 INTRODUCTION

Problems associated with riverbank erosion and channel migration have plagued societies reliant on engineered river crossings for thousands of years. Engineers have dealt with these problems by attempting to site bridges in particularly stable or laterally constrained reaches, over-engineering bridges to withstand all but catastrophic erosion, or building bridges that are easy to replace. However, the risks associated with channel migration at bridge crossings have necessitated that regular inspections be conducted to identify erosion problems and that repairs and maintenance be implemented to avoid bridge failures. Despite all that has been done to avoid or identify the hazards posed by channel migration, no methodology for routine prediction of meander migration in the vicinity of bridges exists, and uncertainty concerning the level of risk remains unacceptably high.

Most streams that present a hazard through lateral migration at road crossings are alluvial. In alluvial streams, the channel is formed by the action of flowing water on boundary materials that have been deposited by the stream and that can be eroded and transported by the stream. In alluvial streams, it is the rule rather than the exception that the banks will migrate through erosion and accretion and that floodplains, islands, and side channels will undergo modification with time. This is particularly the case in actively meandering streams, which continually change their positions and shapes as a consequence of fluvial processes and hydraulic forces exerted on their beds and banks. These changes may be incremental or episodic, gradual or rapid, and systemwide or local in scale. Meanders grow and move naturally, but human activities may accelerate the rate of change or trigger new changes caused by morphological response in the stream system. The fact that highway infrastructure is stationary makes it subject to potentially serious impacts caused by bend migration in actively meandering alluvial streams.

Bend migration is a major consideration in designing bridge crossings and other transportation facilities in meandering channels because it causes the channel alignment and approach conditions present during construction to deteriorate as the upstream channel location and orientation change with time. Channel migration can result in damage or destruction of the bridge through the following:

- Excessive bridge pier and abutment scour,
- Flanking of bridge approaches and other highway infrastructure,

- Excessive scour and pressure loading caused by debris accumulation, and
- Loss of conveyance through bridge openings because of misalignment and point bar development.

Bend migration may be characterized by lateral channel shift (expressed in terms of distance moved perpendicular to the channel centerline, per year) and down-valley migration (expressed as distance moved along the valley, per year). It is a natural phenomenon that occurs in the absence of specific disturbances, although it may be exacerbated by basin-wide factors such as land use changes, gravel mining, dam construction, and removal of vegetation. Engineers must recognize that processes operating in upstream reaches and subwatersheds may affect rates of lateral bend shift and down-valley migration in the vicinity of the bridge or highway. Therefore, any attempt at predicting bend migration must consider all factors that may affect channel migration rates, including the magnitude and frequency of formative river flows and past, present, and possible future disturbances to the upstream watershed and drainage system that might affect channel processes.

Channel migration in meandering streams is driven primarily by the tendency of meander bends to grow in amplitude and move downstream with time. However, meander growth means that a bend eventually may become so extended and tightly curved that it is abandoned by a chute or neck cutoff. Hence, channel migration is predominantly a progressive process that may be punctuated periodically by abrupt changes in channel alignment and position because of cutoffs. On meandering streams, a problem at a bridge site may become apparent only two or three decades after the bridge is constructed.

Channel migration is often evident along considerable reaches of river in a drainage basin; however, it can be localized in the vicinity of a bridge. Remedial action, such as constructing spurs or installing bank protection along substantial reaches of a meandering channel, is expensive and difficult to justify economically except in areas with very high land values. Remedial action is also dependent on the risk to the existing structure and the cost of replacement. Given that channel migration at the reach-scale is likely to persist, a practical methodology is needed to evaluate the potential for bend movement, to define the rates and direction of historic channel shifts, and to predict future channel migration in order to evaluate the hazard posed by channel migration to highway infrastructure within its design life.

For highway engineering purposes, a stream channel can be considered unstable if the rate or magnitude of change is such that the planning, location, design, or maintenance considerations for a highway crossing are significantly affected during the life of the facility. The kinds of changes that are of concern are (1) lateral bank erosion and incremental channel migration; (2) aggradation or degradation of the streambed; (3) short-term fluctuations in streambed elevation (scour and fill); and (4) avulsion. *NCHRP Report 533: Handbook for Predicting Stream Meander Migration* (*Handbook*) is concerned specifically with lateral channel instability (including bend radius expansion, across-valley extension, and down-valley migration) resulting from incremental meander migration. The *Handbook* covers the following topics:

- Screening and classification of meander sites,
- Sources of mapping and aerial photographic data,
- Basic principles and theory of aerial photograph comparison,
- Manual overlay techniques,
- Computer-assisted techniques,
- Measurement and extrapolation techniques based on geographic information systems (GISs),
- Frequency analysis,
- Sources of error and limitations, and
- Illustrated examples using manual overlay techniques.

Chapter 1 provides an introduction to the *Handbook* and a discussion of a range of potential applications of the techniques described in the *Handbook*. Chapter 2 describes the basic principles and processes of stream channel meander migration and discusses the potential hazards caused by meander migration as well as by avulsions and cutoffs.

Chapter 3 presents a geomorphic classification scheme, modified from the channel pattern classification originally developed by Brice (1975), as an approach for both screening and classification. The most common river types (or meander modes) likely to be encountered by hydraulic engineers in the field are addressed by this classification. The screening procedure to identify *stable* meandering stream reaches ensures that engineering and inspection resources are not allocated to locations where there is little probability of a problem developing.

The basic principles of photogrammetry, the types and sources of aerial photography, and the application of aerial photography to meander migration analysis are discussed in Chapter 4.

Chapter 5 describes a manual overlay technique that uses historic bankline positions acquired from sequential historic maps and aerial photos to assess historic channel position. By inscribing and tracking the movement of circles of known radius on a bend over time, a prediction can be made on the probable position of the bend at some point in the future. Chapter 5 provides information on three ways to apply the overlay technique: (1) using a manual method, (2) using computer-assisted methods, and (3) using the ArcView-based Data Logger and Channel Migration Predictor tools developed for use with the *Handbook*.

The potential sources of error and limitations associated with the use of historic aerial photographs and maps in conducting a meander migration assessment and prediction are described in Chapter 6.

A detailed description is provided in Chapter 7 of manual, computer-assisted, and GIS-based methodologies using map and aerial photo comparison techniques to conduct the overlay and prediction of meander migration over time. The GIS-based measurement and extrapolation tools are included on *CRP-CD-48,* which is provided on the back inside cover of the *Handbook.* The use of the frequency analysis results developed under NCHRP Project 24-16 to assist in accurately predicting meander migration is described as well.

Chapter 8 provides detailed, step-by-step examples of assessing historic meander migration and predicting future meander development using the methodologies described in the previous chapters.

Appendix A describes how to download TerraServer images from the Internet for use in the analysis and prediction of meander migration. Methods for delineating the bankline of a channel and determining the radius of a meander bend are provided in Appendix B. Instructions on installing the ArcView–based Data Logger and Channel Migration Predictor tools are provided in Appendix C. Tips for delineating banklines from historic aerial photos that are not georeferenced for use with the Channel Migration Predictor can be found in Appendix D. Appendix E supplements the basic prediction techniques by providing a method to consider bend rotation. A glossary of terms used in the *Handbook* is provided in Appendix F.

1.2 APPLICATIONS

Although the methodologies provided in the *Handbook* were developed to assist in identifying potential hazards to highway facilities from active channel migration, there are a number of other applications in which these methodologies could be used. When used properly, the *Handbook* will allow the user to identify potential problems associated with channel migration and determine the need for revetments, structural solutions, or biotechnical solutions to counter the threat posed by an actively migrating channel.

1.2.1 Transportation Facilities

The techniques described in the *Handbook* could be used to assess the potential threat to an existing or proposed transportation facility or to evaluate the need for structural solutions or countermeasures to inhibit or halt active channel migration in the proximity of an existing or proposed transportation facility.

Active channel migration poses a significant threat to the stability of existing bridges and other highway facilities. Bend migration, as it moves through a bridge reach, may pose a major hazard to a bridge, especially those bridges with bents located in the floodplain. In many locations where bridges

span rivers and their floodways, only the bents and pilings within the channelized section have deep foundations, whereas those located on the floodplain or marginal to the channel may have shallow foundations. When channel migration removes a significant amount of bankline underneath a bridge, floodplain bents and pilings with shallow foundations may become exposed and undermined and may potentially fail. In some cases, the failure of only one bent may be sufficient to cause a significant portion of the entire bridge to collapse, as was the case of a major highway bridge over the Hatchie River in Tennessee in 1989 (see HEC-23, Design Guideline 1 [Lagasse et al., 2001]).

In addition, significant bankline loss associated with either incremental (see Figure 1.1) or catastrophic (see Figure 1.2) channel migration can threaten to undermine or flank the bridge abutments, especially where they rest on, or are shallowly founded in, floodplain soils. In contrast, the components of a bridge and its approach embankments may exacerbate or hinder the processes associated with meander migration.

The techniques described in this *Handbook* can also be used to evaluate the potential threat from channel migration to existing highway embankments, especially where the embankment is located on the active floodplain and runs parallel to the flow direction of a meandering stream.

1.2.2 Urban and Commercial Development

Urban and commercial developments are increasingly encroaching into the floodplain. Although the law requires that these developments are to be built so that they are above or outside the limits of the 100-year floodplain for flood insurance purposes, the potential threat posed by active channel migration is not a consideration in many floodplain regulations. In addition, developers and city planners rarely recognize the potential hazards posed by active channel migration until it is too late. The *Handbook* can be used to identify
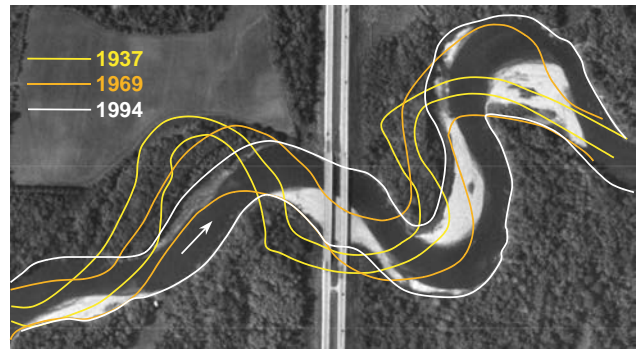
Figure 1.1. Aerial photo of a bridge over the Wapsipinicon River near De Witt, Iowa, showing the incremental shift of the outer bank of the bend as a result of meander migration over time. The bridge was installed after 1969.

potential threats to existing structures from channel migration and to identify and delineate areas where active channel migration may pose a serious hazard to new developments.

1.2.3 Flood Control Facilities

In many areas along larger river systems and in close proximity to large urban areas, flood control facilities such as levees, dikes, and flood relief structures are used to protect the public from major flood events. However, as shown in the Chapter 8 examples on the Sacramento River (Sections 8.4 and 8.5), these flood control facilities are often located in, or in close proximity to, the active meanderbelt and can be threatened by active channel migration. On the Sacramento River as well as along many other major rivers and streams across the country, the U.S. Army Corps of Engineers regularly conducts studies to determine the potential threat to the levee system posed by channel migration. Although most threats are iden-

Figure 1.2. The US-95A bridge over the Carson River near Weeks, Nevada, in 1975 and 1986. Significant meander migration during the 1986 flood caused severe erosion of the south embankment and flanking of both bridge abutments, which ultimately resulted in failure of the bridge.

tified early, major floods can cause significant channel migration over the duration of the flood event. In these cases, the U.S. Army Corps of Engineers may be required to perform emergency repairs or install emergency countermeasures to halt the degradation of a levee or flood control structure. Because this type of analysis is not a common practice among private levee districts, smaller municipalities, and private owners, the *Handbook* can provide these groups with a simple procedure necessary to successfully counter possible threats posed by active channel migration within their districts and river reaches.

1.2.4 Riparian Corridor

In numerous locations throughout the United States, floodplain encroachment by urbanization and development have significantly reduced the amount of riparian land along river and stream corridors. In many places, efforts are being made to acquire, maintain, and increase remaining riparian lands for ecological and biological purposes. Because riparian corridors are often fairly narrow, the erosion and removal of mature riparian vegetation on one side of the channel by active channel migration can be sufficiently rapid to reset or significantly alter the natural establishment and succession of new vegetation on the opposite side of the river or stream. Because active meander migration is generally necessary to maintain a healthy riparian community, a meanderbelt that is sufficiently wide to allow for active channel migration should be maintained. The *Handbook* can be used to define the width requirements of a healthy riparian corridor taking into account an actively migrating channel.

1.2.5 Agriculture

Many areas along a migrating stream that are not urbanized or are not riparian are agricultural. In many locations where there is a minimal riparian corridor and no urban development, farm fields or pastures border streams and rivers, often with cropland extending to the very edge of the channel. In these areas, active channel migration not only results in a loss of private property but also in a loss of productive land and a reduction in annual crop yields. Active channel migration can also threaten irrigation diversion, intake, and return structures; irrigation canals; and other agricultural facilities. Thus, the methodologies described in the *Handbook* can be used to assess the potential long-term impacts from the loss of productive land associated with active channel migration. The procedures in the *Handbook* can also be used to aid in stabilizing existing irrigation structures and in siting new irrigation structures with regard to potential channel migration.

1.2.6 Channel Restoration/ Rehabilitation Works

There are many examples of streambank stabilization and rehabilitation measures that failed because they were placed on actively migrating streams and rivers without evaluating the characteristics of channel migration at those locations. The analysis of radius of curvature and migration rate for numerous bends on the Sacramento River conducted by Water Engineering and Technology, Inc. (WET) (WET, 1988) and described in Chapter 2 is a good example of using meander migration analysis to evaluate the potential effectiveness and survivability of bank protection works. The method of assessing meander migration with regard to radius of curvature to width ratio versus migration rate (WET, 1988) can be used on straightened or channelized streams where meanders are to be restored or incorporated into channel rehabilitation and restoration efforts. This can be done by evaluating active channel migration on nearby streams and then designing the new or restored meanders of the rehabilitated channel based on the stable meander patterns identified from nearby streams.

CHAPTER **2**

BACKGROUND

2.1 PROJECT DESCRIPTION AND OBJECTIVES

Channel migration has important implications for the design, maintenance, and inspection of bridges and other highway facilities. Bend shifting or cutoffs upstream of a bridge reach can produce poor alignment of the channel approaching the bridge, high angles of attack, and an increase in vegetative debris from bank erosion. Migration downstream of a bridge can also have negative impacts. For example, downstream channel migration can lead to a meander cutoff with commensurate degradation that can extend upstream into the bridge reach. In either case, the result at the bridge can be excessive abutment and pier scour, debris loading, loss of conveyance, or erosion of bridge approaches.

The *Handbook* was developed under the National Cooperative Highway Research Program (NCHRP). NCHRP Project 24-16 had as its principal objective the development of a practical methodology to predict the rate and extent of channel migration (i.e., the lateral shift and down-valley migration) in proximity to transportation facilities (Lagasse et al., 2003).

Predicting channel migration requires consideration of both systemwide and local factors. The morphology and behavior of a given river reach are strongly determined by the water and sediment discharges from upstream. In dynamically adjusted systems, the rate of lateral shifting increases with the supply of water and sediment from upstream. Changes in runoff and sediment yield, as a result of natural processes or human activities, will trigger changes in rates and modes of channel migration.

Locally, the distribution of velocity and shear stress and the characteristics of bed and bank materials will control channel behavior. Therefore, local channel morphology such as dimensions (width, depth, meander wavelength, and amplitude), pattern (sinuosity and bend radius of curvature), shape (width/depth ratio), and gradient will not only reflect upstream controls but also provide information on the direction and rate of channel migration.

While geomorphologists may view channel stability from the perspective of hundreds or thousands of years, for highway engineering purposes, a stream channel can be considered unstable if the rate or magnitude of change is such that the planning, location, design, or maintenance considerations for a highway crossing are significantly affected during the life of the facility. In the context of a bridge crossing, meanders may be regarded as stable if they do not migrate appreciably during the design life of a bridge crossing (75 to 100 years).

In streams with actively migrating meanders, the kinds of planform changes that are of concern are (1) incremental channel shift from meander migration and (2) episodic channel shift (avulsion) that occurs when a meander bend is cut off. Predicting hazards to highway facilities from incremental planform changes is the principal objective of the *Handbook* (as stated in Section 2.4). Consideration of hazards related to episodic or avulsive channel shifts is beyond the scope of the *Handbook,* but in Section 2.5 they are briefly discussed along with the potential for predicting planform change from the second area of concern listed above.

The *Handbook* deals specifically with incremental channel shift from meander migration and provides a methodology for predicting the rate and extent of lateral channel shifting and down-valley migration of meanders. The methodology is based primarily on the analysis of bend movement using map and aerial photo comparison techniques; however, frequency analysis results are provided (Section 7.5) to supplement the comparative analysis. The methodology enables practicing engineers to evaluate the potential for adverse impacts caused by incremental meander migration over the design life of a bridge or highway river crossing and to ascertain the need for countermeasures to protect the bridge from any associated hazards.

The methodology can be applied to locate and design a new bridge or highway facility to accommodate predicted channel migration during its design life. Predictions of channel migration could also be used to alert bridge inspection personnel to the potential for channel migration that could affect the future safety of a bridge.

The *Handbook* provides aerial photograph comparison techniques to predict channel migration in proximity to transportation facilities that will enable informed decision making at all levels. The methodologies will be useful in reconnaissance, design, rehabilitation, maintenance, and inspection of highway facilities. The end result will be more efficient use of highway resources and a reduction in impacts associated with channel migration at bridges and/or other highway facilities. As discussed in Chapter 1, the prediction techniques can also be used by practitioners responsible for river channel maintenance, river restoration/rehabilitation, and floodplain planning and management.

2.2 RIVER CHANNEL PATTERNS

Rivers may be categorized as straight, meandering, braided, or anastomosing. The great majority of alluvial streams have meandering planforms, and the *Handbook* is intended for use only on meandering streams.

Braided rivers are high-energy rivers with abundant coarse sediment loads that feature multi-thread flow in subchannels (anabranches); mobile braid bars; and rapidly shifting, highly erodible banklines. Braided rivers present particular problems for the designers of bridge crossings (Neil, 1973). Because the analysis of braided rivers is beyond the scope of the *Handbook,* the reader is directed to consult Hooke (1997), Thorne (1997), Klingeman et al. (1998), and Knighton (1998) for information on the processes and morphologies of these rivers.

Anastomosing rivers feature multiple channels (anabranches) separated by stable, vegetated islands or floodplain elements and are associated with low-energy fluvial systems (Miall, 1977; Smith and Smith, 1980). The individual anabranches behave almost independently of each other and are relatively stable compared with multi-thread braided rivers. Highway crossings of anastomosing rivers usually treat each anabranch as a separate alluvial stream. The methodology provided in the *Handbook* could be used on anastomosing channels displaying a meandering planform to predict the migration rate and risk posed by shifting of individual anabranches.

Naturally straight alluvial streams are rarely encountered. Usually, a straight river is constrained by geology or bank protection works, or it has insufficient stream power to erode its boundaries. In such cases, the stream is not alluvial and falls outside the scope of the *Handbook.* However, some alluvial streams may possess a straight planform associated with past engineering for flood control or land drainage. Such streams often display a sinuous thalweg with bars or shoals occurring on alternate sides of the channel, spaced at between five and seven times the channel width. In this situation, the hydraulic engineer or bridge inspector should be aware of the potential for deflection of the flow and local bank erosion caused by alternate bars that can initiate meandering of a straight stream with a sinuous thalweg. If evidence of meander initiation is present, then the methodology presented here can be used to predict the possible rate of bend growth and migration once bank retreat commences.

2.3 STREAM MEANDERING

2.3.1 Stable Versus Active Meandering

This section is a summary of Chapters 2 and 6 of FHWA's *Hydraulic Engineering Circular No. 20* (Lagasse et al., 2001) on the characteristics of meandering streams and the geomorphic factors affecting stream stability and meander migration.

Meandering streams can be classified as either stable or actively meandering. An actively meandering stream has sufficient energy (stream power) to deform its channel boundaries through active bed scour, bank erosion, and point bar growth. Active meanders are the result of contemporary fluvial processes. They evolve and respond to every discharge event with sufficient stream power to mobilize bed and bank sediments. Conversely, a stable meandering stream is one that, under current conditions, has insufficient stream power to

erode its banks. Stable meanders do not migrate appreciably during the design life of a bridge and generally pose little or no risk to bridge crossings.

Clearly, it is essential to differentiate between stable and active meandering when predicting future rates of lateral migration. In this regard, the first step in screening streams in the methodology presented here is to determine whether a meandering stream is active or stable (see Chapter 3).

2.3.2 Flow Patterns and Cross-Sectional Geometry of Meander Bends

The main features of the flow and geometry at meander bends (depicted in Figure 2.1) are the following:

- Superelevation of the water surface against the outside bank (see Figure 2.1B).
- Helicoidal flow directed toward the outer bank at the surface and toward the inner bank at the bed producing a strong secondary circulation superimposed on the main downstream flow in the mid-channel (thalweg) region of the cross-section (see Figure 2.1C).
- A small secondary-current cell rotating in the opposite direction of the main helicoidal circulation in the outer bank region, especially where the bank is steep (see Figure 2.1B and C). The strength of this cell increases with the strength of the main, helicoidal circulation. Interaction of the main and outer bank cells generates plunging flow that scours the bed and lower bank leading to bank undercutting.
- An area of outward-directed transverse flow in the inner bank region caused by convective acceleration above the shoaling point bar (see Figure 2.1C). Outward flow forces the core of maximum velocity rapidly toward the outer bank (Dietrich and Smith, 1983; Dietrich, 1987).
- A maximum-velocity thread that moves from near the inner bank at the bend entrance to near the outer bank at the bend exit, crossing the channel at the zone of maximum bend curvature (see Figure 2.1A [ii]).
- Progressive shifts in maximum shear stress zone through the bend from close to the inner bank at the bend entrance, to the channel centerline at the apex, and to the outer bank at the bend exit as a result of the bar-pool topography and cross-sectional asymmetry characteristic of meander bends (see Figure 2.1A [i]).
- A highly asymmetrical cross section featuring deep scour in the thalweg adjacent to the outer bank, a shallow point bar at the inner bank, and a steeply sloping point bar face separating these two regions (see Figure 2.1 C).

The flow pattern at a bend is not constant but varies with discharge. Primary flow effects are dominant at high discharges because the main flow follows a straighter path, but secondary currents are relatively strong at intermediate discharges (Bathurst et al., 1979). Consequently, the point and severity of maximum erosive attack of the outer bank moves as a function of stage. At intermediate stages, attack is con-
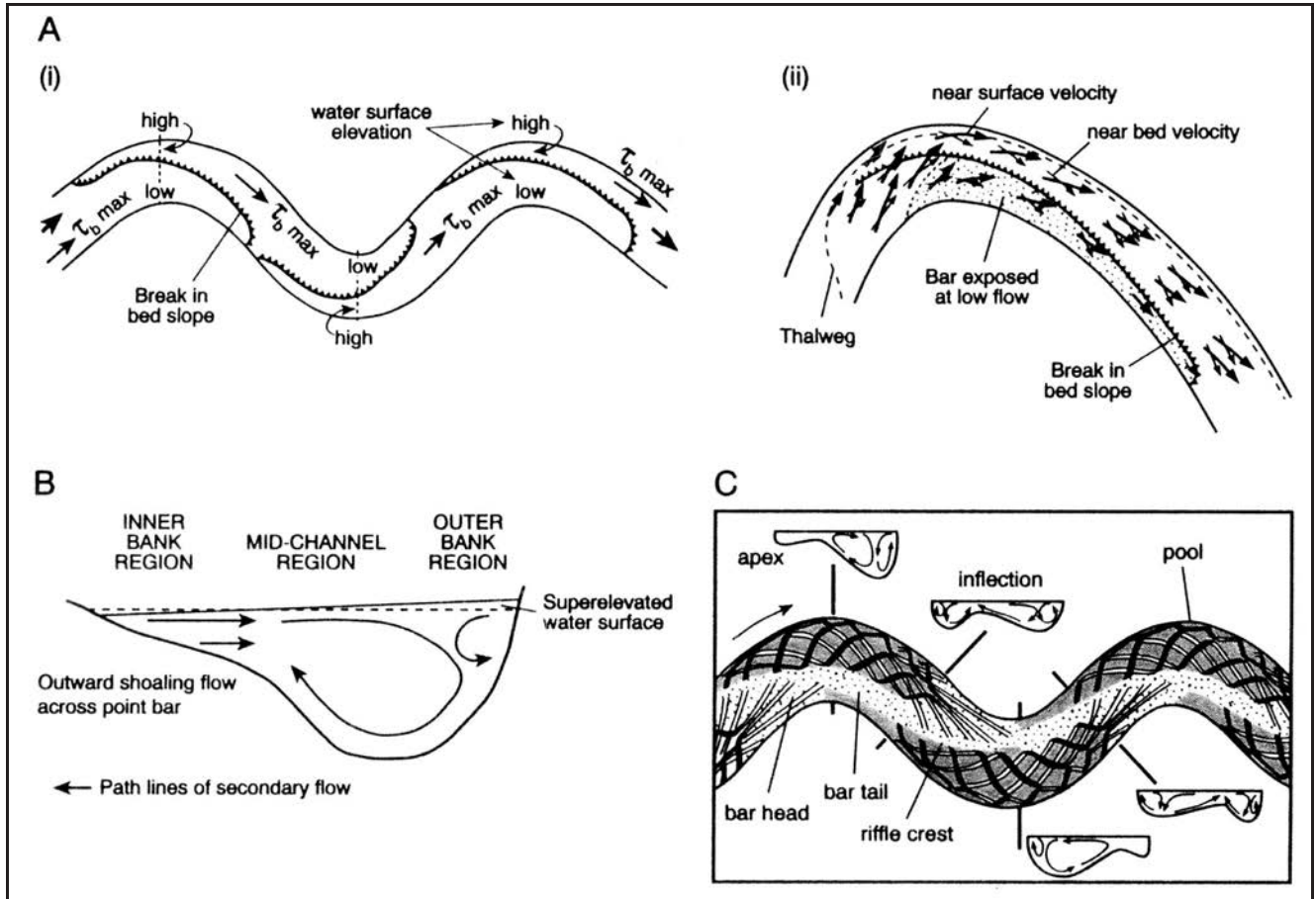
Figure 2.1.   Flow patterns in meanders: (A) (i) location of maximum boundary shear stress (τ_b) and (ii) flow field in a bend with a well-developed point bar (after Dietrich, 1987); (B) secondary flow at a bend apex showing the outer bank cell and the shoaling-induced outward flow over the point bar (after Markham and Thorne, 1992); and (C) model of the flow structure in meandering channels (after Thompson, 1986). Black lines indicate surface currents and white lines represent near-bed currents. (Figure caption is from Knighton, 1998).

centrated between the bend apex and exit, leading to simultaneous lateral growth and down-valley migration of the bend. However, during high in-bank flows, the point of greatest attack moves downstream of the bend exit, leading to rapid bend migration downstream.

The degree of superelevation of the flow and the strength of the secondary circulation increase in tighter bends (low ratio of bend radius of curvature [R_C] to channel width [W]). In bends where $R_C/W < 2$, flow impinges on the outer bank at an acute angle, causing flow separation and generating a strong back eddy along the outer bank near the bend apex, possibly inducing sedimentation along the outer bank upstream of the bend apex (Hickin and Nanson, 1975, 1984).

The channel width/depth ratio (W/D) also exerts a major influence on flow pattern (Markham and Thorne, 1992). Point bar development is more extensive in bends with high width-to-depth ratios, and the shoaling effect over the bar directs the inner bank flow radially outward over a large percentage of the width, concentrating helical flow close to the outer bank. Conversely, in narrow, deep channels, especially where

W/D < 10, wide bars are less likely to form, reducing the shoaling effect and allowing an inward movement of near-bed flow.

The morphological features typical of meander bends are shown in Figure 2.2. Point bars form at the inner banks of meander bends because of sediment accumulation there. The width of the point bar is often taken to indicate the intensity of meander growth and migration. For example, the presence of a wide and unvegetated point bar may be attributed to a rate of bar growth and lateral advance that is too rapid for vegetation establishment. However, the establishment of vegetation on a point bar also depends on factors other than the rate of growth, such as climate, availability of seeds for pioneer species, and the recent record of major floods. Therefore, the absence of vegetation on a point bar is not conclusive evidence of rapid channel migration.

Where point bars become very wide, they often feature chute channels cutting across the inside of the bend. These chute channels are activated during high in-bank flows and can indicate that the channel may have the potential to cut off.
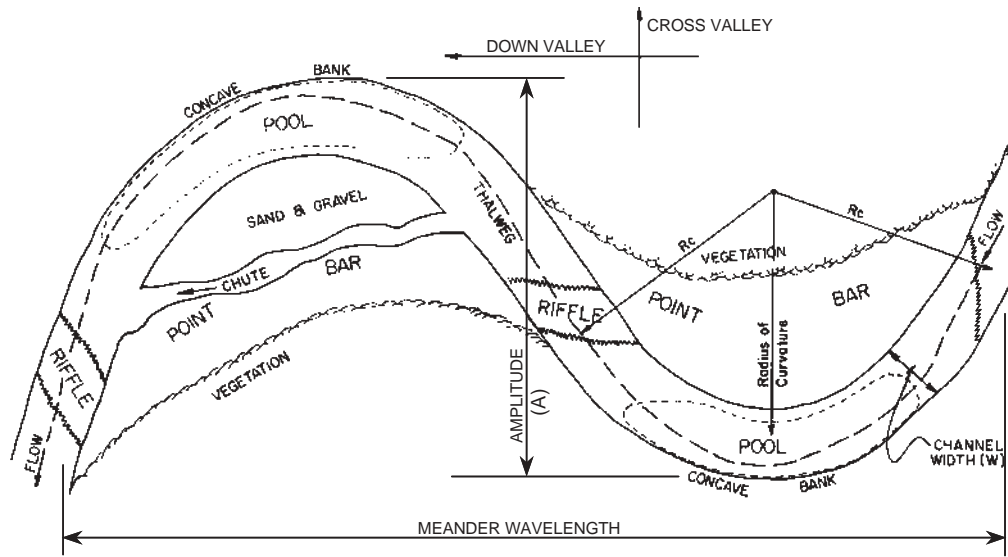
Figure 2.2. Plan view of a meandering stream.

Chute channels are associated with relatively high stream powers, abundant bed material loads, erodible banks, and high rates of lateral migration.

2.3.3 Characteristics of Meandering Streams

The intensity of meandering is most often characterized by channel sinuosity, which is defined as the ratio of the channel centerline length to the valley length. The valley length is either measured along the valley centerline or along a straight line connecting the ends of channel reaches defined by regional changes in channel direction. Straight stream reaches have a sinuosity of one. The maximum value of sinuosity for natural single-thread meandering streams is about four.

Idealized meandering streams are depicted as a sequence of symmetrical curves with similar geometries and dimensions. In fact, symmetrical meander loops are uncommon, and a sequence of two or three identical symmetrical loops is rare in nature. In addition, meander loops are rarely of uniform size. The variability of bank materials and the fact that lateral activity by the stream encounters and produces features, such as clay plugs, distort bend form to produce a wide variety of bend shapes. For example, Fisk's (1944, 1947) work on the lower Mississippi River indicates that the form of most meanders is influenced by local variations in the erodibility of the materials encountered in the outer bank. More generally, analysis of actual meandering streams indicates that the largest bends are commonly about twice the diameter of the smallest.

Meander loops move at unequal rates because of their different stages of development and variations in the erodibility of the banks. Consequently, a bend at any moment may be atypical of morphological conditions, and years of observation may be required before planform parameters characteristic of average conditions in the stream can be identified.

Bends in meandering streams are connected by crossings (short straight reaches) that are generally shallower and narrower than typical cross sections at bends (see Figure 2.2).

Sediment eroded from the outside bank is deposited in the crossing to form a prominent bar, termed a riffle, and large sandbars may form if the channel is laterally unconfined. The banklines in crossing reaches are usually less mobile than at bends, although significant erosion of the down-valley bank may occur during large in-bank and overbank floods.

2.3.4 Meander Planform Geometry

Meander bends are defined by their shape, bend radius, amplitude, and wavelength (see Figure 2.2); and general morphological descriptions and relationships exist between these planform characteristics and channel width.

Langbein and Leopold (1966) characterized the shape of meanders as a sine-generated curve, which closely approximates the curve of minimum variance, or least work, in turning around the bend. This concept describes the form of symmetrical meander paths relatively well. However, real meanders are asymmetrical and deviate significantly from idealized, perfectly symmetrical, sine-generated curves. Bend asymmetry occurs because the point of deepest scour and maximum attack on the outer bank in a bend is usually located downstream of the geometric apex of the bend, causing bends to become skewed in the down-valley direction as they migrate downstream (see Section 2.3.2).

Leopold and Wolman (1957, 1960) established that the meander wavelength (λ) is generally 10 to 14 times the width. They further noted that the radius of curvature (R_C) of a well-developed bend is generally two to three times the width at the crossing. They found these relations to hold over several orders of scale of flow in a variety of natural environments.

Schumm (1968) analyzed large empirical data sets for sand bed channels in an attempt to account for the effect of boundary materials on meander wavelength explicitly by using a weighted silt-clay index of the bed and bank sediments. He determined that meander wavelength decreases as the proportion of fine material in the bed and banks increases. This

indicates that the greater erosion resistance of silt-clay banks results in tighter, shorter wavelength bends than those channels with less cohesive, easily eroded banks. Schumm has also demonstrated that changes to the weighted silt–clay index (M) produce changes in the channel sinuosity and width/depth ratio. The relationship links the characteristic pattern of a meandering channel to its cross-sectional shape and the nature of the boundary materials. By combining the width and bend radius described above, it can be shown that radius of curvature (R_C) is approximately equal to about two to three times the channel width (W) in mature bends.

For R_C/W values of 2 to 3, Bagnold (1960) showed that energy losses caused by the curving of flow in the bend were minimized. Plots of both meander migration rate and bend scour depth as a function of bend tightness also peak sharply at an R_C/W of between 2 and 3, indicating that these bends are the most effective at eroding their bed and banks. The fact that many bends in nature develop and retain an R_C/W value of 2 to 3 while migrating across the floodplain may be consistent with their conformance to the most efficient hydraulic shape, which also maximizes their geomorphic effectiveness (Thorne, 1997).

Thorne (1992) examined the distribution of bend scour with bend geometry in a study of the Red River and determined that in very long radius bends (R_C/W > 10) mean pool scour depth is about one and a half times the mean riffle (crossing) depth, while the maximum scour depth is between one and seven tenths and two times the mean crossing depth. Scour depths ranged from two to four times the mean crossing depth for bends with R_C/W values between 2 and 4, with the deepest scour associated with an R_C/W of about 2. Evidence suggests that maximum scour depths decrease with decreasing bend radius for extremely tight bends with R_C/W < 2.

Although these morphological relationships are useful, caution should be taken when using them to predict channel geometry and scour depth at specific sites. As Knighton (1998) states: "These various relationships indicate a self-similarity of meander geometry over a wide range of scales and environmental conditions. However, the regularity which they imply is not everywhere apparent, and the use of single parameters provides only a partial and often subjective characterization of meander form."

2.3.5 Bank Erosion in Meander Bends

Bank retreat in actively meandering streams is responsible for lateral channel migration. There are two mechanisms by which stream banks retreat: (1) fluvial entrainment (detachment of grains or aggregates by the flow) and (2) mass failure (slumping or sliding caused by gravity). The specific retreat mechanisms at a given location are related to the characteristics of the bank material. Severe bank retreat often results when mass failure and fluvial entrainment act in concert. Fluvial erosion scours the lower bank and bank toe, leading to oversteepening and mass failure of the upper bank. Removal of failed bank material from the base of the bank follows through fluvial erosion and the cycle of retreat is repeated.

It is important to note that fluvial erosion of previously failed bank material plays a significant role in determining the rates of bank retreat. Fluvial activity controls the state of basal endpoint control, or the amount of basal accumulation of bank material, which ultimately controls the stability of the bank. Removal of the failed material results in the formation of steeper banks and may induce toe erosion by removing the material along the toe that buttresses the bank slope (Thorne, 1981). These factors renew the process of bank erosion by mass failure. Without basal erosion, mass failure of the bank material would lead to bank slope reduction and stabilization within a relatively short period of time (Lohnes and Handy, 1968; Thorne, 1981).

Curved flow around a bend causes erosion at the toe of the outer bank and subsequent bank failure because of high near bank velocities, plunging flow, and increased shear stresses around and downstream of the bend apex. As a bend tightens, flow may approach the outer bank at a very acute angle, generating extremely severe toe scour, erosion, and bank retreat through impinging flow. However, if the bend tightens further, flow at the outer bank separates, leading to reduced erosion in the zone of separation and possible bar accumulation at the outer bank. Separated flow at the outer bank may deflect the filament of maximum velocity so that it attacks the inner bank in the bend or the down-valley bank in the crossing downstream. In either case, the distribution of bank retreat and meander migration will be radically altered in a manner that is very difficult to predict.

2.3.6 Modes and Rates of Meander Migration

Although no two meanders migrate in exactly the same way, the movement of bends in a particular stream reach tends to conform to one of the several modes of behavior illustrated in Figure 2.3, which is based on a study of about 200 sinuous or meandering stream reaches (Brice, 1977). Rates of lateral movement generally scale to the size of the channel with annual migration rates generally being 10 percent of the channel width but sometimes reaching as high as 20 percent (Hooke, 1997). In large rivers, these dimensionless rates convert into considerable absolute rates, and meanders have been observed to move at 2,500 ft/year (750 m/year) in large alluvial rivers (Lagasse et al., 2001).

Mode a in Figure 2.3 represents the typical development of a loop of low amplitude, which decreases in radius as it migrates downstream. Mode b occurs only where meanders are confined by artificial levees or by valley sides on a narrow floodplain. Well-developed meanders on streams that have moderately erodible banks are likely to follow Mode c. Mode d applies mainly to larger loops on highly sinuous or tortuous streams. The meander has become too long in relation to stream width, and secondary meanders have developed, making a compound loop. Mode e also applies to highly sinuous meandering streams, usually with relatively narrow point bars and no chutes. An elongated loop has formed without a chute cutoff, but the neck of the loop is gradually being closed and a neck cutoff will eventually occur. Modes f and g occur mainly
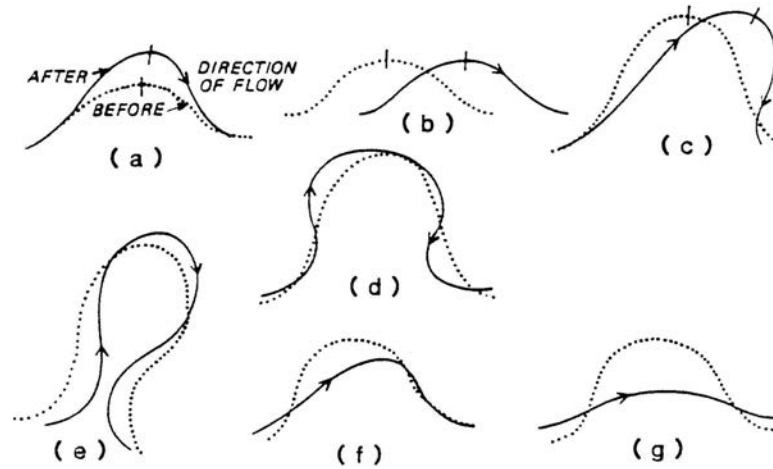
SOURCE: Modified from Brice, 1977

*Figure 2.3.   Modes of meander loop development: (a) extension,
(b) translation, (c) rotation, (d) conversion to a compound loop,
(e) neck cutoff by closure, (f) diagonal cutoff by chute, and (g) neck
cutoff by chute.*

in less sinuous meandering streams with easily eroded banks and wide point bars. Low-amplitude loops are cut off by chutes that break diagonally or directly across the point bar.

The rate of migration is largely controlled by bend geometry, especially by channel curvature as represented by R_C/W. Hickin and Nanson (1975, 1984) and Nanson and Hickin

(1986) demonstrated through detailed studies of more than 125 bends on 19 river reaches in Canada that the rate of migration reaches a maximum when $2 < R_C/W < 3$. This relationship between form and rate of change for meanders (see Figure 2.4) has been further substantiated by Biedenharn et al. (1989) and Hooke (1987). The rate decreases rapidly on either
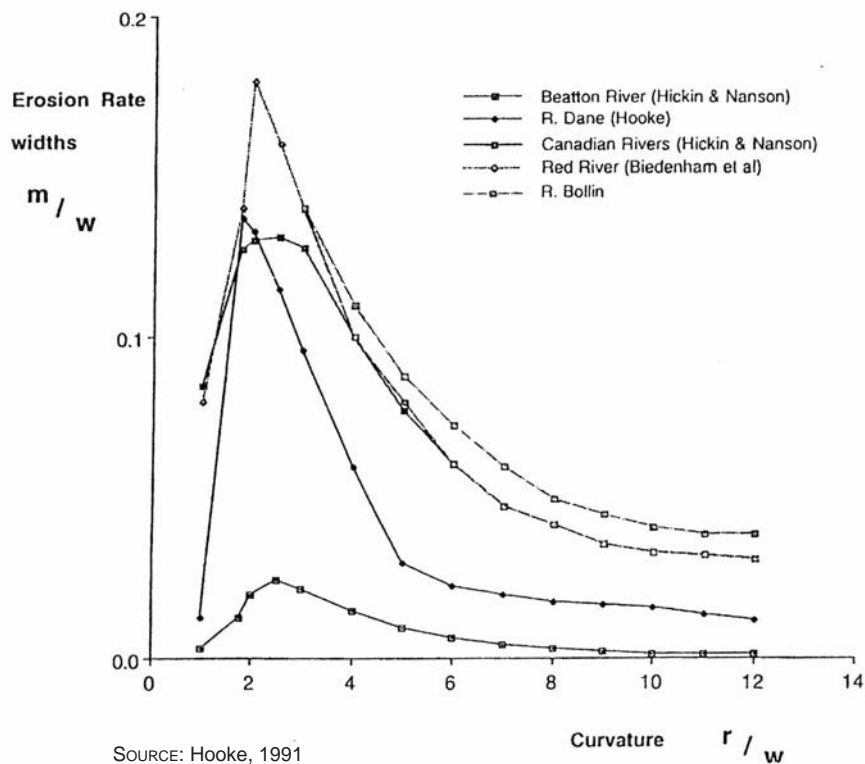
SOURCE: Hooke, 1991

Figure 2.4.   Relationship between erosion (migration) rate and bend curvature.

side of this range. At the lower end of the range, the decrease may be attributable to the large increase in resistance or a decrease in outer-bank radial force as R_C/W falls below 2.

Observations indicate that river meanders tend to an R_C/W value of between 2 and 3. Because of the loss of energy associated with flow through a bend, a maximum bend sharpness exists beyond which further significant lateral erosion is unlikely to occur. It has been shown that the maximum lateral erosion rate for a meander bend occurs when the ratio of radius of curvature to channel width is in the range of about 2 to 4 (see Figure 2.4). For R_C/W values less than about 2, the erosion rate reduces sharply because of energy loss in the bend; and, in very tight bends ($R_C/W < 2$), deposition may actually occur along the outer bank of the bend. Under this condition, the rate of lateral migration significantly decreases or migration stops, and the bend either cuts off or avulses (i.e., undergoes an abrupt shift in channel course).

Oxbow lakes are formed by the cutoff of meander loops, which occur either by gradual closure of the neck (see Figure 2.3e) or by a chute that cuts across the neck (see Figure 2.3g). Commonly, a new meander loop soon forms at the point of cutoff and grows in the same direction as the previous meander. Although recently formed oxbow lakes along a channel are evidence of recent lateral migration, the presence of abundant oxbow lakes on a floodplain does not in itself indicate rapid channel migration because an oxbow lake may persist for hundreds of years.

Usually, the upstream end of the oxbow lake fills quickly to bank height. Overflow during floods and overland flow entering the oxbow lake carry fine materials into the lake area. The lower end of the oxbow remains open, and drainage entering the system can flow out from the lower end. The oxbow gradually fills with fine silts and clays, which are plastic and cohesive. As the stream channel meanders, old meander bends filled with cohesive materials (referred to as clay plugs) are sufficiently resistant to erosion to serve as semi-permanent geologic controls that can drastically affect planform geometry.

The local increase in channel slope caused by cutoff usually results in an increase in the growth rate of adjoining meanders and an increase in channel width at the point of cutoff. Typically, the effects of a cutoff do not extend very far upstream or downstream. The consequences of cutoffs are an abruptly steeper stream gradient at the point of the cutoff, scour at the cutoff, and a propagation of the scour in an upstream direction. Downstream of a cutoff, the gradient of the channel is not changed, and, therefore, the increased sediment load caused by upstream scour will usually be deposited at the site of the cutoff or below it, forming a large bar.

2.3.7 Measuring Meander Migration

Before predictive tools for channel migration can be developed, one must be able to measure and describe channel migration. A standard approach to analyzing data sets must be developed, and this approach should be adhered to for all subsequent measurements.

The initial or existing meander bend should be represented by a starting point (upstream end), an ending point (downstream end), a location of the center of bend radius (bend centroid), an orientation with respect to a baseline (e.g., down-valley direction), and an outside bank radius of curvature (R_C). As shown in Figure 2.5, it can be assumed that the bend starts and ends at the flow crossing (shown as "riffle" in Figure 2.2).

Bend migration can be reasonably described by four modes of movement. Extension is across-valley migration and is easily measured at the bend centroid. Similarly, translation is down-valley migration and is also measured at the bend centroid. Expansion increases bend radius; contraction decreases bend radius. Rotation is a change in the orientation of the meander bend with respect to the valley alignment.

Predicting four modes of movement is a significant task for every bend of interest (see Figure 2.5). However, actual bend migration is even more complex. For example, one part of the bend may be expanding faster or translating down valley faster than another, resulting in changes in bend symmetry. As a concession to practicality, one must limit the number of modes of movement to the fewest possible. In the methodology developed in Chapter 7, extension and translation are considered directly (as a vector sum). Expansion (a change in R_C) is included because it could have a major impact on the location of the outer bank and because rates of migration appear to be correlated to R_C/W (bend radius of curvature/width). If movement in these three modes can be predicted, the primary threats to a bridge, highway, or other facility will be established. Rotation is considered only indirectly as a component of the combined movement in the other three modes relative to adjacent bends.

2.4 HAZARDS TO HIGHWAYS CAUSED BY INCREMENTAL MEANDER MIGRATION

A number of hydraulic problems may stem from meander migration in the vicinity of a highway crossing. These include the incremental shift of flow direction (angle of attack) approaching bridge piers or abutments; development of an extensive point bar in the bridge reach with the commensurate loss of conveyance; lateral channel erosion at piers, abutments, or approaches; and possible flanking of the bridge approaches. Meander migration can also exacerbate scour and pressure loading because of debris accumulation.

For example, failure of a major bridge on the Hatchie River near Covington, Tennessee, in 1989, has been attributed in part to lateral migration of the channel in the bridge reach (Bryan, 1989; NTSB, 1990). Significant migration of the right bank of the channel between 1975 and 1989 had undermined the foundation of a support bent previously located in the floodplain and contributed in part to the collapse of three spans of the roadway and the deaths of eight people. The maximum bank migration rate of 4.5 ft (1.37 m) per year occurred between 1975 and 1981.

The chapters of the *Handbook* that follow this one provide screening and classification procedures and methodologies to

Across Valley

Rc

Channel Centerline

Down Valley

Upstream
End (crossing)

Downstream
End (crossing)

Flow

Initial Bendway

Extension (Across-Valley Migration)   Translation (Down-Valley Migration)

Expansion (Increasing Radius)   Rotation

All Four Modes of Movement
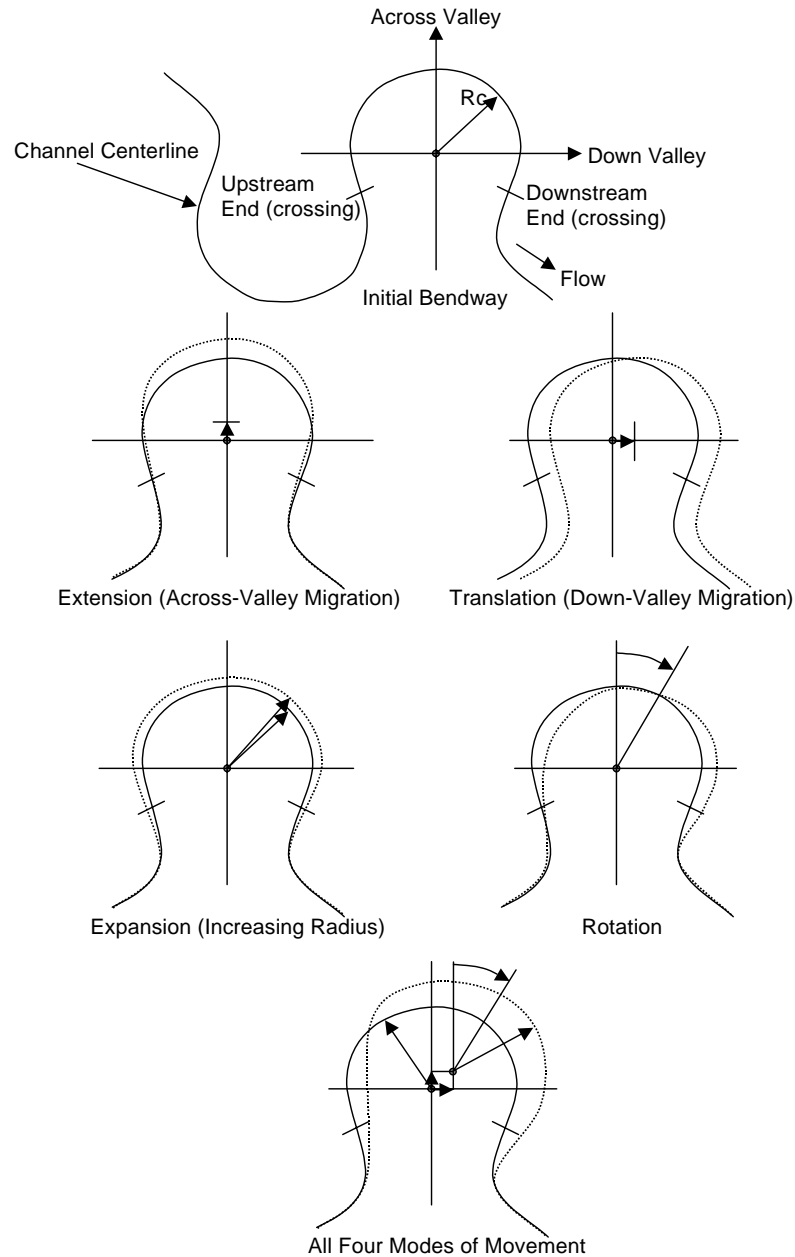
Figure 2.5.   Measuring meander migration.

predict the rate and extent of incremental channel shift as a result of meander migration. Aerial photograph comparison and frequency analysis techniques are provided to predict the potential impact of meander migration on highway facilities for specific classes of meandering channels.

2.5 HAZARDS TO HIGHWAYS CAUSED BY AVULSIONS AND CUTOFFS

The scope of NCHRP Project 24-16 specifically limited the investigation of meander migration to *incremental* channel shift (i.e., lateral channel shift and down-valley migration).

It was beyond the scope of the project to develop a methodology to predict *avulsive* or catastrophic channel shift; however, the process of avulsion, or cutoff of a meander, can also have a significant impact on the stability of a highway facility. These impacts include accelerated erosion of adjacent bends, especially the bend immediately downstream; degradation in the upstream channel reach; and aggradation in the downstream channel reach.

An avulsion is a sudden change in the river channel course that usually occurs when a stream breaks through its banks. Avulsions are often associated with a major flood or catastrophic event. A cutoff is an avulsion related to a single meander loop and can be defined as a natural or artificial channel

that develops across the neck of a meander loop (neck cutoff) or across a point bar (chute cutoff).

The following discussion from a study of the cutoff of meander bends on the Sacramento River is provided to indicate the potential for developing a predictive methodology for avulsions and cutoffs (WET, 1988; Harvey, 1989).

Meander bends eventually cut off when the radius of curvature (R_C) becomes too short, primarily as a result of the arrest of one limb of the bend by more erosion-resistant material. This is a manifestation of reduced hydraulic slope, which causes a reduction in sediment-transport capacity of the flows within the upstream portion of the bend and leads to sediment deposition within the channel and reduced hydraulic capacity in the channel (Harvey, 1989). Reduced hydraulic capacity in the upstream portion of the bend increases the frequency of flows over the point bar, which leads to chute development and eventually bend cutoff. Cutoffs can occur as a result of chute development or neck closure.

Recent and historic cutoffs on the floodplain of the Sacramento River were investigated to evaluate whether cutoffs could be predicted (WET, 1988; Harvey, 1989). A dimensionless cutoff index, which was defined as the ratio of the centerline radius of curvature to the migration distance (R_C/MD), was developed to predict cutoff occurrence. For the coarse-grained meanderbelt section of the Sacramento River, the dimensionless cutoff index was

$$1.7 < R_c/MD < 3.7 \tag{2.1}$$

For the fine-grained meanderbelt section, where the floodplain sediments are more cohesive, the cutoff index was

$$2.5 < R_c/MD < 4.3 \tag{2.2}$$

Associated with these values are two other characteristics that were identified on aerial photographs: (1) the presence of a mid-channel bar in the upstream limb of the bend and (2) the presence of chute channels across the point bar. The cutoff index was tested independently on bends in the Butte Basin reach of the Sacramento River, and it was evident that there is a relationship between the cutoff index and the presence of the two ancillary features.

It should be noted that the cutoff indices developed for the Sacramento River are site specific and have not been generalized for application to other river systems. They are presented here only as evidence that it should be possible to develop predictive relationships for channel avulsions or cutoffs. Developing these predictive relationships was beyond the scope of NCHRP Project 24-16, and the *Handbook* does not provide a methodology to predict episodic channel shift. However, the possibility of a neck cutoff can be identified using the techniques presented in the *Handbook* when the predicted incremental migration leads to meander neck closure.

CHAPTER **3**

SCREENING AND CLASSIFICATION OF MEANDERING STREAMS

3.1 INTRODUCTION

Initial screening is performed to determine whether a channel is straight, meandering, anabranched, or braided. The methodology presented here applies only to meandering channels; braided and anabranched streams are screened out. The planform characteristics of meandering streams are classified using a form of the Brice (1975) method that has been modified in the *Handbook* to cover the geomorphic stream types that users will likely encounter in the field. Secondary screening is then applied to identify stable meanders based on the degree of channel width uniformity. This allows the hydraulic engineer to screen out stable meanders that generally pose little or no threat through lateral migration.

3.2 INITIAL SCREENING

Alluvial streams can be classified according to their patterns as single-thread, braided, or anastomosing (see Figure 3.1). The appearance of the stream when viewed on aerial photographs is used to screen out braided and anastomosing channels, which are beyond the scope of the methodologies presented in the *Handbook.* Only channels identified as meandering will be analyzed beyond the initial screening.

3.3 MEANDER CLASSIFICATION

A number of morphological classification schemes for alluvial rivers were evaluated (Brice, 1975; Schumm, 1977; Schumm and Meyer, 1979; Schumm, 1981; Montgomery and Buffington, 1997; Rosgen, 1994). The utility of different methods was investigated with the aim of producing a classification system that has the following attributes:

- It is simple and directly applicable to the meanders encountered in the field.
- The classification provides a rational basis for screening out stable and highly unstable patterns.
- It is in pictorial format, requiring only a map, aerial photograph, or visual inspection to apply.
- Its application does not require field data (e.g., sediment sampling).
- It requires minimal training and/or instruction for end users.

Based on these criteria, the Brice (1975) method was found to be the most appropriate. However, using the Brice classes to stratify the large data set used in developing the methodology to predict channel migration under NCHRP Project 24-16 revealed that not all the channel classes that Brice identified would commonly be encountered by hydraulic engineers working in the field. Hence, a modified Brice (1975) method was developed. This consists of nine channel categories that were optimized for use in bend classification and secondary screening for meander migration prediction, as shown in Figure 3.2.

3.4 SECONDARY SCREENING

Before predicting migration rates for selected bends along a meandering stream, it is necessary to identify whether meandering is stable or active. The method employed for this purpose is that of Brice (1982), who was able to discriminate qualitatively between stable and laterally active channels on the basis of the degree of width variability along the course of the stream. Through extensive historical documentation and field observations of streams, he discovered that channels that do not vary significantly in width are either static or relatively stable, whereas channels that are wider at bends migrate actively. In Brice's study, highly sinuous, equal-width streams were the most stable, equal-width streams of lower sinuosity were slightly active, and wider-at-bend streams had the highest migration rates. Testing Brice's hypothesis against the larger database assembled for NCHRP Project 24-16 validated this screening procedure.

As a result, secondary screening of meandering channels using the Brice width-variability criterion can be used to differentiate between stable meandering streams and channels with actively migrating bends. Bends of stable meandering streams can be considered sufficiently stable that bend migration is unlikely to pose a threat to bridges or highway structures; no further analysis of these streams is required.

In the modified classification scheme (see Figure 3.2), equal-width rivers in classes B_1 and G_1 are static or relatively stable and are screened out on this basis. Equal-width, deep, or incised channels of Class A are also screened out. Class A channels may not migrate because they are deeply inset into geologically competent materials such as bedrock, or they may be actively cutting through erodible materials but not migrating laterally to any significant degree.

Class F streams are compound channels with a "wandering" low-water channel, wide bars, and back channels. Wandering

SOURCE: Thorne, 1997 (modified from Brice, 1975)

Figure 3.1.   Alluvial channel pattern classification. Degree of anabranching pertains to anastomosing channels.

streams feature lateral activity that is sporadic and spatially disorganized. Lateral migration in such situations is highly unpredictable, and wandering streams should be screened out as potentially so unstable and unpredictable that further evaluation would not be likely to produce a meaningful prediction of meander migration.

Migration rates for meander bends on rivers classified as any of the remaining categories (B_2, C, D, E, and G_2) are amenable to prediction by photogrammetric comparison techniques (see Chapters 5 and 7). Illustrated examples of the application of the classification and screening techniques are presented in Chapter 8.
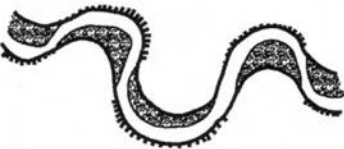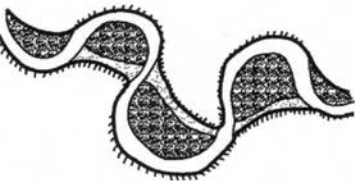
MODIFIED BRICE CLASSIFICATION	SCREEN
A SINGLE PHASE, EQUIWIDTH CHANNEL INCISED OR DEEP	*
B_1 SINGLE PHASE, EQUIWIDTH CHANNEL	*
B_2 SINGLE PHASE, WIDER AT BENDS, NO BARS	
C SINGLE PHASE, WIDER AT BENDS WITH POINT BARS	
D SINGLE PHASE, WIDER AT BENDS WITH POINT BARS, CHUTES COMMON	
E SINGLE PHASE, IRREGULAR WIDTH VARIATION	
F TWO PHASE UNDERFIT, LOW-WATER SINUOSITY (WANDERING)	*
G_1 TWO PHASE, BIMODAL BANKFULL SINUOSITY, EQUIWIDTH	*
G_2 TWO PHASE, BIMODAL BANKFULL SINUOSITY, WIDER AT BENDS WITH POINT BARS	
NOTE: WHERE SCREEN = *, CLASS FALLS OUT DUE TO IMPLICATIONS OF CONSIDERABLE STABILITY OR EXCESSIVE INSTABILITY	

Figure 3.2.   Modified Brice classification of meandering channels.

CHAPTER **4**

PHOTOGRAMMETRY

4.1 INTRODUCTION

Accurate calculation and prediction of bend migration rates from historical sequences of aerial photographs requires the application of the principles of photogrammetry. The American Society of Photogrammetry and Remote Sensing defines photogrammetry as the art, science, and technology of obtaining reliable information about physical objects and the environment through processes of recording, measuring, and interpreting photographic images and patterns of recorded radiant electromagnetic energy and other phenomena (Wolf and Dewitt, 2000). Originally, photogrammetry consisted of analyzing photographs, and aerial photos remain the principal source of information today. However, photogrammetry now includes the analysis of other records, such as digital imagery.

This chapter describes the basic principles of photogrammetry, the application of these principles to meander migration analysis and prediction, the map and photographic requirements necessary for a detailed study of meander migration, and the major sources of maps and aerial photographs.

4.2 BASIC PRINCIPLES OF PHOTOGRAMMETRY

4.2.1 Types of Photogrammetry

There are two fields of photogrammetry: metric and interpretive. Metric photogrammetry consists of making various types of precise measurements on photos and other information sources, with the most common application being the preparation of planimetric and topographic maps and digital orthophotos. Determining the significance of recognized and identified objects through careful analysis is the field of interpretive photogrammetry. Both fields are used in the analysis of channel migration.

The principal types of records available for photogrammetric analysis are photographic and digital. Photographic exposures are taken from the ground (terrestrial) or from the air (aerial) with different types of cameras using a wide variety of lenses and filters. Negatives and positive contact prints are then made from the exposed film under darkroom processing procedures.

A digital image is a computer-compatible pictorial rendition in which the image is composed of a fine grid of picture elements (pixels). Digital images are produced through the process of discreet sampling, whereby a small image area

(pixel) is "sensed" to determine the amount of electromagnetic energy emitted by the corresponding patch of surface on the object. Each pixel in a black and white image is defined by an array of integers (digital numbers) that quantifies its gray level, or degree of darkness. The output image, which appears as a continuous-tone picture, consists of many thousands to millions of these pixels. A digital color image is also composed of pixels; the color of the pixels is represented by an ordered triplet consisting of a blue, green, and red value. The shades of color in digital color images are represented by varying the levels of brightness of the three primary colors or channels individually within each pixel, similar to the principles used in a color television screen.

4.2.2 Aerial Photography

Aerial photography, which is the principal type of photography used in meander migration analysis, is obtained via an airborne platform, such as an airplane or satellite. Aerial photos are classified as either vertical or oblique. Oblique photos are taken with the camera axis intentionally tilted away from vertical and produce a panoramic view. Vertical aerial photos are taken with the camera axis as nearly vertical as possible. Unavoidable aircraft tilt creates some minor photographic tilt; this is accounted for in metric photogrammetry through the use of precise photogrammetric instruments and procedures.

The most common and versatile type of vertical aerial photo is the standard 9 in. × 9 in. (23 cm × 23 cm) black and white panchromatic print using a metric format camera. Other types of aerial photos, including color and color infrared (CIR or false color), are available and are used in meander migration analysis as well. Metric format means that the camera and lens have been calibrated in a laboratory. The calibration includes determining lens distortions, lens focal length, and film flatness and making precise measurements of the camera fiducials. Fiducials are the crosshair marks one sees in the corners and sides of an aerial photograph. They are used to establish a photo coordinate system when highly accurate measurements from the photograph are desired.

Although they vary, the most common flight altitudes from which aerial photos are taken range from 5,000 to 30,000 ft (1,524 to 9,144 m). The aircraft's height above the ground and the camera's focal length determine the scale of the aerial photo. The most common aerial photo obtained today is taken with a 6-in. (152-mm) focal length camera at an altitude of about 20,000 ft (6,096 m). This would produce

a photo that covers an area of about 33 mi^2 (85 km^2) at a scale of 1:40,000. The scale 1:40,000 means 1 in. on the photo is equal to 40,000 in. or about 3,333 ft (1 cm = 400 m) on the ground.

Vertical aerial photography is usually flown along a series of parallel passes, called flight strips. The photos on a given strip are exposed such that there is overlap of the coverage of the previous photo (known as end lap), and parallel flight strips are flown such that there is lateral overlap (side lap) between adjacent flight strips. Aerial photography for the purposes of mapping is usually acquired with a 60 percent overlap to allow photogrammetrists to view the mapping area in three dimensions for collection of elevation data. The common area of coverage in adjacent pairs of photos that are end lapped produces stereoscopic coverage, and the pair of overlapping photos is called a stereopair.

Although aerial photos are flat surfaces, they record pronounced relief that can be seen in three dimensions, or "stereo," using a stereoscope. A simple pocket stereoscope, one of several types of stereoscopes, can be used to view the relief recorded by stereopairs. The use of stereopairs allows the user to identify features, such as an obscured stream bank, that may not be readily visible in an individual photograph. In addition, stereoscopic views can be used to estimate relative heights of objects, especially if an object of unknown height is compared with one of known height. For example, a stream bank height may be estimated by comparing its height with that of a bridge or structure of known height nearby.

Because an aerial photograph is a perspective view, rather than an orthogonal view as provided by most maps, an effect called relief displacement must be understood before measurements are attempted. Relief displacement is the shift, or displacement, in the photographic position of an object caused by the height of an object. Objects above the average terrain elevation in a photo appear to displace outward from the center of the photo. Objects below the average terrain elevation of a photo appear to displace inward toward the center of the photo. The effect is most clearly seen in urban areas with tall structures, where buildings and smokestacks tilt away from the center of the photo (see Figure 4.1). Relief displacement can affect the accuracy of measurements made from an aerial photo, and its effect can be eliminated. How it is eliminated depends on what technique is used to make measurements. This effect is not significant with regard to low relief features such as rivers, but it can be an important factor when using tall or high elevation features to make distance measurements or when registering photos to each other.

Users need to know the average scale of an aerial photo before accurate measurements can be made. The scale of an aerial photograph is the relationship between a measurement

Figure 4.1.   Vertical aerial photograph illustrating relief displacements.

on the photo and a measurement on the ground. Scale can be expressed as a representative fraction or a unit equivalent. For example, the representative fraction of 1:5,000 means 1 unit on the photo is equal to 5,000 units on the ground, whereas the unit equivalent of 1 in. = 2,000 ft means 1 in. on the photo is equal to 2,000 ft on the ground. The scale of the photo is determined by the elevation of the airplane and the focal length of the camera lens at the time the photo is taken (i.e., scale is the ratio of focal length to flying height). The scale determines the accuracy of measurements taken from an aerial photo—the greater the flight altitude, the lower the accuracy of measurements taken from the photo.

Scale also varies across an aerial photo because of terrain height differences and tilt in the camera when the photo was taken. If the camera is not pointing straight down at the time of exposure, the scale of the photo will vary, depending on location. Also, as the terrain changes in elevation, so does the scale; a mountaintop in a photo has different scale than a valley bottom on the same photo. The photogrammetrist can account for both camera tilt and terrain height differences before measurements are taken through processes that are described below.

Most aerial photography has a scale printed on it. However, if the scale is unknown, one method of scale determination is to measure between two points on the photo that have a known distance on the ground. For example, if there is a football field in the photo, measure the distance between the goal lines in the photo. If the distance is 1 in. in length, then the scale of the photo is expressed as 1 in. = 300 ft or 1:3,600 (1 in. = 3,600 in.).

Another simple method of determining scale is to identify two points on the photo with the same two points on a map having a published scale and measuring the distances between them. For example, measure the distance between two road intersections in the photo and the same two road intersections on a United States Geological Survey (USGS) 7.5-minute topographic quadrangle map (scale: 1 in. = 2,000 ft). If the distance on the photo is 3 in. and the distance on the map is 6 in., then the photo scale can be calculated by using the map distance to determine the ground distance. In this case, 6 in. on the map is equal to 12,000 ft on the ground. That same 12,000-ft distance is represented by 3 in. in the photo, so the scale of the photo is 3 in. = 12,000 ft, or 1 in. = 4,000 ft.

There are three methods of making horizontal position measurements off a single aerial photo. The least accurate method of making a horizontal measurement involves using a scale or ruler. Once the scale of the photo is known, one simply measures between objects and converts the measured photo distance to a distance on the ground by using the photo scale. This only yields a distance, however, and most measurements need to be related to a known ground coordinate system to be useful. The photo can be referenced to a ground coordinate system using a scale and a map, but the method is very cumbersome and rarely done. This method assumes the scale across the photo is constant, which is never the case, and it does nothing to mitigate the effects of relief displacement.

The second method involves a simple rectification of the photo. The rectification process references the photo to a ground coordinate system first so that all subsequent measurements are made in a ground coordinate system. This is accomplished using a scanned digital image of the photo, preferably the negative; a map of the same area, usually a USGS 7.5-minute topographic quadrangle map; and a computer program for rectification. After picking at least six points on the photo that can be clearly seen on the map, the ground coordinates of these points are established by reading their coordinates off the map. The ground coordinates of the points are used by the computer program along with the point locations on the digital image, which are measured in an established photo coordinate system (often the Universal Transverse Mercator [UTM] coordinate system). With this information, the computer program performs a simple rectification and georeferences the photo to the ground coordinate system. The rectification process eliminates the effect of scale differences across the photo, but it does not eliminate the effect of relief displacement. (Relief displacement is the inward or outward shift in the photographic position of an object because its elevation is above or below a selected datum.) Measurements can then be made off the digital image using a computer and a mouse or other pointing device. The accuracy of this method depends on the number and accuracy of the points used to georeference the photo. For example, the accuracy of a point interpolated from a 7.5-minute topographic map is ±40 ft, whereas the accuracy that can be attained using modern survey methods is easily within inches.

The last and most accurate method is to make horizontal measurements from a digital orthophoto. The creation of a digital orthophoto requires a scanned digital image of the photo, a way of georeferencing the image, a digital terrain model (DTM) or digital elevation model (DEM), and associated computer software. Users can georeference the image for an orthophoto using the simple rectification process, or they can use a more accurate technique called aerotriangulation. Aerotriangulation requires stereo photo coverage of the area and usually involves surveying high-accuracy ground points. Regardless of the method used for georeferencing, the image is laid over a DTM or DEM surface. The DTM or DEM provides the necessary elevation information to eliminate the effect of relief displacement. This, along with the elimination of scale differences through rectification, produces a perspective-free or orthogonal digital image called a digital orthophoto. Measurements can now be made quickly using a mouse and computer software. All other input data being equal, the digital orthophoto is inherently more accurate than a simple rectified image because the effect of relief displacement has been eliminated as a source of measurement error.

4.2.3 Photogrammetric Products

Photogrammetry has been used to produce topographic maps for many years and is still the principal means of

producing maps. The U.S. Geological Survey (the agency tasked with mapping the United States) and most state departments of transportation compile nearly 100 percent of their maps photogrammetrically. Many of the maps and aerial photos that are presently available can be obtained as digital image files.

Digital image files are most commonly available in TIFF (Tagged Image File format) and GIF (Graphics Interchange Format), as well as in JPEG (Joint Photographic Experts Group) file format. TIFF, which is recommended, contains the maximum number of colors possible and performs very limited compression in a manner that does not affect image quality (lossless). TIFF is a tag-based format compatible with a wide range of software applications and can be used across platforms such as Macintosh, Windows, and UNIX. TIFF is complex, so TIFF files are generally larger than GIF or JPEG files. Although TIFF supports lossless compression, compressed TIFFs take longer to open.

A JPEG image also contains the maximum amount of color information possible, but it has much stronger compression (the image can be up to 30 times smaller than a TIFF). A JPEG file supports 24 bits of color information and is most commonly used for photographs and similar continuous-tone bitmap images. The JPEG file format stores all of the color information in a red, green, and blue (RGB) image and then reduces the file size by compressing it, or saving only the color information that is essential to the image. However, depending on how much an image is compressed, JPEG compression can compromise image quality.

GIF saves space by maintaining the sharpness of an image but drastically reducing the amount of color information contained. This makes GIF a poor choice for most photos. It is most commonly used for bitmap images composed of line drawings or blocks of a few distinct colors. GIF supports only eight bits of color information or less.

Orthophotos and DEMs are two relatively new photogrammetric products that are now often used together to replace traditional topographic maps. Orthophotos are produced from aerial photos that have been modified so that their scale is uniform throughout. This uniformity is accomplished through the process of differential rectification, which eliminates image displacements caused by photographic tilt, terrain relief, and photograph distortion. Orthophotos are equivalent to planimetric maps; but, unlike planimetric maps, which show features by means of lines and symbols, orthophotos show the actual images of features. Orthophotomaps offer significant advantages over aerial photos and line and symbol maps because they combine the features of both.

As described earlier, a DEM is a discrete representation of a topographic surface. The DEM, which is an area composed of an array of points that have had their X, Y, and Z coordinates determined, provides a numerical representation of the topography of the area such that contours, cross sections, and profiles can be computed from it. In some cases, a DEM is also known as a DTM or a digital terrain elevation model (DTEM). Unlike DEMs, digital line graphs (DLGs) are digital planimentric representations of the points, lines, and areas that define natural and cultural features, but DLGs provide no elevation information. A digital raster graphic (DRG) is a digitally scanned image of a topographic map.

Because orthophotos, DRGs, DLGs, and DEMs are in digital form, they are commonly applied in connection with GISs. These photogrammetric products provide a major contribution to GISs through their use in generating spatially accurate layers of information for GIS databases, which can ultimately be used in problem solving.

4.3 APPLICATION OF PHOTOGRAMMETRY TO MEANDER MIGRATION ANALYSIS

The most accurate means of measuring changes in channel geometry and lateral position is through repetitive surveys of channel cross sections referenced to fixed monuments. However, these data are rarely available. A relatively simple and accurate method of determining migration rate and direction is through the comparison of sequential historical aerial photography (photos), maps, and topographic surveys.

The first major use of photogrammetry in the evaluation of fluvial systems was conducted on the Mississippi River Valley. Fisk (1944) used maps, aerial photographs, and ground investigations to document historic and prehistoric Mississippi River channel patterns and valley train positions in the lower Mississippi River Valley. He also examined the effects of fine-grained alluvial deposits on the activity of the contemporary river (Fisk, 1947).

Brice (1975) developed a classification system of alluvial rivers by analyzing the planform properties of 200 river reaches from topographic maps and aerial photos in order to correlate aspects of river behavior, such as rate of lateral erosion and depth of scour, with river type. From this, he developed a comprehensive methodology for conducting a stream stability and meander migration assessment using a comparative analysis of aerial photos, maps, and channel surveys (Brice, 1982).

Since Fisk's work, numerous researchers have used photogrammetry to document channel planform changes, erosion and sedimentation patterns, and meander migration rates on a wide variety of streams in geographically diverse regions. For example, Hooke (1977, 1984) used historic aerial photos and maps to document the lateral mobility of rivers in Devon, England, over a 50-year period. Williams (1978) used photos taken of the Platte River in Nebraska to document the spectacular reductions in channel width that have resulted from river regulation since 1900. Burkham (1972) used surveys, maps, and photographs to document channel changes on the Gila River in Arizona, and Ruhe (1975) used maps covering the period from 1852 to 1970 and aerial photos from 1925 to 1966 to document changes of the Otoe bend on the Missouri River. Using historic maps and aerial photographs, WET (1988, 1990) conducted a geomorphic analysis of more than 100 miles of the Sacramento River in California. Migration rates for specific bends, a bend evolution model, and a bend cutoff index were developed to identify critical sites requiring bank protection and sites where the potential for cutoffs was high (see Section 2.5).

4.4 MAP AND AERIAL PHOTOGRAPHY REQUIREMENTS AND SOURCES

Historical and contemporary aerial photos and maps can be obtained inexpensively from a number of federal, state, and local agencies. Table 4.1 lists some of the main sources. The Internet provides a wealth of sites with links to data resources and sites having searchable databases pertaining to maps and aerial photography. Often, just typing a few keywords relative to aerial photos or maps for a particular site into a search engine will generate a large number of links to related Web sites, which can then be evaluated by the user.

Extensive topographic map coverage of the United States at a variety of scales can be obtained from the local or regional offices of the U.S. Geological Survey (USGS). In general, both aerial photos and maps are required to perform a comprehensive and relatively accurate meander migration assessment. Because the scale of aerial photography is often approx-

imate, contemporary maps are usually needed to accurately determine the true scale of unrectified aerial photos.

Georeferenced and rectified maps and aerial photos are the most desirable for analysis of meander migration, but they can often be expensive to obtain. Presently, aerial photos for the 1990s for most areas of the United States can be obtained from three major sources, the Microsoft TerraServer Web site, the United States Department of Agriculture (USDA) Farm Service Agency, and the USGS (see Table 4.1).

A major public source of aerial photos from the 1990s is the TerraServer Web site operated by Microsoft Corporation. TerraServer, in partnership with the USGS and Compaq, provides free public access to a vast data store of maps and aerial photographs of the United States. Aerial photos and topographic maps at a wide variety of resolutions can be downloaded free of charge from the TerraServer Web site. The advantages of the TerraServer images are that they are rectified, georeferenced, and in digital format so that they are easily

TABLE 4.1   Sources of contemporary and historical aerial photographs and maps

Source	Internet Address	Comments
Microsoft TerraServer—USA	www.terraserver.microsoft.com	Free downloads of contemporary digital topographic and aerial photo files. Operated by Microsoft in conjunction with Compaq and USGS.
USGS EROS Data Center Sioux Falls, South Dakota	For photos go to Photo Finder at edcwww.cr.usgs.gov/Webglis/glisbin/finder_main.pl?dataset_name=NAPP For maps, go to the USGS store at http://store.usgs.gov/	Operated by the USGS. Interactive database search for historic and contemporary topographic maps and aerial photos.
USDA Farm Service Agency Aerial Photography Field Office (FSA—APFO) Salt Lake City, Utah	www.apfo.usda.gov/filmcatalog.html	Operated by the Farm Service Agency. Catalog of historic and contemporary aerial photos for much of the United States. Sources include Soil Conservation Service (SCS) (now called the Natural Resources Conservation Service [NRCS]), the Forest Service, the Bureau of Land Management (BLM), the National Park Service, and other government agencies.
USGS Special Collections Library Denver, Colorado Reston, Virginia	library.usgs.gov/specoll.html	The Field Records Collection is an archive of historic records including maps and aerial photography collected by USGS scientists dating back to 1879. The map collection includes topographic maps for all states dating back to early 1880s.
National Archives and Records Administration (NARA)—Cartographic and Architectural Records Washington D.C.	www.archives.gov	Archive of historic maps and pre-1941 aerial photos.
Western Association of Map Libraries (WAML) San Diego, California	www.waml.org/wmlpubs.html	References to information on obscure historic maps and where they can be found for reproduction.
U.S. Army Corps of Engineers	www.usace.army.mil	Corps districts often have a wealth of historic photos, maps, and survey data.

manipulated by a wide variety of software and can be used in GIS applications. General instructions on downloading TerraServer images can be found in Appendix A. It may be necessary to download a number of higher-resolution map or photo images and splice them together to obtain the amount of detail desired.

For sites where TerraServer photographic coverage from the 1990s is unavailable, aerial photos can be ordered from the USGS Earth Resources Observation Systems (EROS) Data Center in Sioux Falls, South Dakota, or from the USDA Farm Service Agency Aerial Photography Field Office (APFO) in Salt Lake City, Utah. Both agencies have World Wide Web sites (see Table 4.1) with searchable catalogs of available contemporary and historic aerial photography.

Aerial photographs from the EROS Data Center that were flown in the 1980s and 1990s are usually part of the National Aerial Photography Program (NAPP) or the National High Altitude Photography Program (NHAP) and are at scales of 1:40,000 (1 in. = 3,333 ft) or 1:60,000 (1 in. = 5,000 ft). Because of the scale of these photos, small objects may be difficult to see, the resolution of enlarged portions may be poor, and measurements made from the photos may be inaccurate. Historic aerial photos ordered from EROS or APFO range in scale from 1:5,000 to 1:40,000, with most flights having optimal scales of 1:20,000 or 1:24,000. Although both agencies have the ability to enlarge any photo to specification, some resolution is lost with increasing enlargement.

Topographic maps, in paper or electronic format, can be obtained from a variety of sources. Paper copies of topographic maps can be obtained from the USGS or any commercial map supplier. Digital maps (DRGs, DEMs) can be downloaded free from the EROS Web site or purchased from commercial suppliers. Most digital maps are georeferenced and can be loaded directly into GIS-based applications. Portions of georeferenced topographic maps can be downloaded free from the TerraServer Web site and pieced together to form a complete map of a given area or used to fill in gaps. Care should be taken when using digital maps and photos because the georeferenced coordinates and dimensions are usually in metric (SI) units, whereas the contours and spot elevations shown on the maps may be in U.S. customary units.

CHAPTER **5**

MAP AND AERIAL PHOTO COMPARISON TECHNIQUES

5.1 INTRODUCTION

A large number of geographic features and geomorphic planform characteristics used in the evaluation of meander migration are readily discernible on aerial photographs and topographic maps. Thus, a comparison of many of these features and characteristics over time can be made to determine the rate and extent of historic changes and assess potential future changes. The *Handbook* deals with assessments using aerial photos, but the methods described in the *Handbook* can be used when making assessments or measurements from maps.

Bank retreat and meander migration can be physically measured in the field using repeat surveys and erosion pins. However, the most common (or traditional) methods for assessing lateral bank erosion and meander migration use measurements acquired from maps and aerial photographs. Bank retreat and meander migration can be determined in three ways:

- Estimated by visual comparison of two aerial photos taken at different times,
- Measured by scaling distances directly from the bank to common reference points on sequential, historic aerial photographs, and
- Measured on a drawing on which historic channel banklines taken from sequential aerial photos are superimposed at the same scale.

Visual comparison of aerial photos provides a preliminary assessment of stability, especially where significant changes in bank position have occurred. Scaling distances on aerial photos requires making measurements on two photos along a line described by two reference points on each side of the river. The scaling method will usually provide only a few accurate measurements along the bank, depending on the number of reference points and the number of lines that can be drawn across the bend. Additional problems may be associated with the location of the lines because they may not be perpendicular to bank retreat or allow a measurement at the point of maximum retreat. The overlay method is relatively easy and accurate—channel banklines or centerlines from sequential historic aerial photos at a known scale are superimposed on each other and compared. Through this comparison, the rates of bank retreat are determined. Manual overlay techniques are outlined in detail in Sections 5.2 and 7.2.

In addition to the manual overlay techniques, the rate and extent of meander migration can be interpreted from sequential aerial photographs (or maps) using computer-assisted and GIS-based approaches. Computer-assisted techniques are summarized in Sections 5.3 and 7.3. GIS-based measurement and extrapolation techniques are discussed in Section 5.4. The user guides for the GIS-based tools are included in Section 7.4 of the *Handbook,* and the supporting software is included on *CRP-CD-48,* which is provided on the inside back cover of the *Handbook.*

5.2 MANUAL OVERLAY TECHNIQUES

An easy and relatively accurate method of determining migration rates and direction is through the comparison of sequential historical aerial photography, maps, and surveys. Accuracy in such an analysis is greatly dependent on the time intervals over which migration is evaluated, the amount and magnitude of internal and external perturbations forced on the system over time, and the number and quality of sequential aerial photos and maps. Geologic and structural features as well as major changes in watershed characteristics and hydrologic conditions can have a profound effect on meander migration patterns and rates.

An analysis of long-term changes can be useful on a channel that has coverage consisting of data sets (aerial photos, maps, and surveys) that cover multiple time intervals over a long period of time (several decades to more than 100 years). Long-term changes can be documented, and changing migration rates can be evaluated with regard to changes in watershed characteristics and hydrology over time.

If only two or three data sets covering a short time period (several years to a few decades) are available, a short-term analysis may be conducted. A short-term analysis covering recent data can provide information on existing migration rates and conditions.

Predictions of migration for channels that have been extensively modified or have undergone major adjustments attributable to extensive land use changes will be much less reliable than those made for channels in relatively stable watersheds.

The manual overlay technique consists of overlaying channel banklines or centerlines traced from successive historic maps or photos that have been registered to one another on a base map or photo. The first requirement of conducting a simple overlay technique is obtaining the necessary aerial photos and maps for the period of observation. The amount of detail available for analysis increases as the length of time between successive maps or photos decreases. However, a longer period of record for comparison will tend to "average out" anomalies

in the record and provide a better basis for predicting meander migration by extrapolation. Abrupt changes in migration rate and major position shifts can be accounted for by analyzing maps and photos for land use changes, and nearby stream gauge records can be examined for extreme flow events.

Distortion of the image on aerial photos is a common problem and becomes greater with distance away from the center of the photo. Expensive equipment that is needed to rectify and eliminate aerial photo distortion is often unavailable to users of aerial photos, so distortion and scale differences must be accounted for by some other means. Although most photos come with an optimal scale (e.g., 1:20,000), the scale is not always accurate for the purposes of analysis. The scale problem can be overcome through the use of multiple distance measurements taken between reference points on both a photograph and a related base map. Measurements of distance for several reference-point pairs common to both the photo and the map are then averaged to define a relatively accurate approximation of the scale of the photos. Common reference points can include constructed features (such as building corners, roads, fence posts, intersections, and irrigation channels and canals) or natural features (such as isolated rock outcrops, large boulders, trees, drainage intersections, stream confluences, and the irregular boundaries of water bodies). The following relationship is used to determine the scale of the aerial photo relative to the base scale of the base map or photo:

$$\frac{\text{Length Between Aerial Photo Reference Points}}{\text{Length Between Same Reference Points on Base}} \times \frac{\text{Base}}{\text{Scale}} = \frac{\text{Aerial Photo Scale}}{} \qquad (5.1)$$

Once the scale of each historic aerial photo is estimated, the photo will need to be enlarged or reduced to the scale of the base, whether it is another photo or a map. This can be done using a copier with a reduction or enlargement mode or using a flatbed scanner. Copied images are generally difficult to use because of poor tonal quality and resolution, and copiers may stretch the image slightly in the direction of scan. It is often better to trace the bankline or centerline and as many geographic features as possible onto a transparent medium and enlarge or reduce the tracing as necessary. The use of a scanner (many scanners are relatively inexpensive) is advantageous because the resolution of the original photo can be retained, and the photo can easily be used in conjunction with computer-aided design (CAD) or GIS software.

Accurate delineation of a bankline on an aerial photo is dependent primarily on vegetation density at the top of the bank. The bank top is most easily defined if stereopairs of photos are available, but individual photos can also be used when evaluated by experienced personnel. A detailed discussion of the methods for delineating a bankline is provided in Appendix B.

For banks with little or no vegetation, the bank top is easily identified in a photo. The abrupt change between the water and the top of the bank along the outer bank in a bend or an eroding cutbank is defined by a sharp change in the contrast and color (color photo) or gray tone (black and white photo). Usually, the water is significantly darker than the bank top. Along the inner bank of a bend, exposed bar sediment is a lighter color or tone than the river or the bank top. The bank top along a point bar is usually defined by well-established vegetation, such as mature trees and shrubs.

Where vegetation is sporadic along a bank, sections of the bank top may be visible so that the bankline can be interpolated between the visible sections. As vegetation becomes more continuous, the bankline may be completely obscured, and the user may have to locate it by approximation. In this case, it can be assumed that the trunks of the largest trees growing along the edge of the stream are nearly vertical and are located just landward of the bank top. Therefore, a line that approximates the bank top may be drawn just riverward of the center of the crown of the tree. The error involved with this method increases with decreasing stream size because of the relationship of stream size to the crown size of the trees.

If the density of vegetation along a stream is such that an accurate delineation of the bankline cannot be made, then the use of the channel centerline may be required. The centerline is drawn with reference to bankfull conditions. Therefore, the channel centerline will frequently cross exposed point bars. Usually, the channel centerline can be delineated more easily than a bankline masked by vegetation because the centerline can be drawn equidistant from the edge of mature vegetation on either side of the channel. However, the outer bank may still erode relatively rapidly while the position of the channel centerline remains unchanged. This can occur following a flood or where significant widening of the channel occurs.

Once the maps and photos have been enlarged or reduced to a common scale, the common reference points have been identified, the banklines or centerlines have been delineated, and these elements (reference points, banklines, or centerlines) have been traced onto a transparent medium, the banklines or centerlines are superimposed on each other. Once the banklines or centerlines have been superimposed on each other, their positions can then be evaluated with regard to migration distance, rate, and direction over time. Using the information and data obtained from this type of analysis, predictions can be made on the potential position of the river at some point in the future.

5.3 COMPUTER-SUPPORTED TECHNIQUES

Thanks to the availability of powerful computers and photo-editing software, most users of the *Handbook* can perform the photo comparison techniques discussed in the previous section relatively quickly and easily. For example, photo comparison and prediction can take advantage of the photo-editing capabilities in Microsoft Word or PowerPoint. These features were used to develop the illustrative examples provided in Chapters 7 and 8.

In addition, computer-aided design and drawing (CADD) software (such as AutoCAD and Bentley's MicroStation) and

GIS-based software (such as ArcView and ArcInfo) can be used in conjunction with a flatbed scanner and digitizing tablet to perform the photo comparisons with greater precision and accuracy, especially when the maps and photos are georeferenced. When digital files of aerial photos are unavailable, a flatbed scanner can be used to scan aerial photos to a relatively high resolution. Software that can manipulate a photographic image, such as MicroStation Descartes, can be used to warp a scanned aerial photo to fit a map or another resolved aerial photo. A digitizing tablet can be used to record the registration points and bankline positions, as well as other features from historical aerial photos, directly onto a georeferenced drawing, map, or photo.

The photos and banklines can also be georeferenced and the associated data can be saved in a GIS. For example, the bend characteristics and meander migration patterns for more than 1,500 bends on numerous rivers distributed across the continental United States were recorded using a digitizing tablet in conjunction with Bentley's MicroStation as part of NCHRP Project 24-16. The acquired data were used to develop the photogrammetric comparison methods to predict the rate and direction of bend migration presented in Chapters 7 and 8.

5.4 GIS-BASED MEASUREMENT AND EXTRAPOLATION TECHNIQUES

ArcView is a GIS and mapping software package developed by Environmental Systems Research Institute Inc. (ESRI). An ArcView extension, the **Data Logger,** is a GIS-based, menu-driven circle template methodology that was developed for NCHRP Project 24-16 to streamline the measurement and analysis of bend migration data and aid in predicting channel migration. The **Channel Migration Predictor** is another ArcView extension that was developed under NCHRP Project 24-16 using the extrapolation techniques described in Chapters 7 and 8. Both extensions were developed using ArcView Version 3.2.

The predictor tool uses the data archived by the Data Logger in predicting the probable magnitude and direction of bend migration at some specified time in the future. The Data Logger and the Channel Migration Predictor are ArcView extensions that were created using Avenue, a programming language and development environment that is part of the ArcView software package. Avenue is used to create specialized graphical user interfaces and to run scripts that customize the functionality of ArcView.

An ArcView project is a file used to store the work done with ArcView on a particular application, such as recording river bankline data. An ArcView project file contains all the views, tables, charts, themes, and scripts associated with an application.

Both the Data Logger and the Channel Migration Predictor consist of a set of ArcView scripts. A script is the component of an ArcView project that contains Avenue code. Just like macros, procedures, or scripts in other programming or scripting languages, ArcView scripts are used to automate tasks and add new capabilities to ArcView.

The Data Logger provides users with a quick and easy way to gather and archive river planform data. The physical banklines are represented by one or more ArcView themes. A theme is a set of geographic features in a view. A view is an interactive map that allows the user to display, explore, query, and analyze geographic data in ArcView. The bend delineation points for each bend and each historical record are archived in individual themes to provide a graphical record of the user's interpretation of each bend. For each river bend and each historical record, the Data Logger records various river characteristics (e.g., bend radius, bend centroid, river widths, bend wavelength, etc.). These data are organized by river reach and recorded in a table identified by the reach name. These tables provide a permanent record of several river planform characteristics that can be further studied using the Channel Migration Predictor or various statistical procedures.

The Data Logger requires the following steps to be performed at each bend for each historical record:

1. Locate the bankline delineation points on the outside of a river bend,
2. Fit a circle to the bankline demarcation points to describe the radius and orientation of the bend,
3. Use consecutive historical records and the data collected in Steps 1 through 3 to estimate the extension and translation rates for a bend, and
4. Use the migration and extension rates to extrapolate and estimate the future bankline locations.

The Channel Migration Predictor examines a table of river reach data for several bends and two or three historical records per bend and then calculates rates of change in bend radius and bend center position. These rate data allow the Channel Migration Predictor to estimate the location of a bend at user-specified times. As discussed above, river reach data tables can be created using the Data Logger. Users can also create tables for input to the Channel Migration Predictor in the form of properly formatted database files using other means, such as Excel or Avenue.

Instructions on installing the ArcView-based Data Logger and Channel Migration Predictor are provided in Appendix C. The file requirements and user's guides for the Data Logger and the Channel Migration Predictor are provided in Section 7.4. Examples using these tools to conduct the planform measurements and meander migration prediction are provided in Section 8.4.

CHAPTER **6**

SOURCES OF ERROR AND LIMITATIONS

6.1 INTRODUCTION

Factors such as human limitations, instrument imperfections, and instabilities in nature often render measured values inexact. There are many potential sources of error associated with maps and photos used in the comparison techniques and with the method, precision, and accuracy of the measurements. The overlay techniques have their limitations, in part, because of these potential sources of error (Wolf and Dewitt, 2000).

Understanding the occurrence and treatment of errors requires an understanding of the concepts of accuracy and precision. *Accuracy* pertains to the degree of conformity to the true value. The level of accuracy can be assessed by checking against an independent, higher accuracy standard. *Precision* is the degree of refinement of a quantity. Repeated measurements to check the consistency of values are used to assess the level of precision. An *error* is the difference between a particular value and the true or correct value. Most measurements of a continuous physical quantity (such as distance) contain some amount of error (Wolf and Dewitt, 2000).

Errors are categorized as mistakes, systematic errors, and random errors. Mistakes are gross errors caused by carelessness. Mistakes can often be avoided through careful procedures, or they can be detected and eliminated or corrected using quality control checks.

Systematic errors are errors that follow some mathematical or physical law. A correction can be calculated and the systematic error can be eliminated if the conditions causing the error are measured and properly modeled. Shrinkage or expansion of photographs, camera lens distortions, and atmospheric refraction distortions are examples of systematic errors in photogrammetry.

Errors that are not mistakes and systematic errors are random and are dealt with according to the mathematical laws of probability. Random errors are usually small and are often compensated for naturally.

6.2 MAP AND AERIAL PHOTO ERRORS AND LIMITATIONS

6.2.1 Errors

The principal errors associated with aerial photos, and ultimately with maps, are systematic errors. The major sources of these errors are the following:

- Film distortions because of shrinkage, expansion, and lack of flatness;
- Failure of fiducial axes to intersect at the principal point;
- Lens distortion;
- Atmospheric refraction distortions; and
- Earth curvature distortion.

A detailed description of the causes of these sources of error is beyond the scope of the *Handbook,* but such a description can be found in most textbooks on photogrammetry (e.g., Wolf and Dewitt, 2000). Depending on the precision and accuracy requirements of a given project, corrections can be applied to eliminate the effects of these systematic errors.

The primary sources of map error are associated with the vertical and horizontal accuracy and the age of the map. Most federal maps are required to meet rigorous standards for accuracy. The National Map Accuracy Standards, which were issued in 1941, apply to all federal agencies that produce maps. The following is a partial list of the standards of accuracy for published maps defined by the federal government (U.S. Bureau of the Budget, 1941, 1943, 1947 [available at http://geography.usgs.gov/standards/]):

- **Horizontal accuracy.** For maps on publication scales larger than 1:20,000, not more than 10 percent of the points tested shall be in error by more than 1/30 in., measured on the publication scale; for maps on publication scales of 1:20,000 or smaller, 1/50 in. These limits of accuracy shall apply to positions of well-defined points only. Well-defined points are those that are easily visible or recoverable on the ground, such as the following: monuments or markers, such as bench marks, property boundary monuments; intersections of roads and railroads, etc.; corners of large buildings or structures (or center points of small buildings); etc. In general what is well-defined will be determined by what is plottable on the scale of the map within 1/100 in. Thus while the intersection of two road or property lines meeting at right angles would come within a sensible interpretation, identification of the intersection of such lines meeting at an acute angle would obviously not be practicable within 1/100 in. Similarly, features not identifiable upon the ground within close limits are not to be considered as test points within the limits quoted, even though their positions may be scaled closely

upon the map. In this class would come timber lines and soil boundaries, etc.

- **Vertical accuracy,** as applied to contour maps on all publication scales, shall be such that not more than 10 percent of the elevations tested shall be in error more than one-half the contour interval. In checking elevations taken from the map, the apparent vertical error may be decreased by assuming a horizontal displacement within the permissible horizontal error for a map of that scale.
- **The accuracy of any map may be tested** by comparing the positions of points whose locations or elevations are shown upon it with corresponding positions as determined by surveys of a higher accuracy. Tests shall be made by the producing agency, which shall also determine which of its maps are to be tested, and the extent of the testing.

Although the federal standards for accuracy may seem reasonable, the accuracy of topographic maps may be insufficient or problematic when using the comparison techniques for defining and predicting meander migration. For example, if the potential horizontal error of the topographic map used in the comparison is a significant percentage of the actual channel width, then there could be a substantial discrepancy between the mapped bankline position and the true bankline position for the same time period and between time periods. The map error may also be problematic if comparisons are made with historic survey data.

Comparison of newer maps and aerial photos with older maps may also pose a problem because the older maps may have been compiled before the use of aerial photos. These maps are based on physical ground surveys, field notes, surveyor descriptions, and sketches made in the field. Therefore, the accuracy of historic maps decreases with increasing age.

Maps that are georeferenced may not match the positions of georeferenced aerial photos. This can occur if georeferenced digital maps are obtained from sources other than the USGS and used in conjunction with georeferenced digital aerial photographs compiled by the USGS or other agencies. The authors of the *Handbook* have encountered this problem many times.

There may also be problems associated with the use of different horizontal "datums." A datum is a system of reference using precisely surveyed control monuments to specify the relative positions of points used for surveying and mapping purposes. The most common horizontal datums used in the United States are the North American Datum of 1927 (NAD27), the North American Datum of 1983 (NAD83), the World Geodetic System of 1984 (WGS84), various statewide high-accuracy reference networks (HARNs), and the International Terrestrial Reference Framework (ITRF). In addition, the U.S. Army Corps of Engineers, local levee districts, and other state and local agencies may have different datums. Therefore, comparisons of maps, aerial photos, and survey data from different sources should be evaluated for different datums. Transformations from one datum to another have become commonplace with the increasing use of GISs. Software (NADCON) to convert NAD27 to NAD83 is readily available from the National Geodetic Survey via the World Wide Web (http://www.ngs.noaa.gov).

6.2.2 Limitations

There are several potential limitations to the use of aerial photos and maps in the comparison techniques and in the evaluation of meander migration. Scale can be a significant limitation to the use of aerial photos and maps. There are potential problems associated with major scale differences between maps and photos and changes in scale on a given photograph because of distortion across the photo. In some cases, only high-altitude aerial photographs (scales of 1:40,000 or 1:60,000) may be available for a particular site. A comparison of bankline positions from high-altitude photos with those from topographic maps may be difficult because of the significant scale difference. In some cases, an enlargement of the aerial photo may provide an image of sufficient resolution or clarity to be used in the comparison. However, this is also dependent on the relative size of the channel with regard to the scale at which it is being evaluated.

Often, the enlargement of high-altitude photos using a copier or a flatbed scanner in conjunction with photo-editing software yields images with poor resolution. Even though an aerial photo can be scanned at a high resolution, the quality of the resolution and the amount of visible detail is greatly dependent on the original image quality and clarity. Moreover, the quality of an enlarged scanned image degrades rapidly after the image has been enlarged to more than two or three times its original size. The resolution of an older aerial photograph will generally be lower than the resolution of a newer aerial photograph because of changes in technology over time. In contrast, digital images such as those found on the TerraServer Web site can be downloaded at various scales and resolutions.

Brightness and contrast also play a role in the usability of an aerial photo. Photos can be too dark or too light, and the contrast may be so coarse that the banklines of a channel may be difficult or impossible to identify. The time of the year or the time of day during which the aerial photo is taken is also important and can affect the usability of a photo. Long shadows, dense vegetation, and cloud coverage may partially or totally obscure the bankline or the entire channel. Aerial photos that were taken at midday and during winter months with little cloud coverage are optimal. Photos taken during early spring, prior to leaf-out, may be useful, but spring floods may obscure the tops of the banks. Photos taken during summer months can be used if the density of the bankline vegetation is sparse enough to allow the user to adequately define the bankline. Otherwise, bankline positions will need to be estimated based on the locations of the crowns of the trees growing at the bankline, as described in Section 5.2. In this case, the accuracy of the measurements is questionable.

The age of an aerial photo and map may also limit their usefulness. Old maps and photos may not have the same

identifiable geographic features or landmarks found on newer maps and photos, so finding identifiable landmarks that can be used as registration points may be difficult. In addition, the township, range, and section lines found on newer topographic maps, whose intersections could be used as registration points, may not be in the same location or may not be available on older maps.

6.3 MEASUREMENT ERROR

As with any methodology that requires the physical measurement of a quantity, the accuracy and precision of the measurements conducted under the comparison techniques described in the *Handbook* can limit the usefulness of the acquired data. Obviously, those measurements made visually using a ruler or engineering scale will be less accurate than those made using a computer. Also, repeated measurements should be made the same way each time.

Scale plays an important role in measurement error as well. Large-scale images (e.g., 1:10,000) show ground features at a larger, more detailed size, and small-scale images (e.g., 1:50,000) show ground features at a smaller, less detailed size. Thus, using identical measurement techniques, measurements made on large-scale maps and photos generally will be more accurate than those made on smaller-scale maps and photos.

Meander bends are rarely perfectly round with smooth banklines. They often are oddly shaped, and their banklines are irregular. As a result, fitting a circle to the channel centerline or outer bank can be very difficult. As a rule, the circle should be fit to the bend centerline or outer bankline between the crossings or at the point where the bend begins to straighten or where there is a major inflection in the channel. As much of the circle as possible should intersect the bankline or centerline, and the amount of area outside the circle should match the amount of area inside the circle as closely as possible. The radius of curvature of a bend centerline or bankline can be significantly different depending on how the circle is fit to the bend, especially on smaller channels. Defining meander bends with best-fit circles is discussed in greater detail in Chapter 7 and Appendix B.

6.4 LIMITATIONS OF OVERLAY TECHNIQUES

Overlay techniques require the availability of adequate maps and aerial photos that cover a sufficient period of time to be useful. Another requirement is the ability to identify and delineate a sufficient number of registration points common to each map and photo. It is not necessary to find all the registration points on all the maps and photos, but an adequate number of registration points identified on each map or photo should match those on the previous or following map or photo. The registration points should bracket the area of interest (this would require at least four common registration points) and should not change significantly in size over time. Even when a sufficient number of registration points are available, photo distortions or inaccuracies in mapping may not allow for an accurate registration of the images. In these cases, the user will need to decide whether "close" is good enough or if the image should be abandoned.

Excessive or very limited movement of the channel, cutoffs, and bank erosion countermeasures will also limit the usefulness of the comparison techniques. An analysis of the rate and extent of historical movement may be useless if excessive meander migration is a problem (as with meander Class F in Figure 3.2). Depending on the scale of the overlays, the amount of migration may be so small as to be undetectable, or the overlays may be at such a small scale that the movement is not measurable.

Countermeasures to halt bank erosion or protect a physical feature within the floodplain can also have an impact on the usefulness of the overlays. These features should be identified prior to developing the overlays. Anomalous changes in the bend or bankline configuration or a major reduction in migration rates may suggest that bank protection is present, especially in areas where the bankline is not completely visible or on images with poor resolution.

Geologic features in the floodplain, such as clay plugs or rock outcrops, can also limit the usefulness of the overlays because they can have a significant influence on migration patterns. Bends can become distorted as they impinge on these features, and localized bankline erosion rates may decrease significantly as these erosion resistant features become exposed in the bank. Where the channel encounters a geologic control or man-made feature, the channel may intersect the feature at a sharp or abrupt angle and migrate more rapidly down valley along the feature, or the channel may become highly distorted. An example of this might be where a channel encounters geologic controls, bank protection, or levees that run parallel to the valley direction.

In some cases, the channel may encounter a very localized outcrop or hard point in the bank creating an irregular bankline or causing the bend to deform around it. In these cases, determining the radius of the outside bankline of a bend may be very difficult. Because any evaluation of meander migration requires an assessment of, among other things, changes in bend radius, the user will need to use judgment in determining the radius of the bend, and possibly the bankline, by defining it with a best-fit circle of known radius (see Section 7.2).

Where the channel makes a sharp or abrupt turn, mud flats or bars may develop along the outer bank in the upstream half of the bend, and the delineation of the outer bankline on a photo or map may be difficult at best. In this case, there are two methods of defining an approximate outer bankline radius. The first method is to identify the radius of the inner bankline by inscribing a best-fit circle on it and then determining the average channel width at the crossings in the reach. Then, the user can add 1.5 to 2 average channel widths to the inner bankline circle to define the outer bankline radius. Once this is accomplished, the user will need to evaluate how well the estimated outer bankline fits relative to the actual channel position, to similar bends that may be located in the reach, and to other features along the channel at the bend.

The second method requires the use of the edge of water at the outer bankline of the channel on the photo or map. This should provide a relatively close approximation of the outer bankline radius of curvature. Although both of these methods can contain significant error, they may provide the only reasonable approximation of the outer bankline and radius of curvature necessary to make a prediction of future bankline position.

In reaches where geologic controls are exposed predominantly in the bed of the channel, migration rates may increase dramatically because the channel bed is not adjustable, which may cause the channel to migrate rapidly across the feature. A fundamental assumption of the overlay techniques based on aerial photo or map comparison is that a time period sufficient to "average out" such anomalies will be available, making the historic meander rates a reasonable key to the future.

CHAPTER **7**

METHODOLOGY

7.1 INTRODUCTION

This chapter defines the steps necessary to conduct a detailed meander migration analysis. The first method (Section 7.2) describes a manual overlay of historic maps and aerial photos for comparative purposes and applies the acquired data and information to predict the position of a bend in the future. The next method (Section 7.3) describes how certain types of common computer software can be used to assist in the historic assessment and prediction of bend migration. The last method (Section 7.4) describes the procedures necessary to use the Data Logger and Channel Migration Predictor software supplied with the *Handbook* to conduct the comparison and prediction steps.

Care should be taken when using the following methodologies in areas where geologic features, structures, erosion control measures, and other "hardening" features may influence the characteristics of meander migration (see Section 6.4).

7.2 MANUAL OVERLAY AND PREDICTION

The following steps provide direction in conducting a simple overlay comparison of historic banklines and making predictions on the potential future position of a bend based on the past channel migration characteristics.

Step 1. The first step in conducting a meander migration analysis using an overlay technique is to obtain aerial photographs and maps for the study area, as described in Section 4.4. Appendix A also provides general instructions on downloading digital aerial photographs and topographic maps from Microsoft's TerraServer Web site.

Step 2. The maps and photos must be enlarged or reduced to a common working scale, as described in Section 5.2. The scale of the most recent map or photo should be used because it will be the basis for comparing historical meander pattern changes and predicting the position of a given bend in the future.

Step 3. After a working scale is defined, the photos and maps are registered to a common base map or photo by identifying several features or points that are common to each photo/map being compared. The registration points of a map or photo do not need to be common to all the maps and photos, only to the subsequent map or photo to which it is being compared, because comparisons can be performed in pairs.

For example, Figures 7.1 and 7.2 show the 1937 and 1966 aerial photos, respectively, for a reach of the White River in Indiana. Four registration points have been identified on the 1937 photo that are also on the 1966 photo. Two registration points are road intersections and two are isolated vegetation (trees or large shrubs). Registration points that bracket the site on both sides of the stream and at both ends of the reach are most useful because they reduce the amount of potential error within the bracketed area. Intermediate points between the end points are helpful in accurately registering the middle sections of the reach. More than five or six registration points can make registration difficult because of the difficulty in aligning all the registration points among the various aerial photos and maps used. However, there will be cases in which there will be very few identifiable common registration points, and these cases may have the potential for significant error.

Step 4. After the registration points are identified, banklines and registration points for each year are traced from the aerial photo onto a transparent overlay. The method for identifying and tracing the banklines is described in Chapter 5 and Appendix B. Registration points are included on the overlay so that they can be easily plotted onto other aerial photos or maps for comparative purposes. The traced banklines and registration points of the White River for 1937 are plotted on the 1966 aerial photo in Figure 7.3 for comparative purposes.

Because most meander bends are not simple loops, the loop classification of Brice (1975) can be used to characterize the shape of each bend that is to be analyzed (see Figure 7.4). Meander bends seldom form single symmetrical loops, but instead are composed of one or more arcs combined to form either symmetrical or asymmetrical loops. Brice (1975) derived the classification scheme for meander loops from a study of the meandering patterns of 125 alluvial streams. The scheme consists of four main categories of loops (simple, compound, symmetrical, and asymmetrical) comprising 16 form types. Although compound loops are regarded as aberrant forms of indefinite radius and length, the meandering patterns can be divided into simple loops whose properties can be described, measured, and analyzed. The radius of curvature of most bends can be defined by fitting one or more circles or arcs to the bend centerline or outer bankline of a meander loop.

The number of loops that describe a bend does not always remain constant as a bend evolves. For example, a bend at Time 1 may be defined by two loops, but as it evolves to Time 2 or Time 3, the bend may become a single loop. In this case, the bends from Time 1 and Time 2 should also be delineated by a single loop when conducting the meander migration
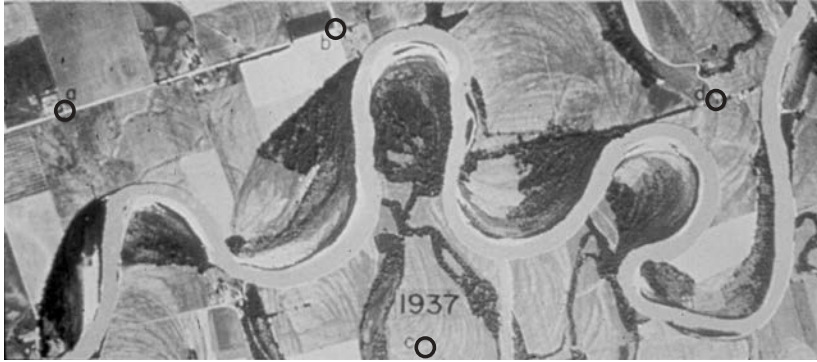
Figure 7.1.   Aerial photograph of a site on the White River in Indiana showing four registration points (circles designated a through d) common to the 1966 aerial photo.
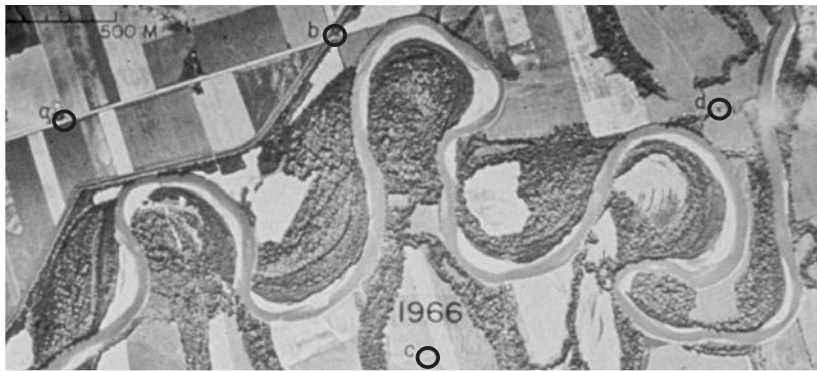

Figure 7.2.   Aerial photo of a site on the White River in Indiana showing the four registration points common to the 1937 aerial photo in Figure 7.1.
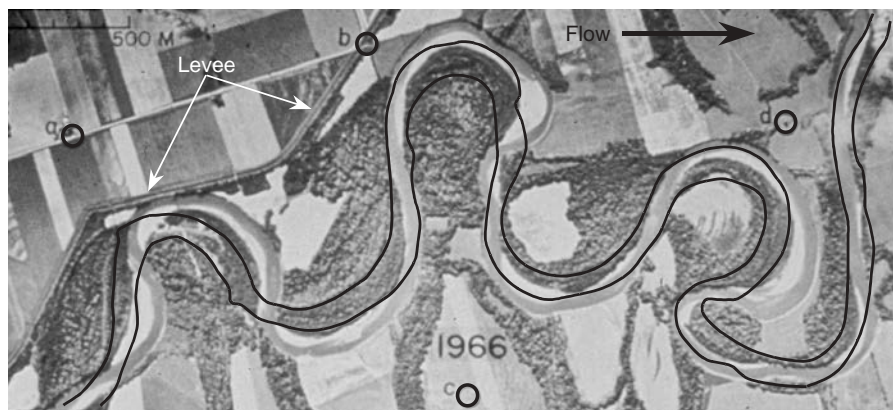

Figure 7.3.   The 1966 aerial photo of the White River in Indiana with the 1937 bankline tracing and registration points.

analysis. The opposite case may also occur, in which the final bend is a double-headed bend (Figure 7.4-H, -I, -M, -N, and -O). In this case, an attempt should be made to delineate the Time 1 and Time 2 bends by two loops in similar positions as the Time 3 loops.

Step 5. Once the banklines for each of the historic aerial photos have been traced, circles are best-fit to the outer bank of each bend to define the average bankline arc, the radius of curvature (R_C) of the bend, and the bend centroid position (see Figure 7.5). The number of circles required to define the bend is based on the loop classification described above and shown in Figure 7.4. A detailed description of the method used to fit a circle to the outer bankline of a meander bend is provided in Appendix B. The radius of curvature and centroid position of the circle used to describe the bend will be
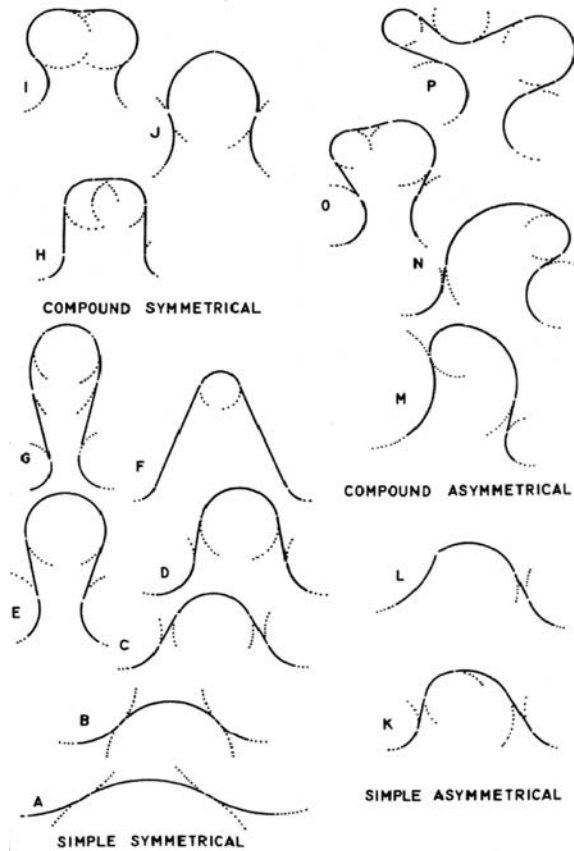
SOURCE: Brice, 1975

Figure 7.4.   Meander loop evolution and classification scheme proposed by Brice (1975). Flow is left to right.

used to make a comparison with the bend measurements of previous and subsequent years. These measurements can then be used to determine migration rates and direction and estimate future bend migration characteristics.

Figure 7.6 compares the best-fit circles and bend centroids for each bend traced from the aerial photographs for 1937

and 1966. The vector arrow at each bend shows the direction and magnitude of movement of the bend centroid between 1937 and 1966. For each bend, this vector may be resolved into cross- and down-valley components to determine the rates of meander migration. The change in radius of curvature of each bend is defined by the difference between the magnitudes of the vectors for 1937 and 1966.

Step 6. The position of the bend at a selected date in the future can be predicted by simple extrapolation if it is assumed that the bend will continue to move at the same rate and in approximately the same direction as it has in the past. To estimate the position of a bend centroid in 1998, for example, the distance the centroid would be expected to move during the 32 years between 1966 and 1998 can be determined by multiplying the annual rate of movement for the 1937-to-1966 period by 32. This distance is plotted along a line starting at the 1966 centroid point and extending in the direction defined by the 1937-to-1966 migration vector. The radius of curvature of the bend in 1998 can be defined by determining the rate of change of the bend radius from 1937 to 1966 as a percentage relative to the 1966 radius and multiplying this value by number of years from 1966 to 1998. A circle with that radius, centered on the predicted location of the centroid, is plotted on the tracing to indicate the expected location and radius of the bend in 1998.

Figure 7.7 shows the expected outer bank circles for each of the bends of the White River in 1998, based on simple extrapolation of the rates and directions of change from 1937 to 1966. Banklines for the 1998 channel can then be constructed on the tracing by joining the outer bank circles through interpolation, with the 1937 and 1966 banklines used to indicate the reach-scale configuration of the channel.

Figure 7.8 shows the 1966 aerial photo overlaid with the banklines observed in 1937 and estimated for 1998. Inspection of the estimated banklines reveals that Bend 1 would encroach into the levee to the north by 1998, while growth of Bend 5 would likely cut off Bends 6 and 7.
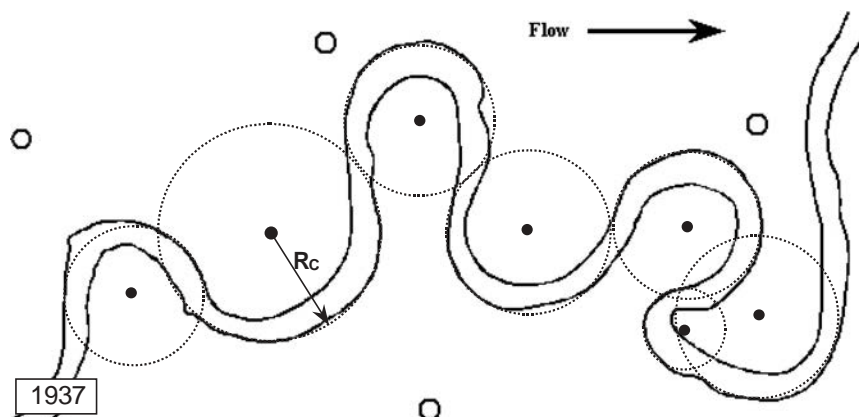
Figure 7.5.   Inscribed circles that define the average outer banklines from the 1937 aerial photo of the White River site in Indiana. Also shown are the bend centroids and the radius of curvature (R_C) for one of the bends.
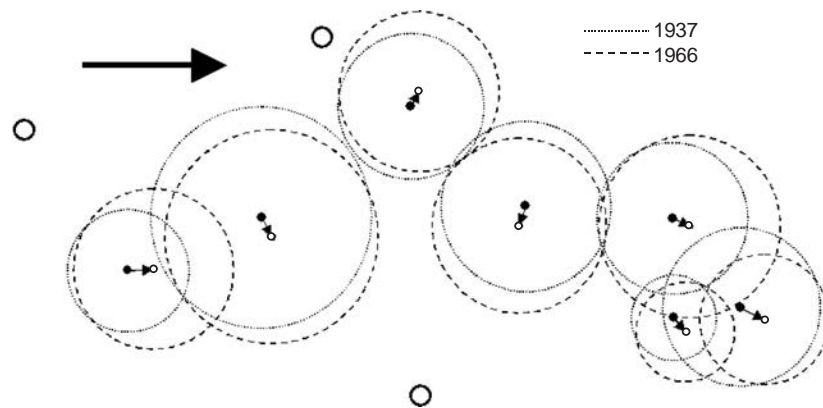
Figure 7.6.   Depiction of the bends from the 1937 and 1966 outer banklines as defined by best-fit circles. The movement of the bend centroids (arrows) defines migration of the bends.
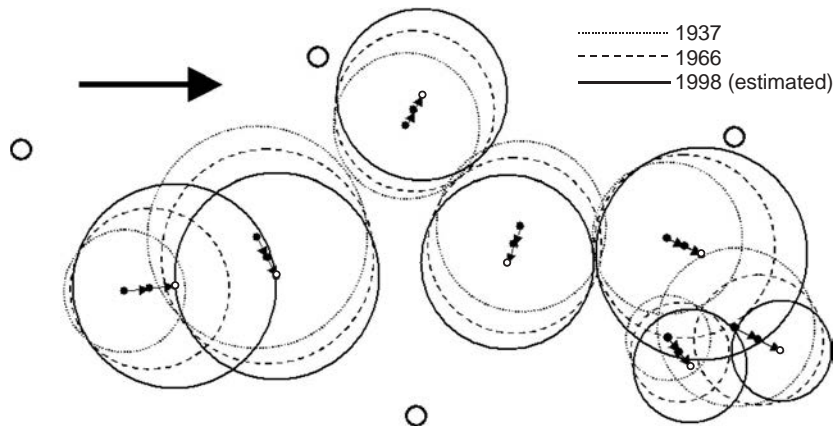

Figure 7.7.   Depiction of the bends from the 1937 and 1966 outer banklines, as defined by best-fit circles, and the predicted location and radius of the 1998 outer bankline circle.
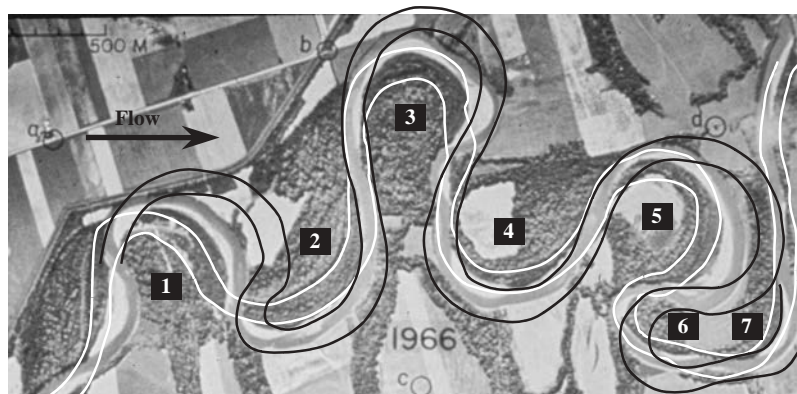

Figure 7.8.   Aerial photo of the White River in 1966 showing the actual 1937 banklines (white) and the predicted 1998 bankline positions (black).

In Figure 7.9, the banklines predicted for 1998 by extrapolation of trends of change between 1937 and 1966 are superimposed on an aerial photograph taken in 1998. Two of the registration points used for this comparison are different because two of the original registration points from the previous aerial photos are no longer present on the 1998 aerial photo.

Comparison of the actual and estimated banklines illustrates that meander migration can be predicted relatively accurately using this simple approach. For example, the positions of Bends 3 and 4 and the cutoff at Bend 5 are accurately predicted. Errors in the predicted banklines can be accounted for by (1) an artificial cutoff that affected Bends 1 and 2, (2) the natural cutoff at Bend 5 that led to Bends 6 and 7 being abandoned, and (3) construction of bank protection at Bends 3 and 5 during the period of 1966 to 1995. The artificial cutoff at Bend 1 may have been in response to the serious threat posed by bend migration toward the nearby levee. That cutoff caused Bend 2 to distort in a way that could not have been predicted from its previous behavior. Outer bank migration at Bends 3 and 5 appears to have been curtailed by bank revetments. The migration of Bends 3, 4, and 5, the cutoff of Bend 5, and the abandonment of Bends 6 and 7 were predicted reasonably well. It is likely that the positions of Bends 1 and 2, as well as the banklines in the revetted portions of Bends 3 and 4, would have been as predicted except for these engineering interventions.

The case study of the White River used a single period (1937 to 1966) to predict the position of the banklines in 1998. To improve the reliability and accuracy of predictions, it may be desirable to use multiple pairs of aerial photographs to generate more than one period of analysis. Through evaluating multiple periods, meander migration analysis can detect trends of change in the rate and direction of bend migration as well as time-averaged values.

For example, the channel positions and circles inscribed on the outer banklines for a hypothetical channel in Years 1, 2, and 3 are shown in Figure 7.10. To predict the amount and direction of migration of a bend at some future date, the amount and direction of migration for previous periods must first be determined.

Figure 7.11 shows the best-fit circles for the outer bank positions in Years 1, 2, and 3; the outer bank radius of curvature for each year (R_{C1}, R_{C2}, and R_{C3}); the angle defined by the change in direction of the bend centroid for each time period (θ_A and θ_B); and the amount of migration of the bend centroid (D_A and D_B). The subscripts A and B refer to Period A (Year 1 to Year 2) and Period B (Year 2 to Year 3), respectively. The aim is to predict the bankline position in Year 4 at the end of Period C (Year 3 to Year 4).

The rate of change of the radius of curvature for the outer bank during Period A (Year 1 to Year 2) is defined by

$$\Delta R_{CA} = (R_{C2} - R_{C1})/Y_A \qquad (7.1)$$

where

ΔR_{CA} = Rate of change in radius of curvature during Period A (ft/yr or m/yr),
R_{C1} = Radius of curvature of outer bank in Year 1 (ft or m),
R_{C2} = Radius of curvature of outer bank in Year 2 (ft or m), and
Y_A = Number of years in Period A.

The rate of change of the radius of curvature for the outer bank during Period B (Year 2 to Year 3) is defined by

$$\Delta R_{CB} = (R_{C3} - R_{C2})/Y_B \qquad (7.2)$$

where

ΔR_{CB} = Rate of change in radius of curvature during Period B (ft/yr or m/yr),
R_{C2} = Radius of curvature of outer bank in Year 2 (ft or m),
R_{C3} = Radius of curvature of outer bank in Year 3 (ft or m), and
Y_B = Number of years in Period B.

To predict the rate of change of the radius of curvature for the outer bank during Period C (Year 3 to Year 4), it is neces-
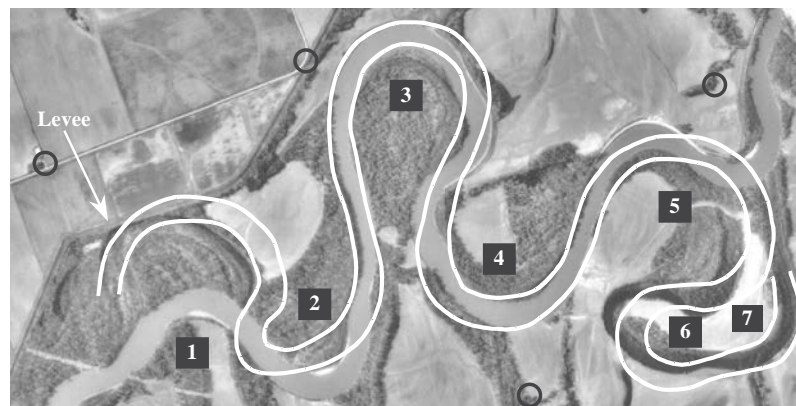

Figure 7.9. Aerial photograph of the White River site in Indiana in 1998 comparing the predicted bankline positions with the actual banklines.
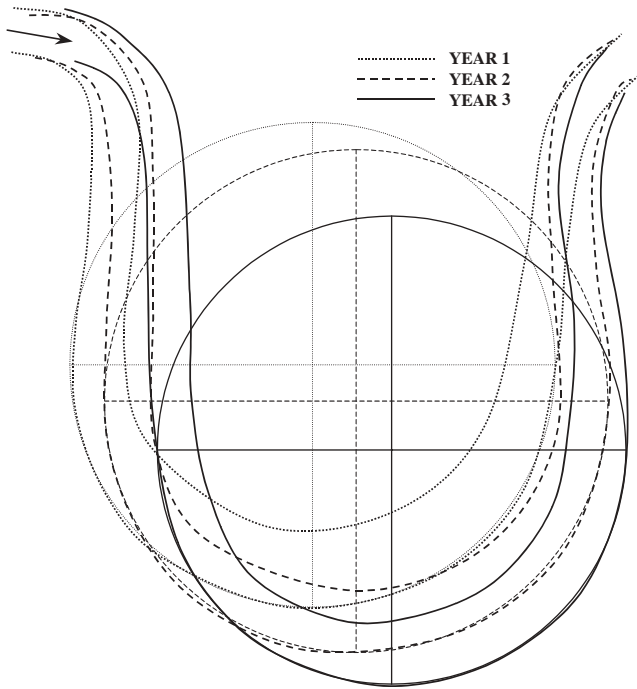
Figure 7.10.   Banklines and circles drawn along outer bankline positions for a hypothetical channel in 3 different years.

sary to decide if the long-term average or the most recent rate will be used. A long-term average rate of change of the radius of curvature is based on the entire period of record, which may be influenced by changes in land use, basin hydrology, or channel modifications. In addition, periods of bend expansion or contraction within the period of record can yield an anom-
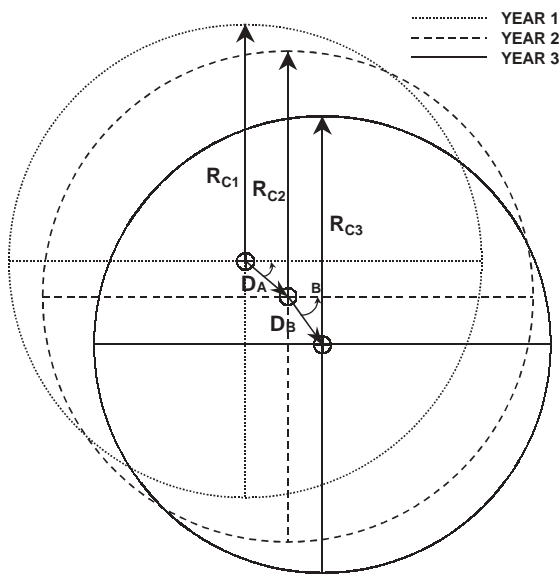

Figure 7.11.   Diagram defining the outer bank radius of curvature in Years 1, 2, and 3 (R_{C1}, R_{C2}, and R_{C3}) and the amount (D_A and D_B) and direction (θ_A and θ_B) of migration of the bend centroid during Periods A and B.

alous rate. Because of problems inherent in using a long-term average rate of change, it is recommended that the most recent rate, the rate of change for the previous period (Period B in this case), be used because it is more closely related to existing conditions and processes. Hence, the predicted radius of curvature of the outer bank in Year 4 is defined by

$$R_{C4} = R_{C3} + \left[\left(\frac{(R_{C3} - R_{C2})}{(Y_B)}\right)(Y_C)\right] \tag{7.3}$$

where

R_{C4} = Predicted radius of curvature in Year 4 (ft or m),
R_{C3} = Radius of curvature of outer bank in Year 3 (ft or m),
R_{C2} = Radius of curvature of outer bank in Year 2 (ft or m),
Y_B = Number of years in Period B, and
Y_C = Number of years in Period C.

Judgment should also be used to evaluate the reasonableness of the predicted radius; the predicted radius should not be significantly smaller than the average radius of small bends within the reach. Another method of determining whether the predicted radius is reasonable is to determine the ratio of the predicted bend radius to the average channel width of the reach. If the ratio falls below 2, it is likely that the bend may cut off or become distorted prior to reaching Year 4.

The angle of migration of the centroid (θ) of the circle that inscribes the outer bank and the amount of migration of the centroid (D) for each period are shown in Figure 7.11. There are two methods of defining the angle of bend migration for Period C. The first is to simply use the same migration angle for Period B (e.g., $\theta_C = \theta_B$). Using the migration angle from the previous period (i.e., Period B) is recommended where geomorphic and hydrologic conditions have not changed significantly. The second method uses the rate of change of the migration angle from the previous period to define the rate of change for the period being predicted such that:

$$\theta_C = \left[\left(\frac{(\theta_B - \theta_A)}{Y_B}\right)(Y_C)\right] + \theta_B \tag{7.4}$$

where

θ_C = Predicted angle of outer bank migration for Period C,
θ_A = Angle of outer bank migration for Period A,
θ_B = Angle of outer bank migration for Period B,
Y_B = Number of years in Period B, and
Y_C = Number of years in Period C.

The second method can be used where geomorphic, hydrologic, and hydraulic conditions have changed significantly. It is recommended that both methods be used and compared for reasonableness. Again, judgment should be used to evaluate the reasonableness of the predicted migration angle with respect to the general alignment of the bends or reaches immediately upstream and downstream. This is particularly important in reaches that may contain features such

as revetment, bridges, and levees that can have a significant influence on meander migration.

The amount of migration of the bend centroid for Period A is D_A, and for Period B it is D_B. The rates of migration during Periods A and B are determined by dividing D_A and D_B by the number of years in the associated period. To predict the magnitude of centroid migration during Period C, it is more accurate to use the most recent Period B rate of centroid shift, which yields the following relationship:

$$D_C = (D_B/Y_B)Y_C \qquad (7.5)$$

where

D_C = Magnitude of centroid migration for Period C (ft or m),
D_B = Magnitude of centroid migration for Period B (ft or m),
Y_B = Number of years in Period B, and
Y_C = Number of years in Period C.

The centroid, radius of curvature, and predicted position of the circle that inscribes the outer bank in Year 4 are shown in Figure 7.12. Figure 7.13 shows an interpretation of the predicted banklines for Year 4 based on the average channel width of the bend from previous periods.

Using a CAD software package will serve to reduce the number of steps in this procedure and also provide more accurate answers for the prediction. The use of a CAD software package involves only two steps, and no change in scale takes place. The user can import a digital image into the CAD program with a given scale; trace the stream banklines; and delineate various features, such as the bend centroid location and the bend radius of curvature. From this CAD file, the user can import the traced banklines into the meander migration

Figure 7.13.   Predicted bankline position of the hypothetical channel in Year 4.

prediction routine described in the next section, measure the various features required by the routine, and use the measured data to predict the location of the bend at some point in the future.

7.3 COMPUTER-ASSISTED METHODOLOGY

The methods described in the previous section can be conducted more easily and efficiently using common computer software such as Microsoft PowerPoint and Jasc's Paint Shop Pro or more powerful and versatile programs like Autodesk's AutoCAD and Bentley's MicroStation.

The photo-editing capabilities of Microsoft Word and PowerPoint were used to perform the comparison and prediction in the previous examples. In Word and PowerPoint, an aerial photo in the form of a JPEG or TIFF file, for example, can be imported into the software using the "Insert> Picture>From File" commands on the main menu.

Right clicking on the main menu area pulls up a list of available toolbars, including the "Picture" and "Drawing" toolbars. The "Picture" toolbar is used to change the attributes of the picture, and the "Drawing" toolbar allows the user to mark the registration points and trace a line for the banklines using the "Autoshapes>Lines" or "Autoshapes>Basic Shapes" commands.

Once the registration points and banklines for each aerial photo have been drawn, they should be grouped using the "Grouping" tool. This enables the user to move all the items together to another picture for comparative purposes. After

Figure 7.12.   Predicted position and radius of curvature of the circle that defines the outer bank of the hypothetical channel in Year 4.

the group of registration points and banklines associated with one aerial photo has been superimposed onto the second aerial photo, the group can be correctly registered on that photo by resizing and rotating the group using the "Format Picture> Size" and "Format Picture>Rotate" tools. Right clicking on the picture accesses these tools.

Although the scale of the aerial photos is not provided by some graphics-editing software, the scale can be found by comparing distances between several points on the photos with measurements between the same points on a map or photo with a known scale. This allows use of the prediction portion of the comparison technique described in the previous section by defining the change in bend radius of curvature and the direction of migration of the bend centroid. The user can then derive and plot the predicted radius and position of the best-fit circle (Figure 7.7) and interpret the future bankline position using the shape of the channel in previous photos (Figure 7.8). The prediction of the 1998 banklines for the White River shown in Figure 7.8 and the analysis leading up to the prediction were completed using the Microsoft PowerPoint tools described above.

7.4 DATA LOGGER AND CHANNEL MIGRATION PREDICTOR

The Data Logger and Channel Migration Predictor are GIS-based, menu-driven ArcView extensions. These extensions were developed to assist in the measurement and analysis of bend migration data and aid in predicting channel migration (see Section 5.4 for basic description).

The Data Logger and Channel Migration Predictor software are included on *CRP-CD-48,* provided at the back of the *Handbook,* and instructions for installing the Data

Logger and Channel Migration Predictor are provided in Appendix C. Tips for delineating and registering banklines from historic aerial photos that are not georeferenced for use with the Channel Migration Predictor are provided in Appendix D.

7.4.1 Data Logger Bankline File Requirements

Users of ArcView can choose from a variety of file types for importing visual representations of banklines into the Data Logger. Supported CAD file formats include MicroStation design (.dgn) files and two kinds of AutoCAD drawing files (.dwg and .dxf). ArcView supports 16 image file formats, including JPEG and TIFF. Digital elevation maps (DEMs) and Triangular Irregular Network (TIN) representations of terrain data can also be used to represent river banklines.

7.4.2 Data Logger Users Guide

Prior to starting the Data Logger, the historic banklines for a given study site need to be digitized and saved. The set of banklines is defined here as a theme, which is just a set of geographic features in a view.

Step 1. Start ArcView and add a theme containing (either two or three) historical channel banklines for a selected reach. Figure 7.14 is an example of a theme with two historical bankline records.

Step 2. Clicking the green diamond, located at the top right of the ArcView button panel (Figure 7.14), launches the "Reach Data" dialog box (see Figure 7.15) of the Data Logger.
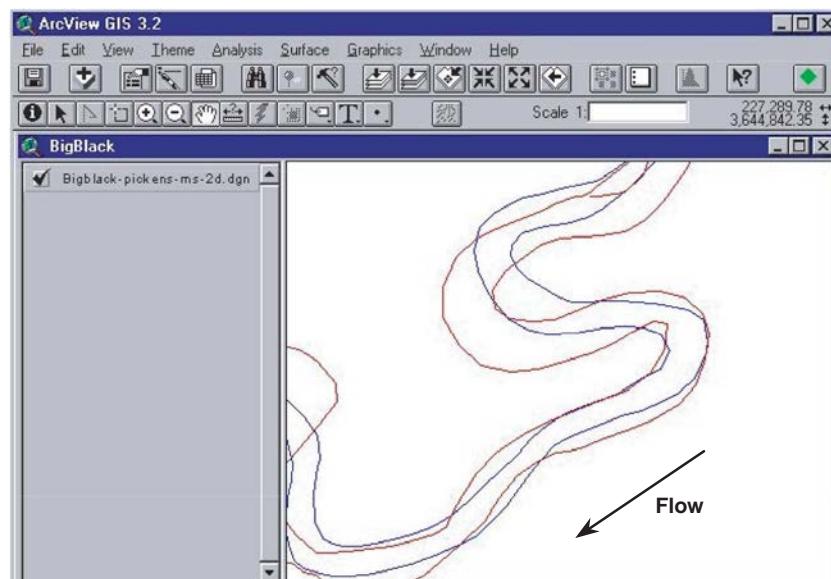

Figure 7.14.   ArcView project with a theme showing two historical bankline records.

Figure 7.15.   "Reach Data" dialog box of the Data Logger.

At this point, the user provides information about the particular reach or sub-reach under consideration.

The "Reach Data" dialog box enables the user to quickly enter information about a particular reach or sub-reach. For convenience, a reach with a large number of bends can be broken into sub-reaches to facilitate a modular approach to data archiving. For example, as indicated in Figure 7.14, the first sub-reach has been chosen to contain three bends. If the next sub-reach has five bends, then the next time the Reach Data dialog box is displayed, the user should enter 5 for the "Number of Bends" and 4 for the "First Bend Number."

It is important that the name entered in "View File Name" form ("BigBlack" in Figure 7.15) be an exact match of the name of the view containing the historical bankline contours ("BigBlack" in Figure 7.14). Also the dates associated with historical banklines must be entered in the "m/d/yyyy" form illustrated in Figure 7.15. The Channel Migration Predictor extension will use these date objects to calculate migration rates and extrapolate bankline positions.

After filling in the various text boxes in the "Reach Data" dialog box, the user then clicks on the "Create Data File" button. The "Create Data File" button launches three ArcView Avenue scripts.

The first script defines one theme for each year and each bend for the archiving of bankline registration points. This script also adds these bend-year registration point themes to the ArcView project shown in Figure 7.14. Figure 7.16 shows the ArcView project with the six new themes added to the view "BigBlack."
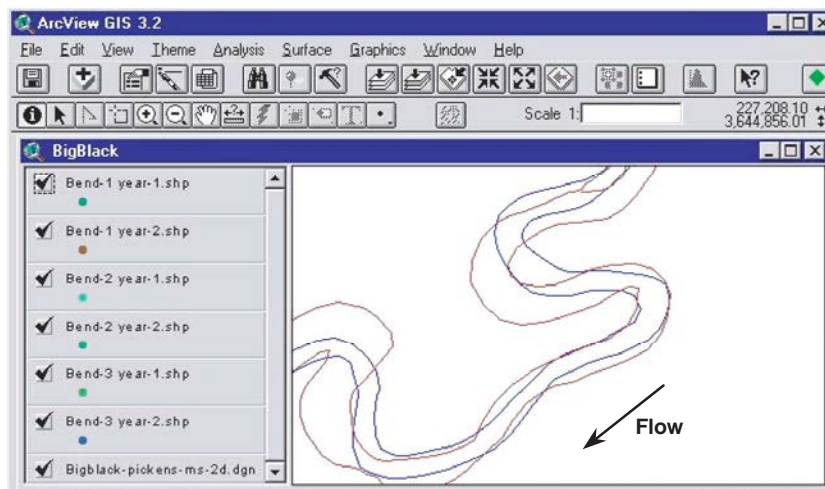
Figure 7.16.   Themes to store the bend registration points have been added to the ArcView project.

The second script prompts the user for a file name in which the Virtual Table (VTab) for this sub-reach is to be stored (see Figure 7.17). This script also formats the VTab to have one record per bend and fields in each record for storage of the data for each bend and each year. Finally, the second script creates a table for viewing the VTab during the data logging procedure. Figure 7.18 shows the initial contents of the VTab. Additional fields will be filled in the next phase of the data logging process.

The third script launches the "Data Manager" dialog box, shown in Figure 7.19. This script also disables the "Create Data File" button on the "Reach Data" dialog box so the user cannot add duplicate bend-year themes to the view containing the bankline records for this sub-reach. The user can reactivate the "Create Data File" button by clicking the green diamond button in the ArcView button panel.

Finally, the third script minimizes the "Reach Data" dialog box and places it at the bottom of the screen. For the remainder of the data collection and archiving, the user interacts with the "Data Manager" dialog box. The "Data Manager" dialog box provides an efficient method for collecting and archiving the data necessary to predict channel migration.

Step 3. This step describes how to locate delineation points along the outer bank of a selected bend. To begin, the user selects the "Enter Bend Delineation Points" tool at the top of the "Data Manager" dialog box. With this tool selected,

the mouse pointer displays as crosshairs when over the current view. The user can move the crosshairs to a desired delineation point and then left-click to position the point on the bankline. Figure 7.20 shows seven delineation points on the outer bank of a bend. (Note: This procedure may also be used to define the channel centerline at a bend if the user is tracking meander migration using centerlines.)

If several of the bankline delineation points have been positioned incorrectly, the "Delete Current Bend Points" button provides the user with the ability to clear all the bankline delineation points and start over. If only a few bankline delineation points appear incorrectly positioned, the "Select Bend Point(s) to Delete" tool enables the user to select one or more points (by holding down Shift key) to delete (by pressing the Delete key after the selection is complete).

When the user is satisfied with the placement of the bankline delineation points on a bend, the fitting of a circle to the bend is performed by pressing the "Fit Circle to Bend" button on the "Data Manager" dialog box. This button runs an Avenue script that determines the center and radius of the circle that best fits (using a least-squares approximation) the bankline delineation points the user has selected on the bend. The script also determines the orientation of the bend as the angle of the line joining the center of the circle to the midpoint of the bend. This angle is measured counterclockwise from a zero angle defined to be due east (Cartesian coordinate system). Figure 7.21 shows the fitted circle and the
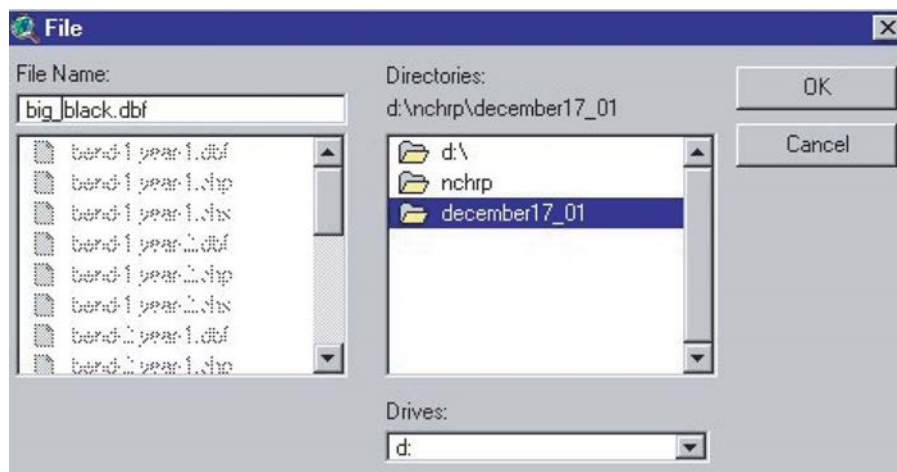

Figure 7.17. File dialog box for choosing a name for the database.

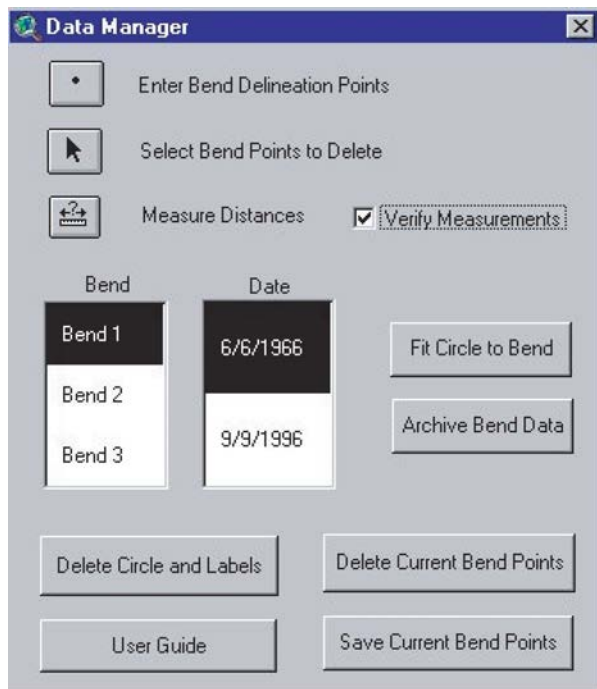*Figure 7.18. Initial contents of the database.*

Figure 7.19.   "Data Manager" dialog box.

orientation line for a selected bend (see Appendix C for the circle-fitting algorithm).

To complete the data collection for this bend, the user selects the "Measure Distances" tool on the "Data Manager" dialog box. Pressing and holding the left mouse button at a given point on the view defines the beginning of a line segment. Dragging the mouse pointer to a second point in the view and releasing the left mouse button defines a line segment whose length is calculated in an Avenue script.

Following the procedure described above, the user must make five distance measurements (see Figure 7.22) at each bend representing the following:

- Upstream channel width (U-U),
- Bend apex channel width (A-A),
- Downstream channel width (D-D),
- Wavelength of the bend (line between U-U and D-D), and
- Amplitude of the bend.

The upstream (U-U) and downstream (D-D) channel widths are measured perpendicular to flow from bankline to bankline at the crossing point between the measured bend and the next upstream or downstream bend. The width of the bend apex (A-A) is measured perpendicular to flow from bankline to bankline at the farthest outward extension of the bend. Wavelength is measured by placing a line between the middle of the channel at the upstream width measurement (U-U) to the middle of the channel at the downstream width measurement (D-D). The wavelength is calculated by the program by doubling the length of this line. The amplitude is determined by placing a perpendicular line from the wavelength line to the outer bank of the bend apex where the width (A-A) was measured. The amplitude is calculated by the program by doubling the length of this line.

A pull-down list dialog box (see Figure 7.23) is provided to assist the user in making and recording these five distance measurements. After making each distance measurement, the user is informed of the distance measured and asked to verify that it is acceptable for later entry in the database. Figure 7.24 shows an example in which the user is asked to verify a measurement of downstream channel width.

Before moving to a new bend or a new historical record, the data for the current bend must be written to the database for this sub-reach. Clicking on the "Archive Bend Data" button (see Figure 7.19) will prompt the user to confirm the bend number and the year number. After confirmation, a script writes the following information to the database:

- Coordinates of the center of the circle,
- Radius of the circle,
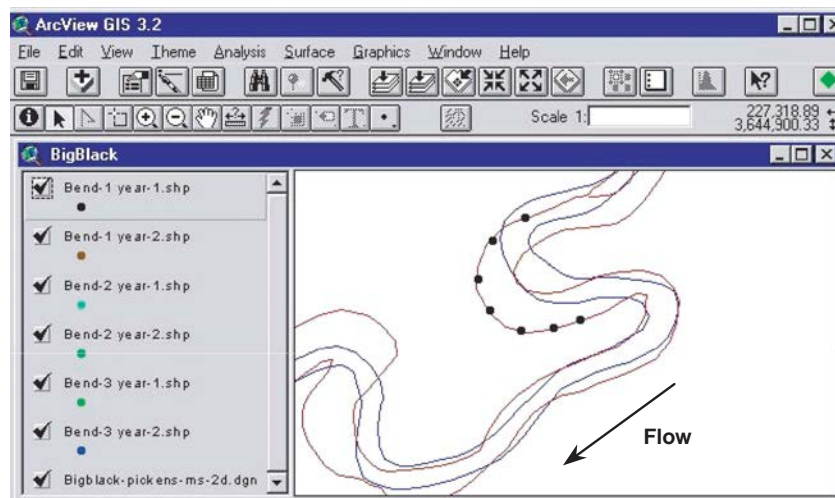
Figure 7.20.   Bankline delineation points on a selected bend.
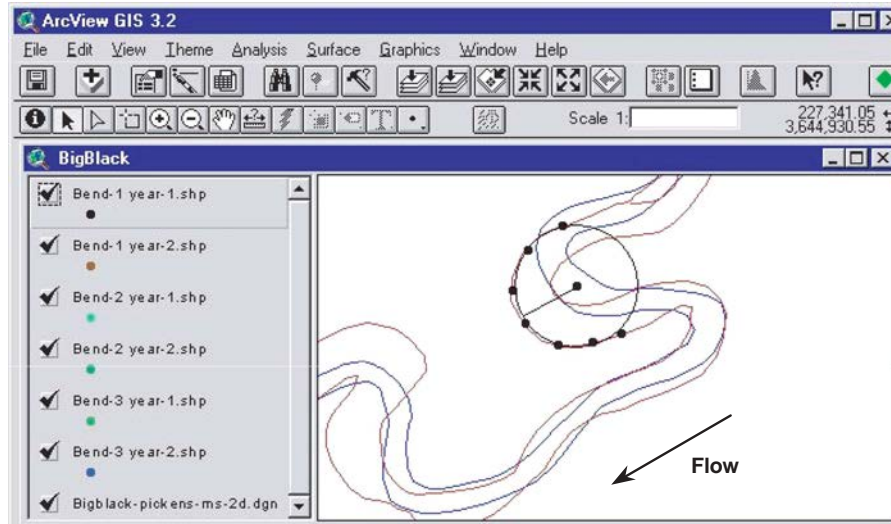
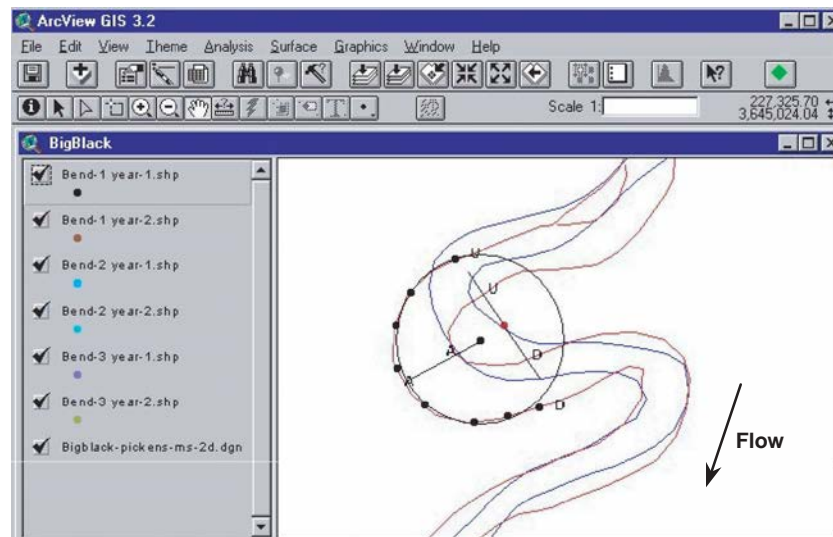*Figure 7.21.   Fitted circle and bend orientation line.*

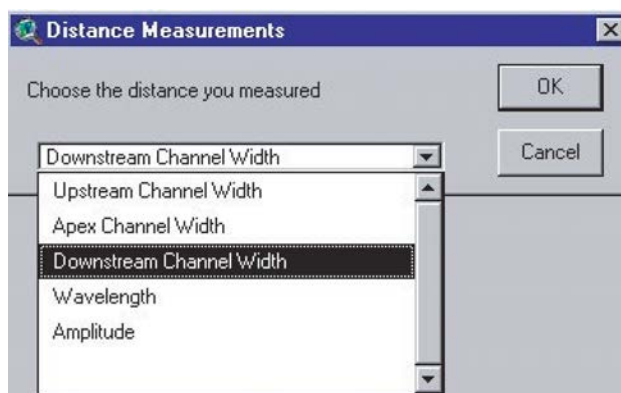*Figure 7.22.   Distance measurements used to describe each bend.*

Figure 7.23.   "Distance Measurements" dialog box.

- Orientation of the centerline of the bend,
- Three channel width measurements,
- Wavelength of the bend, and
- Amplitude of the bend.

Figure 7.25 illustrates the format in which the data are stored. If the user determines that the database contains incorrect values for some bend-year pair, the steps outlined above can be repeated. Archiving the data for a given bend and year overwrites the current field values for that record.

Bankline delineation points for the current bend are stored in a theme attached to the ArcView project for this sub-reach. Because these points can be recovered at any time, use the "Delete Current Bend Points" and "Delete Circles" buttons on the "Data Manager" dialog box to clean the view up before moving to a new bend or a new historical record.
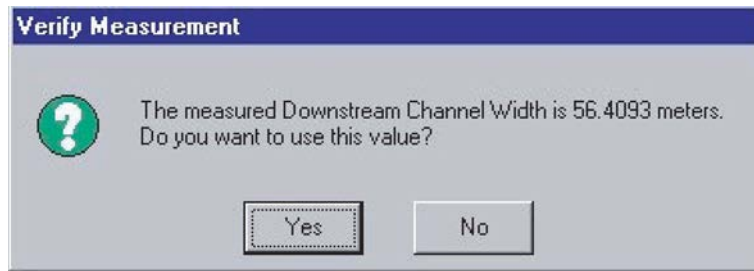
Figure 7.24. *"Verify Measurement" dialog box.*

Figure 7.25. *Some of the data fields for Bend 1 and Year 1.*

When the user has performed the steps described above for each bend and each historical record, the ArcView project for this sub-reach can be closed and should be saved to provide a record of how the database for this sub-reach was created.

7.4.3 Channel Migration Predictor Users Guide

The Channel Migration Predictor uses as input data two or three historical records of bankline position. From this input data, the Channel Migration Predictor calculates and records the extension and translation rates for each bend and each historical interval. Two historical bankline records result in one historical interval, whereas three historical bankline records result in two historical intervals. The Channel Migration Pre-

dictor uses these calculated migration and extension rates to extrapolate and estimate future bankline locations.

Step 1. Start ArcView and add a bankline theme containing the historical records that have been measured and archived using the Data Logger. Figure 7.26 shows an example of such a theme with two historical bankline records. The presence of the blue diamond button in the upper right corner of the project window of Figure 7.26 confirms that the Channel Migration Predictor extension has been loaded into ArcView.

Step 2. Ensure that the ArcView project contains the table of archived, measured data corresponding to the displayed banklines. Figure 7.27 shows the table named "bigblack.dbf"
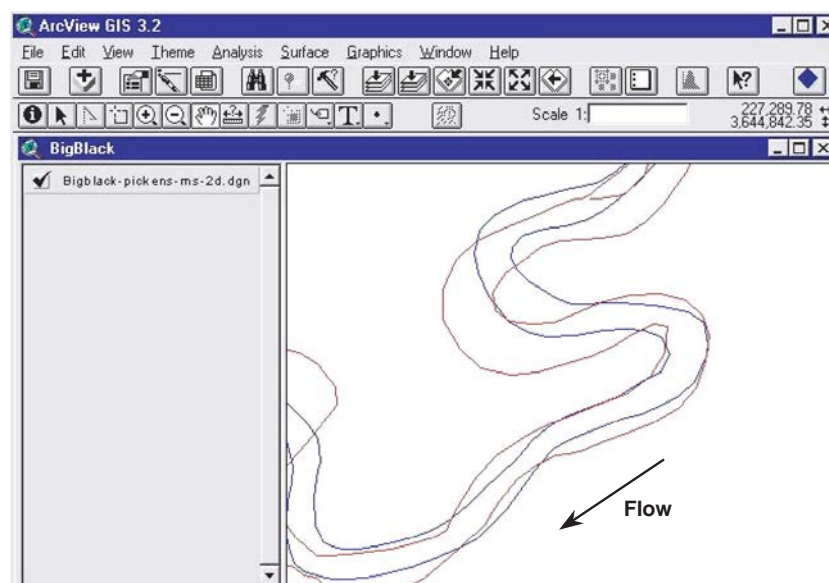
Figure 7.26. *Bankline theme containing two historical bankline records.*
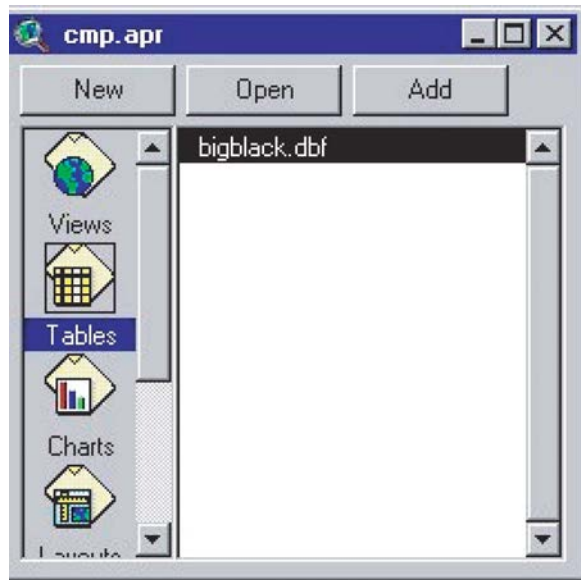
Figure 7.27.   ArcView project tables window.

Figure 7.28.   Channel Migration Predictor interface.

has been added to the project. If the "Tables" list does not contain the database file containing the archived data, then the user must press the "Add" button in Figure 7.27 and add it to the project before launching the Channel Migration Predictor.

Step 3. Press the blue diamond button shown in Figure 7.26 to start the Channel Migration Predictor, which is illustrated in Figure 7.28. The user must provide the name of the archived data file, the "view" name, the number of historical records, the bend number to analyze, and the date for which the bankline is to be predicted.

After providing this information, the user presses the "Continue" button to initiate the calculation of the predicted bankline position. Comparing Figure 7.29 with Figure 7.26, it can be seen that, when the Channel Migration Predictor is started, new themes are added to the view "BigBlack."

Pressing the "Continue" button causes the Channel Migration Predictor to read the database file of archived data and to calculate migration and extension rates. The Channel Migration Predictor then proceeds to create a theme for each historical record and a theme for the predicted bankline. To each of these themes is added a circle indicating the center
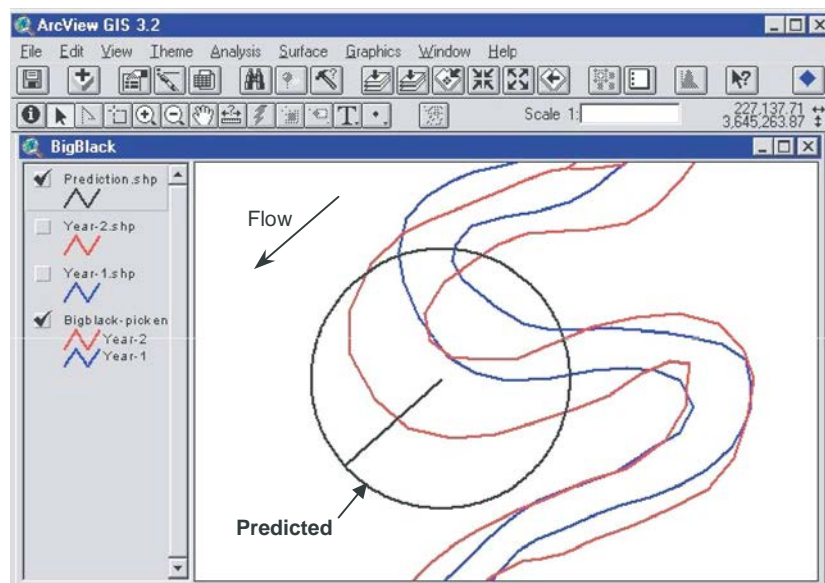
Figure 7.29.   Centroid, radius of curvature, and orientation of the predicted bend.

and radius of curvature of the bend; a line segment indicating the orientation of the bend is also added (see Figure 7.29).

As shown in Figure 7.30, the "Continue" button on the Channel Migration Predictor interface has been temporarily disabled, and check boxes allowing the user to selectively display bend data have been enabled. A change in any of the text fields above the "Continue" button will enable the "Continue" button and disable the check boxes.

7.5 FREQUENCY ANALYSIS

The GIS bend measurement and prediction tools are recommended for predicting future bend migration because the individual bend conditions and history are considered to be the best information for making the prediction. The GIS prediction also computes the rate of migration (in channel widths per year) and provides a comparison of this rate to a database of measured bends. As part of the NCHRP 24-16 research project, a database was developed that includes nearly 2,500 measurements of bend migration. If the time sequence aerial photos are not available and a prediction of bend migration is still needed, the measured amounts of bend migration from the database can provide some guidance. For the modified Brice Class A, B1, B2 and C sites (see Figure 3.2), rates of extension and translation were measured and the cumulative percent, or frequency, of movement was calculated. The number of bends that were included in this analysis are 89, 249, 408, and 915 bends for the A, B1, B2 and C sites, respectively. The rates of movement are shown in Figures 7.31 and 7.32 as cumulative percent of extension and translation in channel widths per year. The figures should be interpreted such that, "x" percentage of the bends were

Figure 7.30.   Enabled check boxes allowing selective viewing of bend data.

migrating at less than the specified rate and 100 minus "x" percentage were migrating faster than the specified rate. These figures show that the C sites migrate faster than the A, B1, and B2 sites. This result agrees with the premise of the screening and classification. These figures also show that rates of translation tend to be greater than rates of extension (bends tend to move faster in the downstream direction relative to their orientation).

Figures 7.31 and 7.32 show that 50 percent of C sites were observed to extend 0.008 channel widths per year and to translate 0.015 channel widths per year. This information can be used to provide an estimate of future bankline positions. For example, suppose an estimate of bankline position for 20 years into the future at a C site bend with a channel width of 140 ft (42.7 m) is needed. The data from Figures 7.31 and 7.32 suggest that half of other similar (C site) bends extended at least 22 ft (7 m) (0.008 channel widths/year × 20 years × 140 ft-width = 22 ft or 7 m) and translated at least 42 ft (13 m) (0.015 channel widths/year × 20 years × 140 ft-width = 42 ft or 13 m). Half of the bends also moved at slower rates than 0.008 (extension) and 0.015 (translation) channel widths per year. This approach requires judgment in selecting a "level of confidence" to use in making the estimate. The "level of confidence" refers to the percentage in the "Cumulative Percent" axis. The higher the percentage, the more likely it is that the bend will be moving less than the computed amount (shown on the "Extension" and "Translation" axes of Figures 7.31 and 7.32, respectively). Thus, selecting a higher percentage will provide a more conservative estimate. More conservative estimates may be desired for more important transportation structures. Returning to the example previously discussed, if a more conservative estimate were wanted, the bend could be assessed for a 75-percent level of movement rather than for a 50-percent level. Figures 7.31 and 7.32 show that 75 percent of the C site bends extended less than 0.018 channel widths per year and translated less than 0.031 channel widths per year and that 25 percent of the C site bends were moving at higher rates. The 20-year prediction using 75-percent rates of extension and translation are 50 ft (15 m) and 87 ft (26 m), respectively.

Using the frequency approach relies on identifying the channel classification and applying a rate based on a selected frequency or percentage. Higher percentages result in more conservative estimates of migration (i.e., the bend will likely move less than the estimated amount). In addition to Figures 7.31 and 7.32, the rates for the modified Brice classes (see Figure 3.2) and different probabilities are summarized in Table 7.1. The cumulative percent can be used as the probability that a bend will migrate less than the given amount. One hundred minus the cumulative percent can be used as the probability that a bend will migrate more than that amount.

Figure 7.33 is an illustration of the frequency analysis approach applied to an A site and a C site assuming similar starting conditions. For the initial condition, both banklines are shown, and for a 30-year future condition several potential
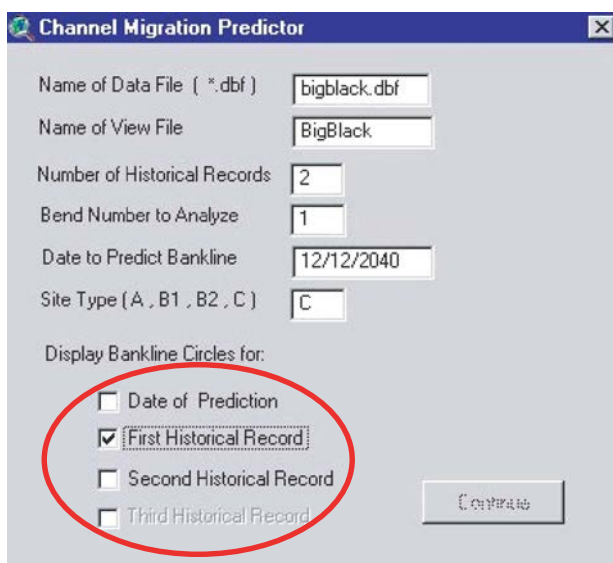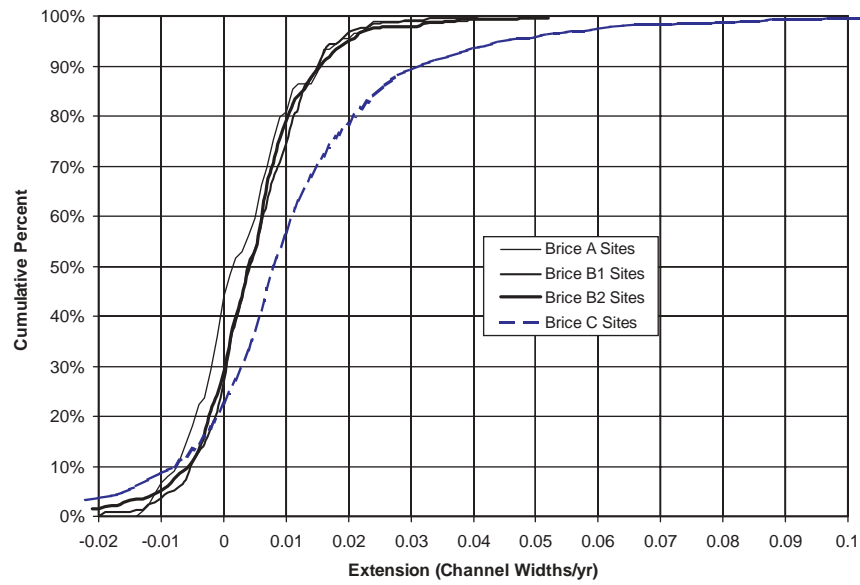
Figure 7.31.   Cumulative percentage of extension in channel widths per year.
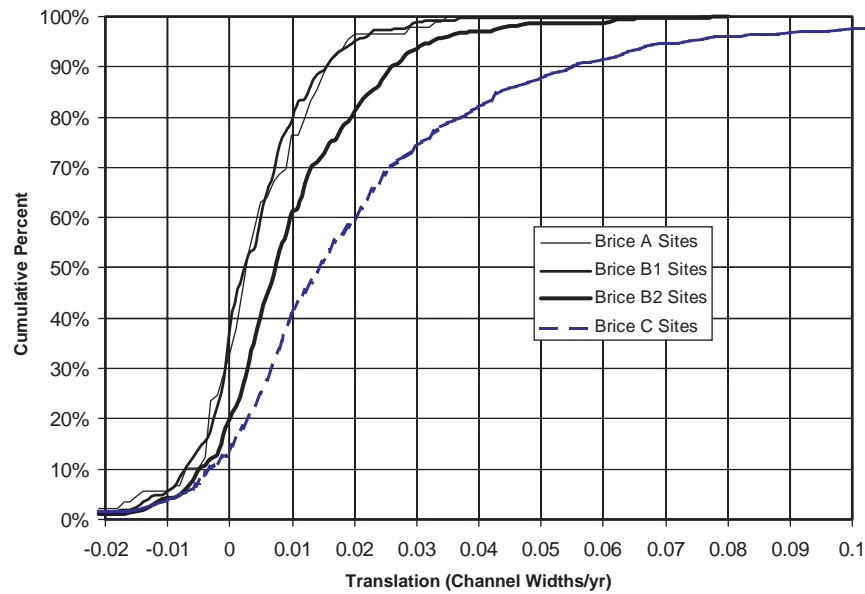

Figure 7.32.   Cumulative percentage of translation in channel widths per year.

TABLE 7.1   Rates of extension and translation

	Extension (channel widths/yr)				Translation (channel widths/yr)			
Cumulative %	50	75	90	95	50	75	90	95
A Sites	0.0015	0.008	0.015	0.018	0.0025	0.010	0.015	0.019
B1 Sites	0.004	0.010	0.015	0.026	0.0023	0.009	0.016	0.020
B2 Sites	0.004	0.009	0.016	0.020	0.007	0.016	0.026	0.033
C Sites	0.008	0.018	0.032	0.045	0.015	0.031	0.055	0.074

46
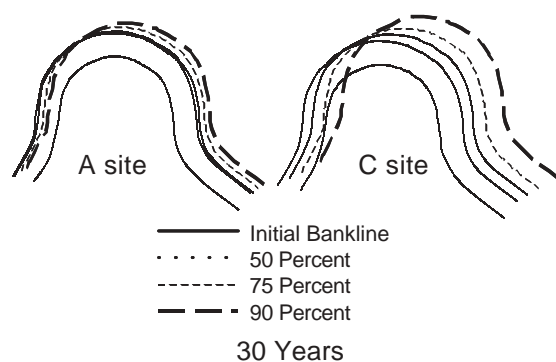
Figure 7.33.   Example movement percentages for a 30-year time period.

channel locations (outer bank only) are shown. At the 50-percent level, the A site shows almost no migration, whereas the C site shows the potential to migrate half the channel width. There is a 10-percent chance that the A site will migrate half a channel width in 30 years (90 percent of A site channels moved less than half a channel width in 30 years) and a 10-percent chance that the C site will migrate nearly two channel widths (90 percent moved less than two channel widths in 30 years). As an alternative to photo comparison, or as a check on the results of the photo comparison, this frequency analysis approach provides reasonable results. However, it should only be considered as an alternative to photo comparison when no data are available for the extrapolation technique using photo comparison.

CHAPTER **8**

ILLUSTRATED EXAMPLES

8.1 INTRODUCTION

This chapter provides the user with illustrated examples of the application of the comparison techniques described in Chapters 5 and 7. This chapter begins by allowing the user to conduct an initial screening and classification of several streams. The chapter then provides the user with step-by-step instructions on conducting the manual comparison techniques using Mylar or acetate overlays.

8.2 SCREENING TASK

The first step in determining the potential for channel migration and the migration history of a channel using the methodology set forth in the *Handbook* is determining whether the channel is a meandering stream. An initial screening should be conducted based on the description of straight, braided, and anabranched streams in Section 2.2. Once a stream has been determined to be a single-thread meandering channel, the user proceeds to classify the stream based on the classification scheme shown in Figure 3.2.

8.3 CLASSIFICATION TASK

Eleven channels are provided in Figure 8.1 to allow the user to conduct an initial screening and classification based on the descriptions of non-meandering stream planform in Chapter 2 and the modified stream classification scheme described in Chapter 3 and shown in Figure 3.2. The classification of each stream shown in Figure 8.1 is provided in Table 8.1.

Stream Reaches 2, 6, and 11 in Figure 8.1 would be screened out from further analysis based primarily on planform characteristics. Stream Reach 2 (Cimarron River) would be screened out because it is a highly unstable, two-phase stream with a low-flow wandering channel. The Henrys Fork River, shown as Stream Reach 6, is classified as a braided river and would be removed from further analysis. Stream Reach 11 (Altamaha River) would be removed because it is an anabranched river; it is multichanneled, stable, and located in a low-energy environment.

The remaining streams would be classified based on the stream classification scheme shown in Figure 3.2. Stream Reach 1 (Smokey Hill River) is classified as Class G_2; it is a two-phase, bimodal sinuosity channel that is wider at the bends because of the presence of point bars. Stream Reach 3 (Pee Dee River) is classified as Class B_1 because it is an equal-width, single-phase channel.

Stream Reach 4 (Licking River) is classified as Class A because it is a deeply incised, single-phase, equal-width channel. The narrow riparian fringe along both sides of the channel and the extensive agricultural fields surrounding the river indicate an incised or deep channel with a narrow terrace or berm and a dense growth of vegetation inset between both banks.

The reach of the Sacramento River shown as Stream Reach 5 in Figure 8.1 is classified as Class D because it is a single-phase channel that is wider at the bends with extensive point bar development and well-developed chute channels across the point bars of both bends. The reach of the Sacramento River shown as Stream Reach 7 is near Stream Reach 5, but Stream Reach 7 is classified as a Class C because no chute channels are present on the point bars of the reach.

The two-phase, equal-width, bimodal sinuosity channel shown as Stream Reach 8 (Saline River) is classified as Class G_1. The channel shown as Stream Reach 9 (Little Pee Dee River) is classified as a single-phase, irregular-width Class E channel. Stream Reach 10 (Neches River) is classified as a Class B_2 channel, which is a single-phase channel that is wider at the bends but has no apparent point bars.

Once a channel reach has been classified, the prediction of the rate and extent of future migration of a given bend or channel reach for B_2, C, D, E, or G_2 channels can be conducted using the aerial photo and map comparison techniques described in Chapters 5 and 7 and in the example in the following section.

8.4 EXAMPLES USING AERIAL PHOTO COMPARISON AND PREDICTION TECHNIQUES

The following sections provide steps for using aerial photographs and maps to conduct a simple comparison of historic bankline positions and for using the manual overlay techniques described in Chapters 5 and 7 to make predictions on potential future migration. The reach of the Sacramento River shown as Stream Reach 7 in Figure 8.1 (a Class C channel) will be used as the example reach in the following discussion.

8.4.1 Manual Bankline Overlay and Circle Template Method

The following steps include delineating the historic bankline positions of the Sacramento River by hand, evaluating bankline shift in the reach using simple overlays, evaluating the historic migration rate and extent using circle templates,
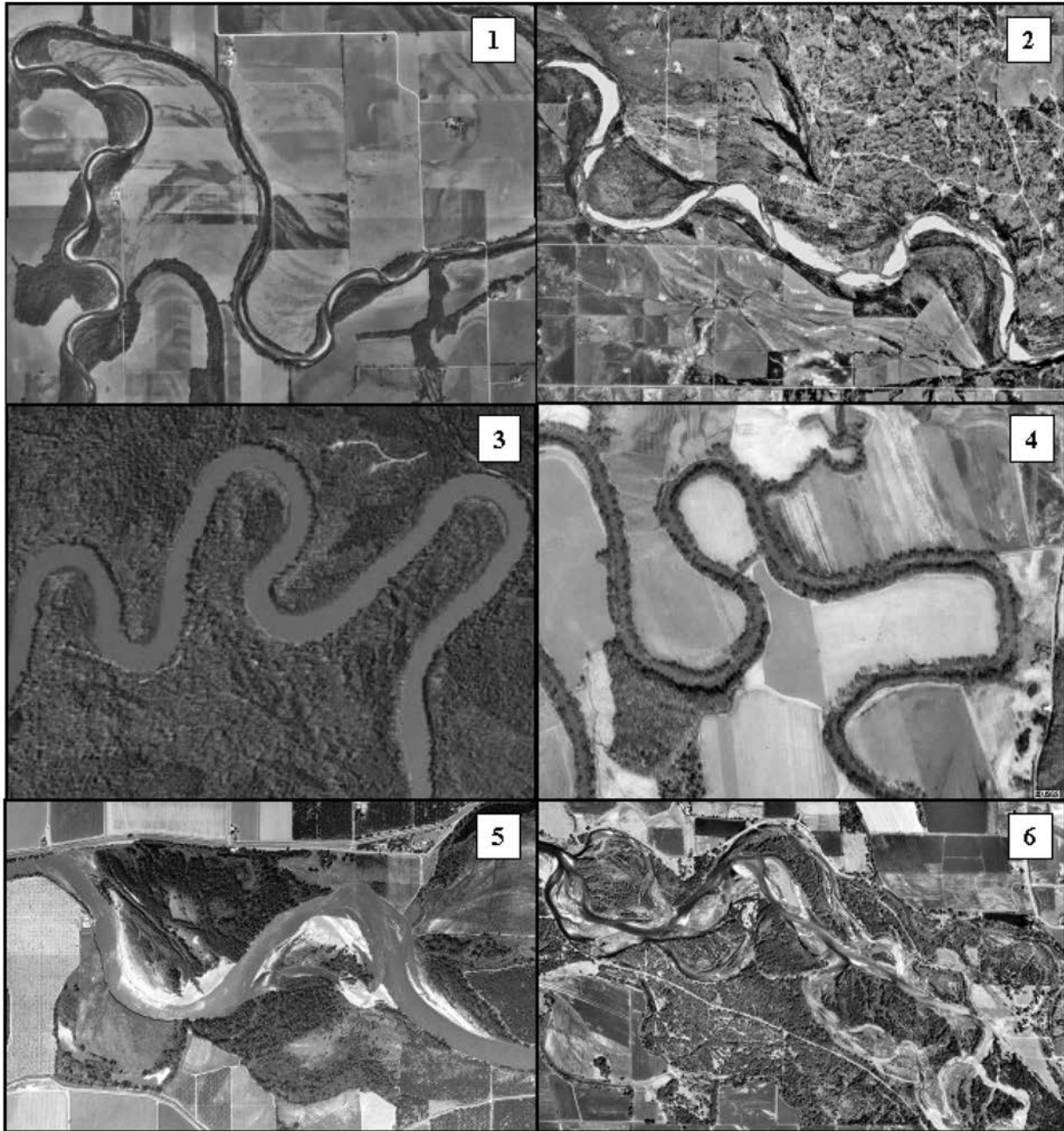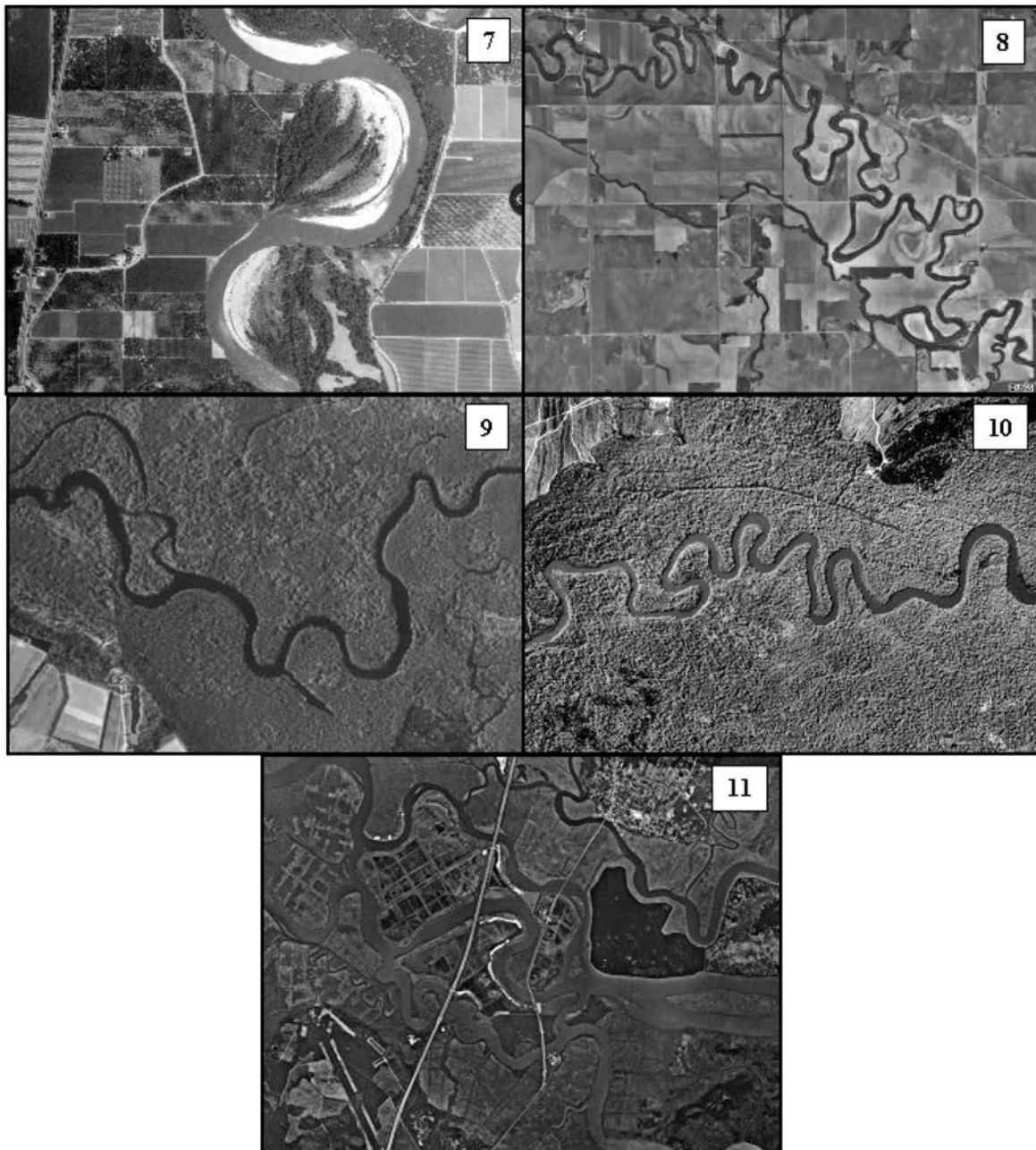
Figure 8.1. Various streams requiring classification by the user based on the initial screening described in Chapter 2 and the classification scheme shown in Figure 3.2. (continued on next page)

and predicting the potential position of the channel in the future.

Step 1. The first step in evaluating the potential for channel migration is acquiring appropriate historic maps and aerial photography of the reach. These can be acquired from a number of federal, state, and local government agencies and private vendors. The addresses for some of the more prominent distributors are provided in Table 4.1. Figure 8.2 shows two maps from a 1937 topographic survey of the Sacramento River

Valley conducted by the U.S. Army Corps of Engineers and acquired from the Sacramento District. Figure 8.3 shows blue-line sheets of 1972 aerial photographs of the Sacramento River acquired from the California Department of Water Resources. A 1998 NAPP black and white aerial photograph of the Sacramento River, shown in Figure 8.4, was acquired from the U.S. Geological Survey EROS Data Center.

Step 2. After the appropriate historic maps and aerial photos have been acquired, the next step is to delineate the

Figure 8.1. (continued) *Various streams requiring classification by the user based on the initial screening described in Chapter 2 and the classification scheme shown in Figure 3.2.*

TABLE 8.1   Classification of streams shown in Figure 8.1

Stream Number	Location	Classification
1	Smokey Hill River near Chapman, KS	G_2
2	Cimarron River near Fairview, OK	F
3	Pee Dee River Near Peedee, SC	B_1
4	Licking River near Romey, KY	A
5	Sacramento River near Butte City, CA	D
6	Henrys Fork River near Rigby, ID	Braided
7	Sacramento River near Butte City, CA	C
8	Saline River near Tescott, KS	G_1
9	Little Pee Dee River near Galivants Ferry, SC	E
10	Neches River near Evadale, TX	B_2
11	Altamaha River near Darien, GA	Anabranched
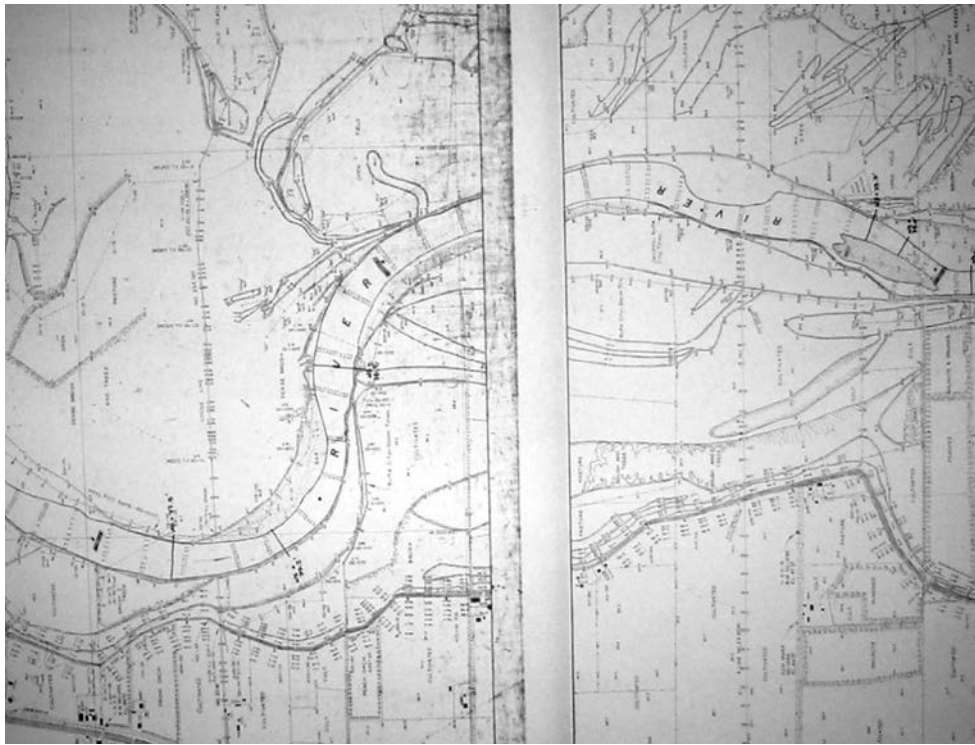
Figure 8.2.   Two sheets showing U.S. Army Corps of Engineers topographic survey maps of the Sacramento River near Butte City, California, from 1937.

Figure 8.3.   Two sheets showing California Department of Water Resources aerial photographs of the Sacramento River near Butte City, California, in 1972.

Figure 8.4.   Aerial photograph obtained from the USGS of the Sacramento River near Butte City, California, in 1998.

banklines and identify the registration points that are common to all the maps and aerial photos. This can be done by hand or electronically. To do this by hand, a piece of Mylar or acetate is laid on top of the map or aerial photo, and the banklines are traced onto it. Registration points that are common to the photos and maps being analyzed are delineated on the tracings as well. A registration point can be any geographic feature (such as a fence, road crossing, or a structure), and the point should bracket the reach at both ends to provide the best fit possible among the historic banklines. Figure 8.5 shows bankline tracings and registration points from the 1972 aerial photos hand drawn on Mylar.

A particular site can often extend over two or more aerial photos or maps from each time period. In these cases, overlapping aerial photographic coverage should be obtained so that the overlapping photos can also be registered together for delineating the channel banklines. When a site falls on two or more maps, the map edges are usually all that needs to be matched together. If adjacent photos and maps do not match, they are probably at a slightly different scale and will need to be enlarged or reduced to match the other photos or maps in the set.

In many cases, the different historic aerial photos and maps used in the comparison may not have the same scale, and, therefore, they will need to be enlarged or reduced to a common scale. By enlarging or reducing the bankline tracings on a copier with a zoom feature, the user can closely match each subsequent bankline to the previous bankline with the registration points.

The same steps can be accomplished more easily using graphics and photo-editing software such as Microsoft PowerPoint or Jasc Paint Shop Pro as discussed in Sections 5.3 and 7.3. The aerial photos and maps should be obtained in digital format for use with this software. This can be accomplished by scanning the images on flatbed scanners or by obtaining the images in digital format directly from a vendor. The aerial photos and maps of the reach of the Sacramento River being used in this example were scanned and converted into digital format. The Sacramento River banklines and registration points were delineated on the 1937 map (see Figure 8.6) and on the 1972 aerial photo (see Figure 8.7) using MS PowerPoint.

Step 3. Once the banklines and registration points have been delineated on each map and photo, the registration points can be matched using a manual or digital overlay technique so that the banklines can be compiled onto a Mylar sheet (manual technique) or digital image (digital technique). Figure 8.8 shows the overlay of both the 1937 and 1972 banklines on the 1972 image of the Sacramento River. As seen in Figure 8.8, the left bank of the river has migrated laterally and down valley as much as 1,370 ft (417 m) in the 35 years between 1937 and 1972. This produces a maximum average migration rate of about 39 ft (12 m) per year. It is also apparent that the meander bend has increased in width over time as a result of the growth of the point bar.

Step 4. Contemporary migration characteristics of this Sacramento River meander bend can be evaluated further by comparing the 1937 and 1972 banklines with the banklines of the river on the 1998 aerial photograph. Figure 8.9 shows the 1998 aerial photo of the river with the banklines and registration points delineated. The banklines from 1937 and 1972 are then superimposed on the 1998 aerial photo (with
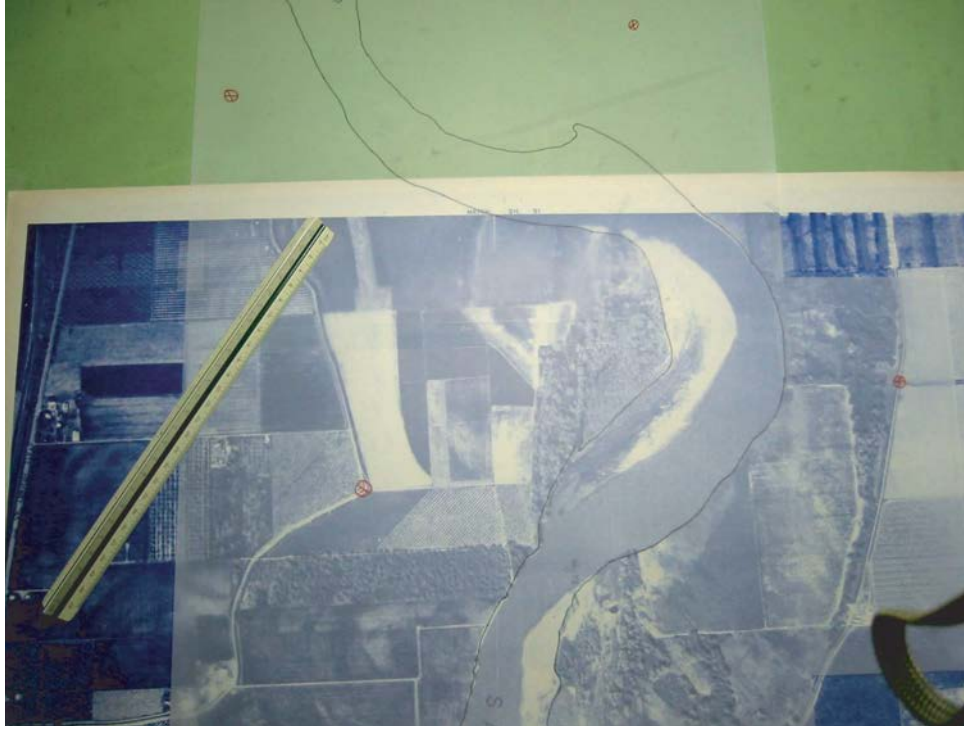
Figure 8.5. Bankline tracings (black lines) and registration points (circled red crosses) delineated on a Mylar sheet laid on top of the 1972 aerial photograph of the Sacramento River near Butte City, California.

the 1998 banklines and registration points delineated) as shown in Figure 8.10. It is readily apparent that the continued migration of this meander bend will soon threaten the flood control levee located less than 250 ft (76 m) from the left bank of the river.

Step 5. The next step in evaluating the migration rate and extent of the bend of the Sacramento River involves delineating the radius of curvature and centroid of a best-fit circle used to define the outer bank for each year in the analysis (see Figure 8.11). The measured radii of curvature of the outer bank of the meander bend in 1937 (R_{C1}), 1972 (R_{C2}), and 1998 (R_{C3}) are 3,650 ft (1,113 m), 2,425 ft (739 m), and 2,650 ft (808 m), respectively. The rate of change in the radius of curvature of the outer bank can then be determined by figuring out how much the radius has contracted or expanded over each period and then dividing the amount of change by the number of years in the period. For the purpose of discussion, the period of time between 1937 and 1972 is defined as Period A, and the period of time between 1972 and 1998 is defined as Period B. For this bend of the Sacramento River, the outer bank radius of curvature contracted 1,225 ft (373 m) between 1937 and 1972. The resulting contraction rate (ΔR_{CA}), derived using Equation 7.1, is as follows:

$$\Delta R_{CA} = (R_{C2} - R_{C1})/Y_A = (2425\,\text{ft} - 3650\,\text{ft})/(35\,\text{yr})$$
$$= 35\,\text{ft/yr}\,(-10.6\,\text{m/yr}).$$

The radius of the outer bank expanded more than 225 ft (68 m) between 1972 and 1998. The resulting expansion rate (ΔR_{CB}), derived using Equation 7.2, is as follows:

$$\Delta R_{CB} = (R_{C3} - R_{C2})/Y_B = (2650\,\text{ft} - 2425\,\text{ft})/(26\,\text{yr})$$
$$= 8.7\,\text{ft/yr}\,(2.6\,\text{m/yr}).$$

Step 6. After delineating the outer bankline radii of curvature with best-fit circles, the circle centroids are delineated, and their migration is plotted as shown in Figure 8.12. The centroid migration distance is defined as the length of the line between the centroid position defined by Period A (D_A) and the centroid position defined by Period B (D_B). The centroid migration distance (D_A) from 1937 to 1972 is approximately 2,700 ft (823 m). The centroid migration distance (D_B) from 1972 to 1998 is approximately 875 ft (267 m). The migration rate for Period A is 77 ft (23.5 m) per year, and the migration rate for Period B is 33.7 ft (10.3 m) per year.

An arbitrary line is drawn vertically from the 1937 bend centroid and is used to define the change in direction of the 1972 and 1998 bend centroids (see Figure 8.12). Line D_A defines the direction of migration of the bend during Period A. The angle θ_A, described by the intersection of line D_A with the arbitrary line, represents the angle of migration of the bend centroid during Period A. The angle θ_B represents the bend centroid migration direction relative to the arbitrary line during Period B. The migration direction of the bend centroid between 1937 and 1972 as defined by angle θ_A is 13.5 degrees. The migration direction of the bend centroid between 1972 and 1998 as defined by angle θ_B is 46 degrees.

Step 7. The final step in the analysis is the prediction of future meander migration. Using the rates and direction of
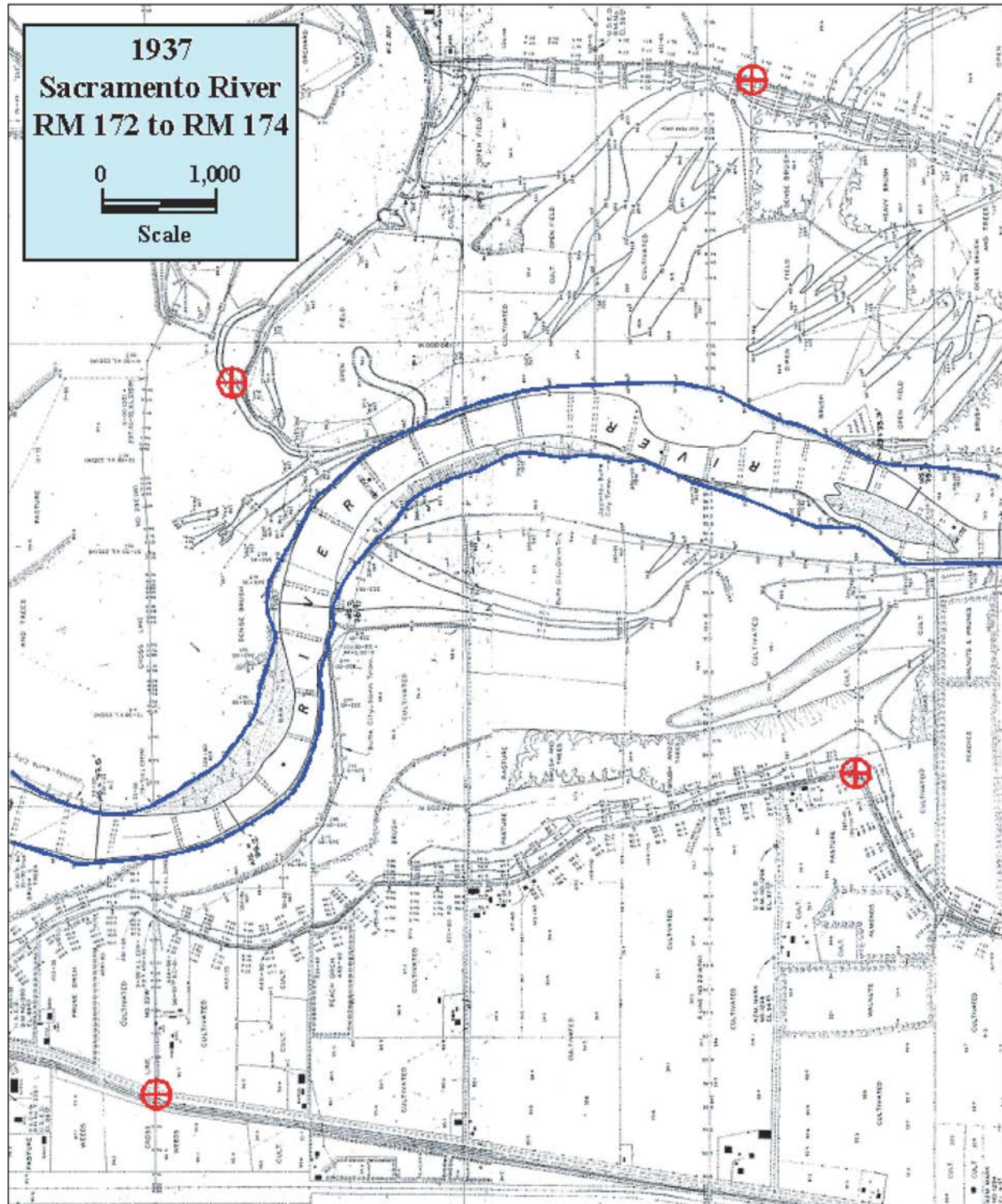
Figure 8.6.   U.S. Army Corps of Engineers 1937 map of surveyed topography of the Sacramento River Valley near Butte City, California. The banklines of the river are defined by blue lines. Common registration points are defined by the red circled crosses. (RM = river mile.)

past migration, a prediction can be made on the position of the outer bankline of a bend in the future. For example, a prediction of where the outer bankline will be in the year 2028 for the example reach of the Sacramento River is provided in Figure 8.13. Prediction of the future migration rate of the bend centroid should use the migration rate for Period B

because the conditions associated with this rate are likely to be more closely related to those in the future. Thus, the predicted migration distance (D_C) during Period C (1998 to 2028), derived using Equation 7.5, is the following:

$$D_C = (D_B/Y_B)Y_C = (875\,\text{ft}/26\,\text{yr})(30\,\text{yr}) = 1{,}010\,\text{ft}\,(308\,\text{m}).$$
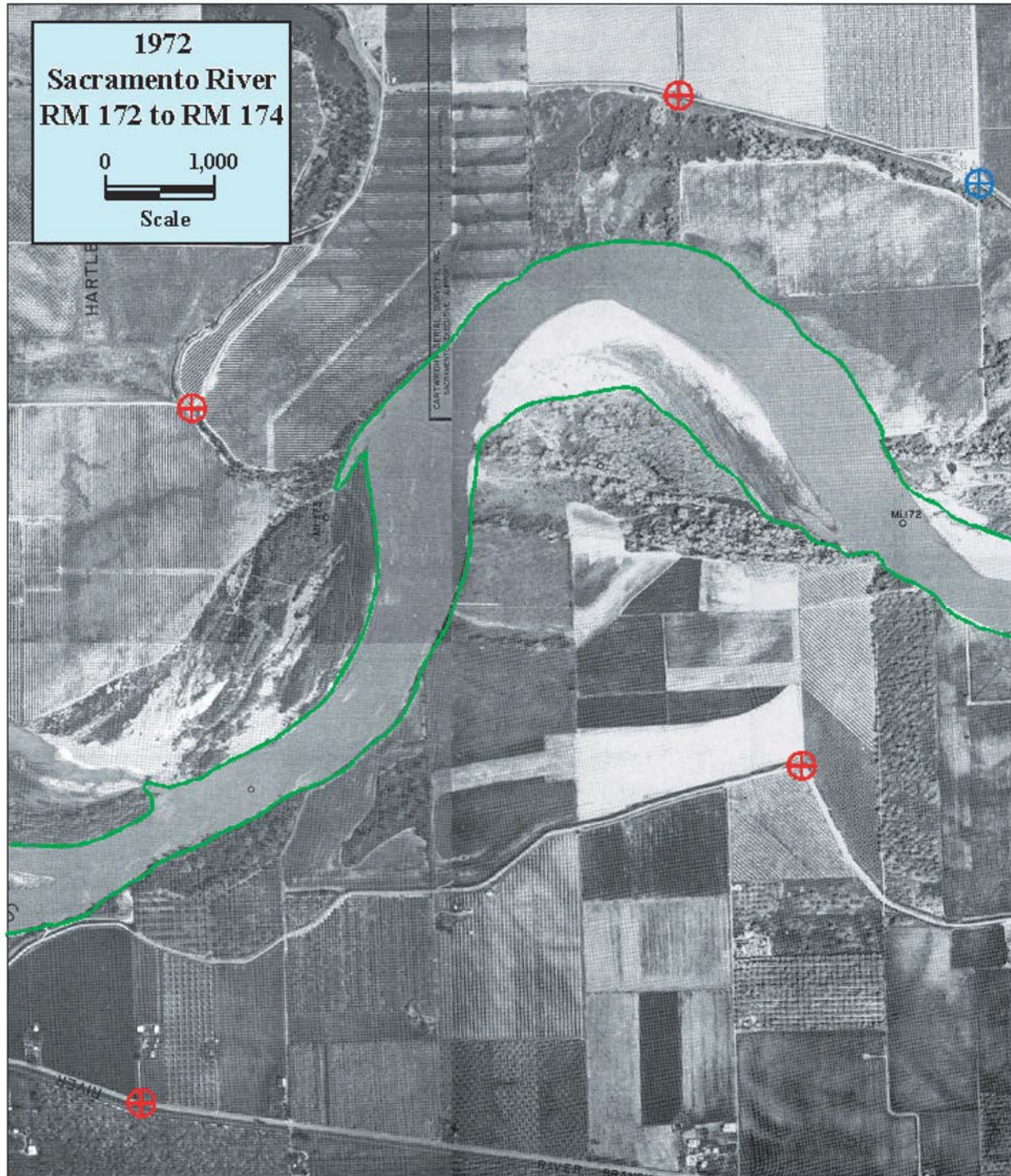
Figure 8.7. California Department of Water Resources 1972 aerial photography of the Sacramento River Valley near Butte City, California. The banklines of the river are defined by green lines. Common registration points are defined by the red and blue circled crosses. (RM = river mile.)

If only one period is available, then it can be assumed that the migration direction does not change ($\theta_C = \theta_B$). If two or more periods are available, a decision should be made as to whether the prediction of future meander migration should include change in migration direction, as described by Equation 7.4 in Chapter 7. It is assumed for the purposes of this example that meander migration will follow the same direction as that of the previous period. The incorporation of change in migration direction for this problem can be found in Appendix E. Consideration should be given to applying both methods in order to define an area over which future meander migration might occur.
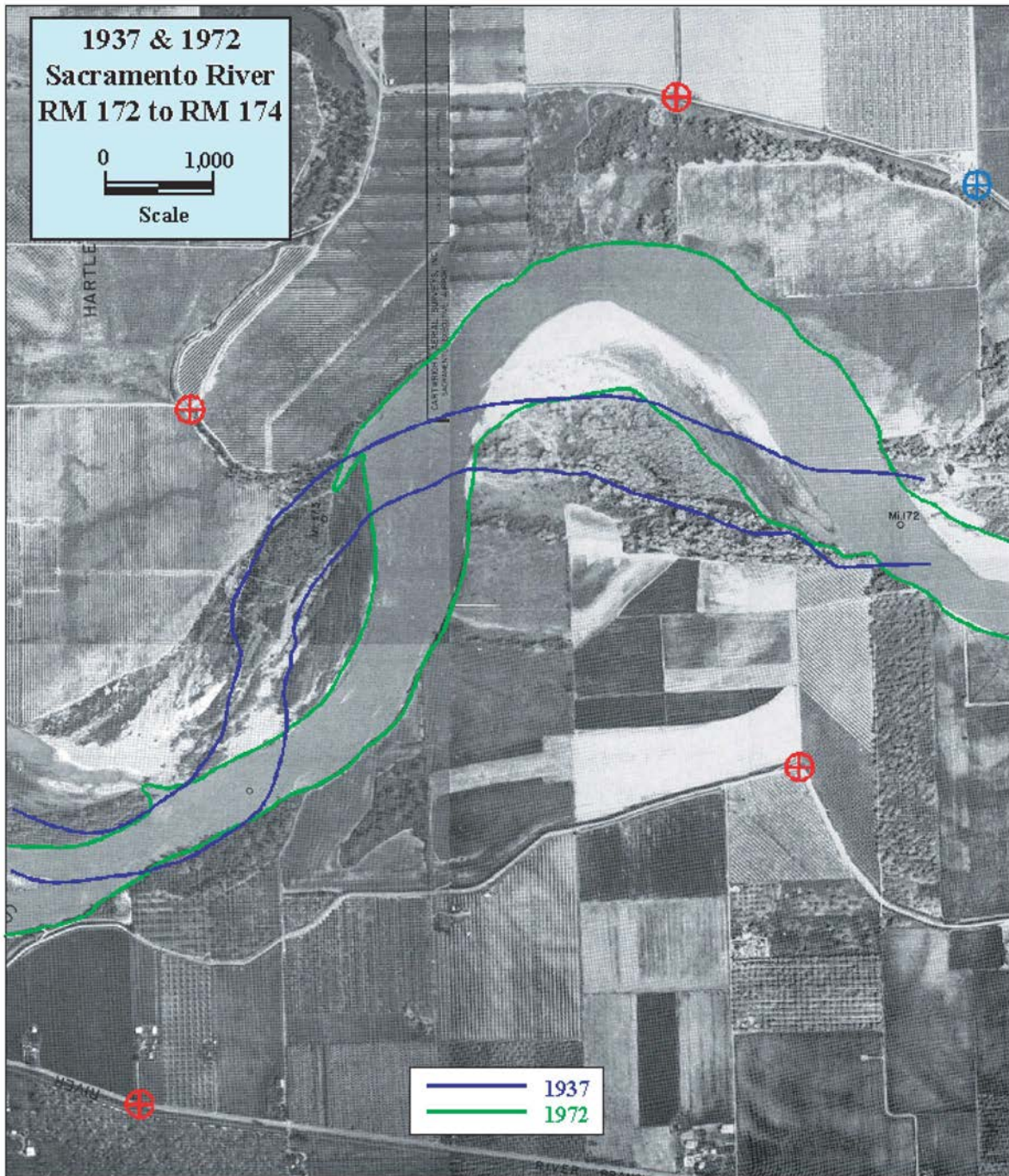
Figure 8.8.   Overlay and comparison of the 1937 and 1972 banklines and common registration points on the 1972 aerial photography. (RM = river mile)

Finally, the radius of curvature for the outer bank of the meander bend in 2028 (R_{C4}) is predicted based on the assumption that the bend will continue to expand (or contract) at the same rate as the previous period (Period B). This is calculated using Equation 7.3, which is the rate of change per year of the radius during Period B (the expansion rate) times 30 years plus the 1998 radius of curvature. Thus, the radius of curvature for the outer bank of the meander bend of the river in the year 2028 (R_{C4}) is predicted to be

$$R_{C4} = R_{C3} + \left[\left(\frac{(R_{C3} - R_{C2})}{Y_B} \right)(Y_C) \right]$$

$$= 2{,}650\,\text{ft} + \left[\left(\frac{(2{,}650\,\text{ft} - 2{,}425\,\text{ft})}{(26\,\text{yr})} \right)(30\ \text{yr}) \right]$$

$$R_{C4} = 2{,}910\,\text{ft}\,(887\,\text{m}).$$

The outer bankline position for the river bend in the year 2028 is defined by a circle with the predicted radius, R_{C4}.
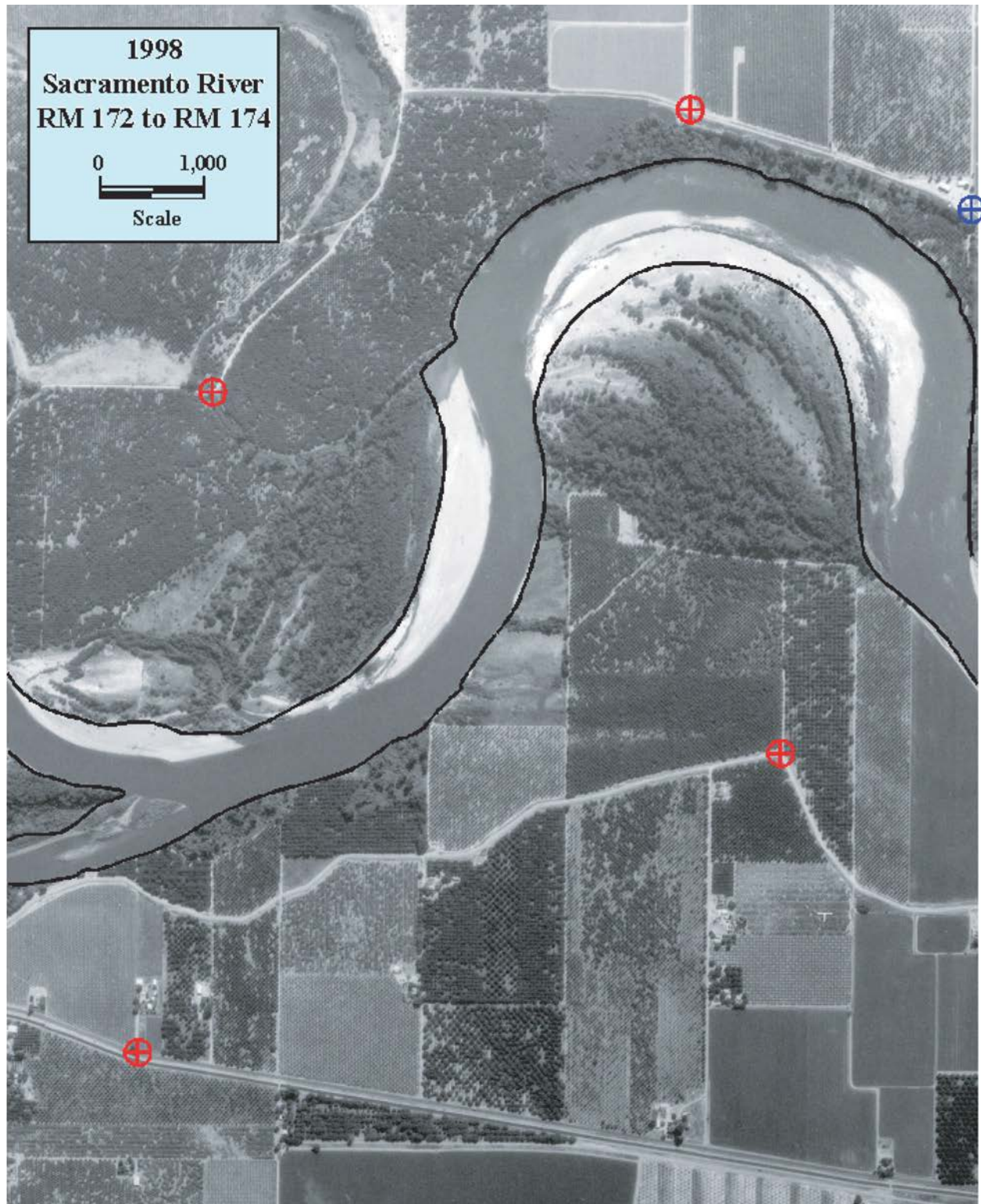
Figure 8.9.   Aerial photograph of the Sacramento River near Butte City, California, showing the bankline positions of the river in 1998. (RM = river mile)
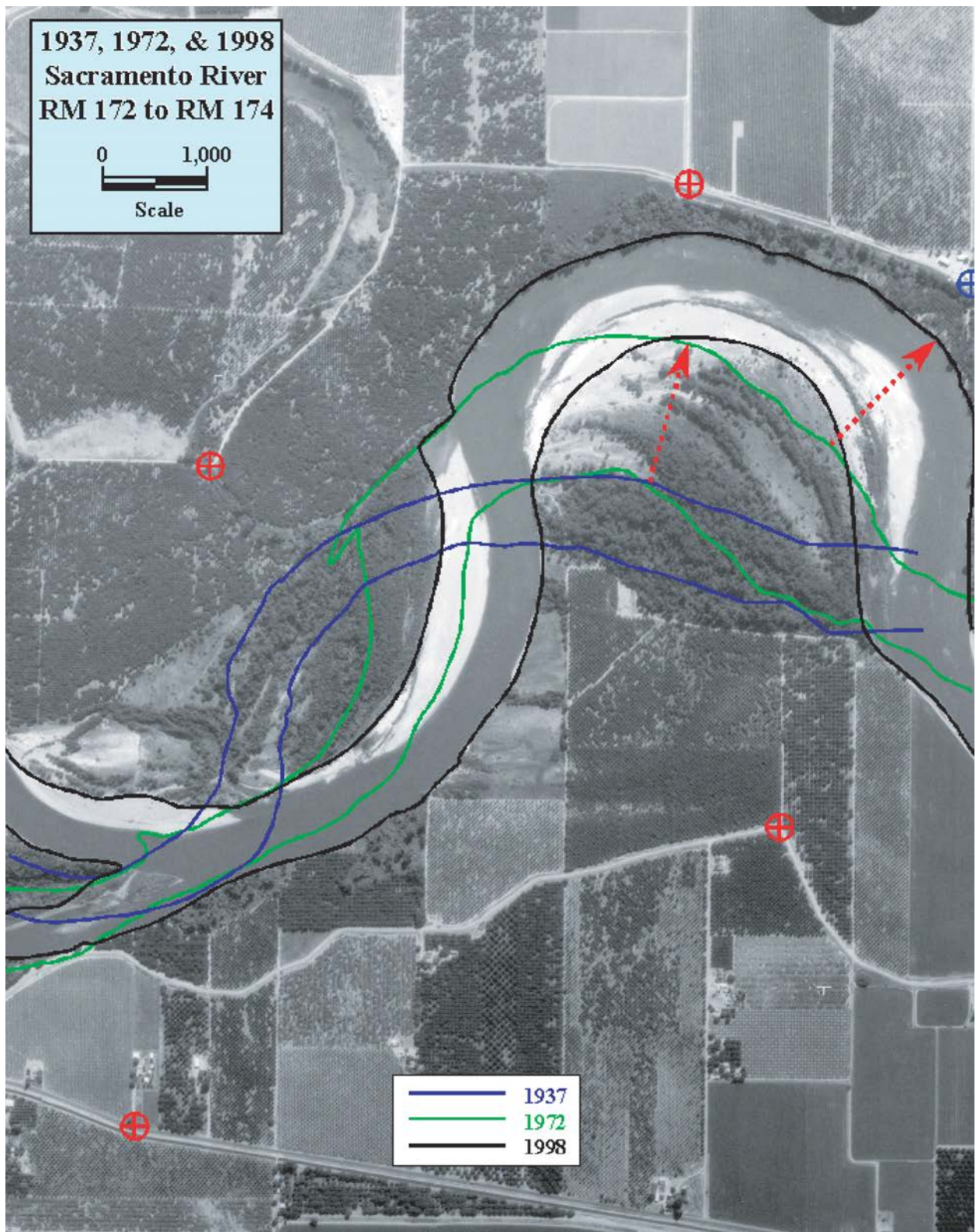
Figure 8.10.   Overlay and comparison of the 1937 (blue), 1972 (green), and 1998 (black) banklines on the 1998 aerial photo of the Sacramento River near Butte City, California. The red arrows show the maximum bankline migration display. (RM = river mile.)
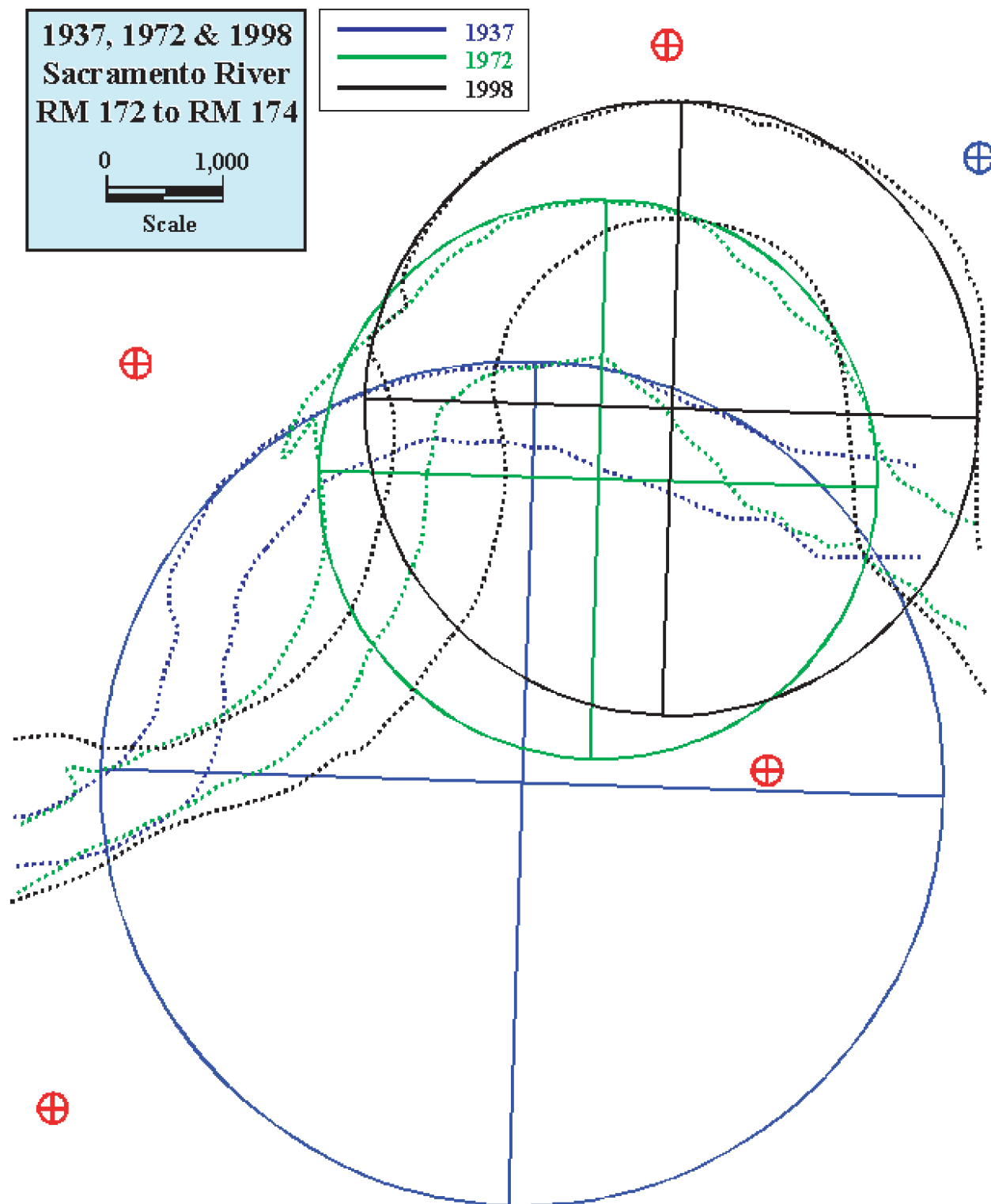
Figure 8.11.   Circles of known radius of curvature fitted to the 1937, 1972, and 1998 outer banklines (dotted lines) of the Sacramento River. (RM = river mile.)
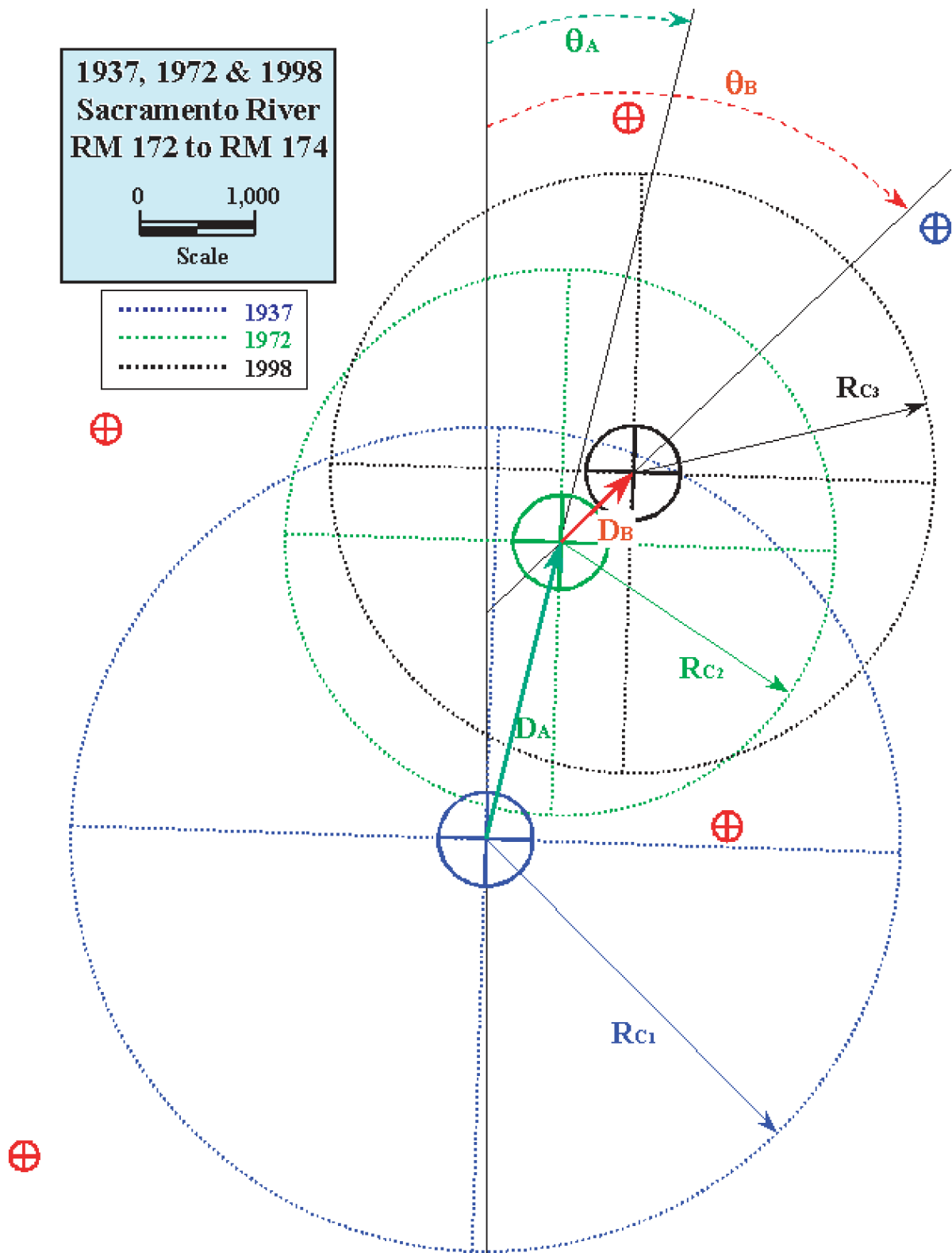
Figure 8.12.   Delineation of the bankline radii of curvature (R_{C1}, R_{C2}, and R_{C3}), bend centroid migration distances (D_A and D_B), and angles (θ_A and θ_B) for Period A (1937 to 1972) and Period B (1972 to 1998). (RM = river mile.)
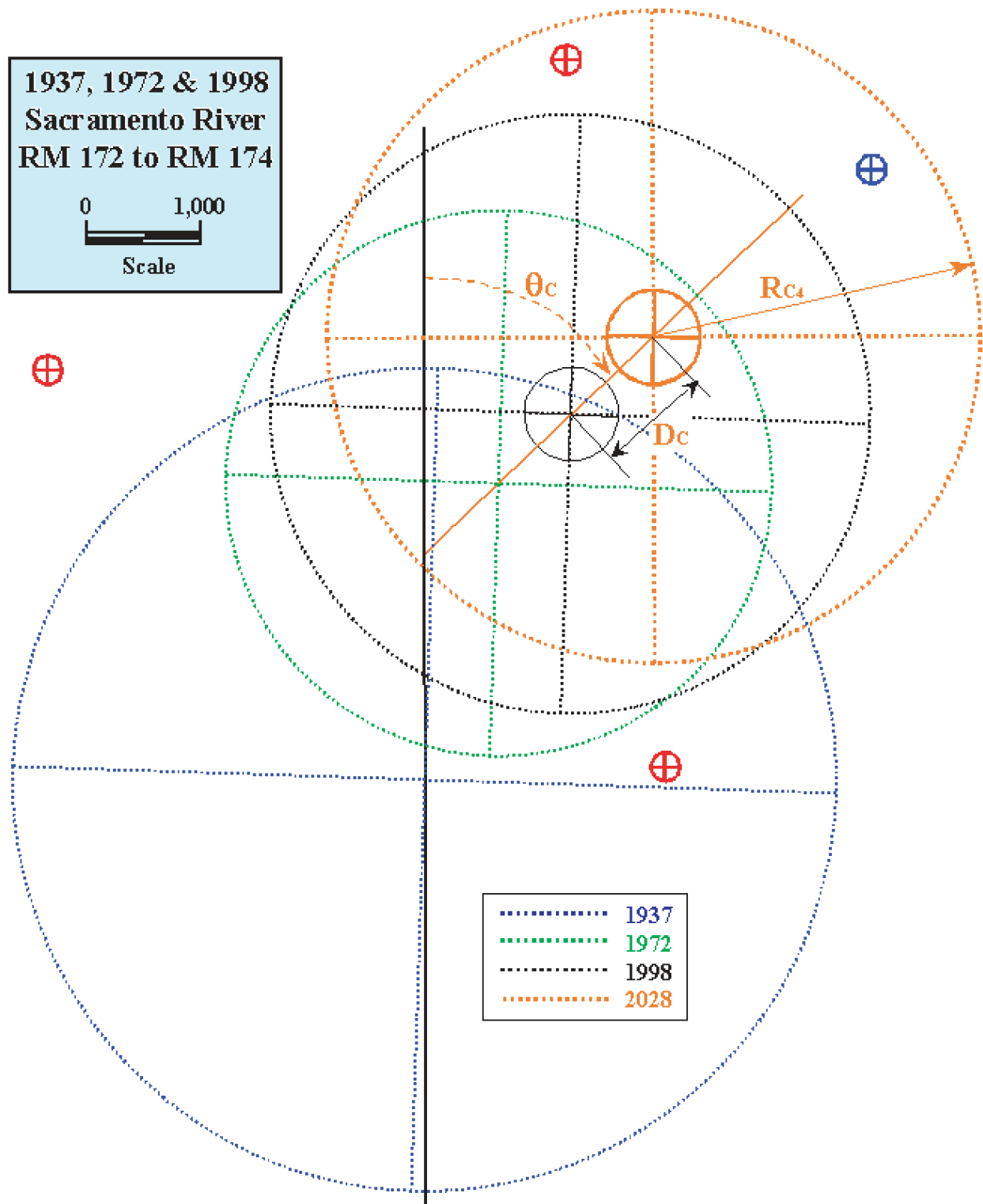
Figure 8.13.   Prediction of bend migration for the period from 1998 to 2028 and the predicted position of the outer bank of the bend in 2028. (RM = river mile.)

Based on past channel configurations, the predicted channel banklines for the year 2028 can be drawn and then superimposed on the 1998 aerial photo. The predicted channel banklines for the year 2028 can be drawn based on past channel configurations and then superimposed on the 1998 aerial photo (see Figure 8.14) to determine the potential hazard to local structures and features posed by continued active migration over the next 30 years. On the basis of the predicted position of the channel in 2028, it appears that a local levee is in the direct path of the migrating bend.

8.4.2 Method Using GIS Applications

All of the steps described in the previous paragraphs can be accomplished using CAD and GIS software. For example, two and three historic aerial photos and maps for more than 1,500 bends were used to evaluate meander migration under NCHRP Project 24-16. In order to accomplish this rapidly and accurately, Bentley's MicroStation was used to import and register corrected and georeferenced aerial photos and topographic maps, and Bentley's Descartes was used to adjust scanned (uncorrected) aerial photos for distortion during the registration process. The banklines for each year were delineated and general measurements were taken using MicroStation. The historic banklines were then exported to files that could be used with the ArcView-based Data Logger and Channel Migration Predictor described in Sections 5.4 and 7.4.

8.5 EXAMPLE USING FREQUENCY ANALYSIS

The results of the previous example of the Sacramento River bend near Butte City, California, are shown below compared with a frequency analysis. To use the frequency results, the rates of extension and translation are selected from Table 7.1 or from Figures 7.31 and 7.32 for a specific channel class (in this case a C site). These rates are then mul-

tiplied by the channel width and time period of interest to arrive at amounts of bend translation and extension. The calculations are shown in Table 8.2 using the C site percentages, a 30-year period, and a channel width (average of the upstream and downstream crossing widths) of 1,000 ft for this site. The 30-year movement of the bend, excluding change in radius, can be plotted by shifting the existing bend by the amounts computed for extension and translation. These amounts are shown in Figure 8.15.

Figure 8.15 shows that the predicted rate of movement for this bend matches the 75-percent frequency bankline very well. At the 75-percent level, three-quarters of C Class bends have moved at a rate less than the predicted rate and one-quarter of C Class bends have moved at a rate higher than the predicted rate. The results do not indicate that the predicted amount is unreasonable, just that it is greater than average. If the predicted rate seems high, then the user should check the accuracy of photo registration, the accuracy and consistency of the banklines and circle fit, and the calculations of translation and extension. Even if the rates appear high, they may not be wrong. The bend may actually be migrating at a high rate. Whether this rate will continue into the future depends on hydrologic variability, bank material characteristics, and land use change, which are not considered in the extrapolation method or the frequency analysis other than by the assumption that past conditions will persist into the future.

Another potential use of the frequency results would be at a site where historic photos are unavailable. If one had a current aerial photo and no other information at a site, one could use the frequency rates to assess potential bend migration. The only conclusion that could be drawn from the frequency analysis is that for this class of channel the measured bends in the database have moved at the indicated rates and frequencies. Clearly, if the Sacramento River bend near Butte City is allowed to migrate unconfined, channel migration into the levee is likely within 10 to 20 years.
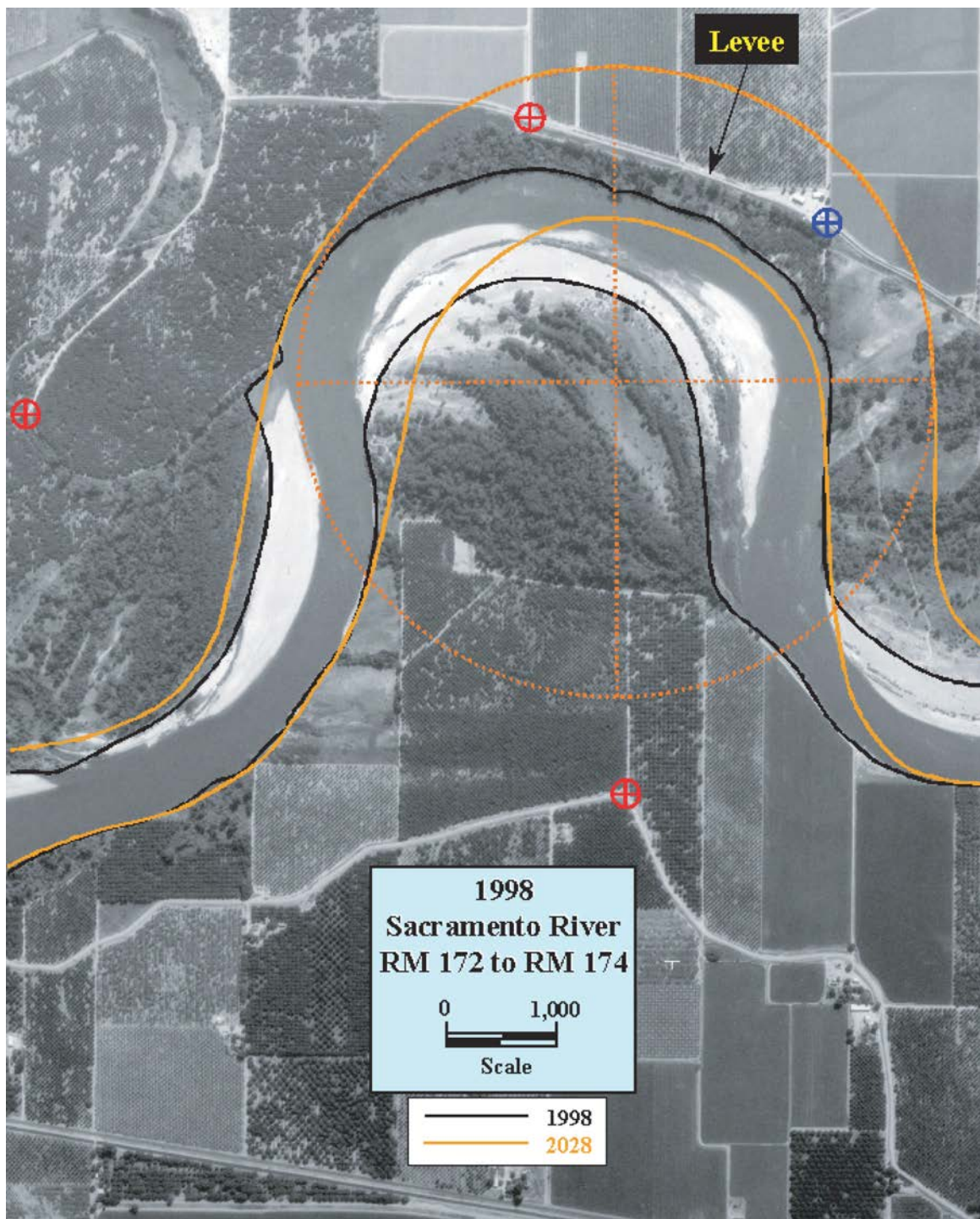
Figure 8.14.   Overlay of the predicted channel position in 2028 on the 1998 aerial photograph of the Sacramento River near Butte City, California. Note the threat to the local levee. (RM = river mile.)

TABLE 8.2   Frequency calculations for Sacramento River example

Cumulative Percent	25	50	75	90	95
			Extension		
C Sites (channel widths/yr)	0.0011	0.008	0.018	0.032	0.045
x 1,000 ft width (ft/yr)	1.1	8.0	18	32	45
x 30 years (ft in 30 yrs)	33	240	540	960	1350
			Translation		
C Sites (channel widths/yr)	0.005	0.015	0.031	0.055	0.074
x 1,000 ft width (ft/yr)	5.0	15	31	55	74
x 30 years (ft in 30 yrs)	150	450	930	1650	2220
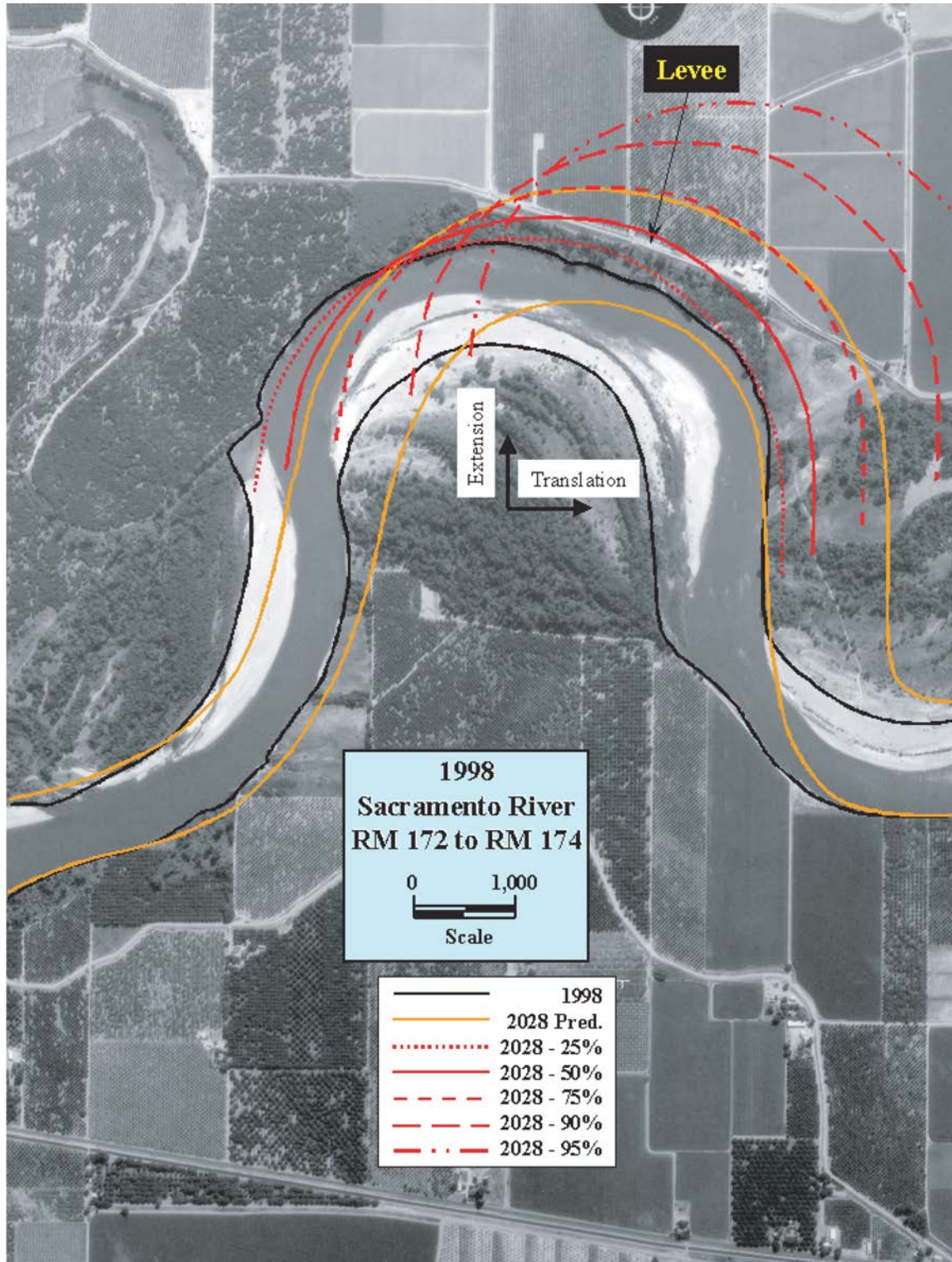
Figure 8.15.   Bend movement for C Class frequencies. (RM = river mile.)

CHAPTER **9**

SUMMARY

Rivers prone to channel migration may be spanned by structures and paralleled by fixed highway alignments and other appurtenances. Channel migration (alluvial river meander planform deformation) is a major consideration in designing bridge crossings and other transportation facilities in affected areas; it causes the channel alignment and approach conditions present during construction to deteriorate as the upstream channel location changes. Channel migration can result in the following: (1) excessive bridge pier and abutment scour, (2) flanking of bridge approaches and other highway infrastructure, (3) excessive scour because of debris problems, and (4) obstructed conveyance through bridge openings.

Channel migration includes lateral channel shift (expressed in terms of distance moved perpendicular to the channel centerline per year) and down-valley migration (expressed in distance moved along the valley per year). Engineers are concerned about predicting channel migration as it moves through the bridge elements (piers and abutments) or endangers other highway infrastructure during the design life of the structure.

The *Handbook* will assist practicing engineers in locating and designing new bridges, highway facilities, or other structures to accommodate anticipated channel migration. The techniques developed in the *Handbook* could also be used to evaluate the risk to existing facilities and, if necessary, determine the need for, and design of, measures to counteract the effects of channel migration. A reliable prediction of channel migration could also alert bridge inspection personnel to the potential for channel change that could affect the safety of a bridge. In addition, the techniques developed in the *Handbook* can be applied to channel restoration and stabilization efforts.

The map and aerial photo comparison and frequency analysis techniques provide a practical quantitative methodology for predicting channel migration in proximity to transportation facilities. The *Handbook* will be useful in reconnaissance, design, rehabilitation, maintenance, and inspection of highway facilities. The result will be a more efficient use of highway resources and a reduction in costs associated with the impacts of channel migration on highway facilities. The prediction techniques can also be used by other practitioners responsible for river channel maintenance, river restoration/rehabilitation, and floodplain planning and management.

REFERENCES

Bagnold, R. A., 1960. *Some Aspects of the Shape of River Meanders,* U.S. Geological Survey Professional Paper 282-E.

Bathurst, J. C., Thorne, C. R., and Hey, R. D., 1979. "Secondary Flow and Shear Stress at Bends," American Society of Civil Engineers, *Journal of Hydraulics* (HY10), Vol. 105, pp. 1277–1295.

Biedenharn, D. S., Combs, P. G., Hill, G. J., Pinkard, C. F., and Pinkston, C. B., 1989. "Relationship Between Channel Migration and Radius of Curvature on the Red River," in Wang, S. Y. (ed.), *Sediment Transport Modeling: Proceedings of the International Symposium,* American Society of Civil Engineers, New York, pp. 536–541.

Brice, J. C., 1974. "Evolution of Meander Loops," *Geological Society of America Bulletin,* Vol. 85, pp. 581–586.

Brice, J. C., 1975. *Air Photo Interpretation of the Form and Behavior of Alluvial Rivers,* Final Report to the U.S. Army Research Office—Durham, Washington University, St. Louis, 10 p.

Brice, J. C., 1977. *Lateral Migration of the Middle Sacramento River, California,* U.S. Geological Survey, Water Resources Investigations 77–43, 551 p.

Brice, J. C., 1982. *Stream Channel Stability Assessment,* Federal Highway Administration, Offices of Research and Development, Report No. FHWA/RD-82/021, 42 p.

Bryan, B. A., 1989. *Channel Evolution of the Hatchie River near the U.S. Highway 51 Crossing in Lauderdale and Tipton Counties, West Tennessee,* U.S. Geological Survey Open-File Report 89-598.

Burkham, D. E., 1972. *Channel Changes of the Gila River in Safford Valley, Arizona, 1846–1970,* United States Geological Survey Professional Paper 655-G.

Dietrich, W. E., 1987. "Mechanics of Flow and Sediment Transport in River Bends," in Richards, K. S. (ed.), *River Channels: Environment and Process,* Blackwell, Oxford, UK, pp. 179–227.

Dietrich, W. E., and Smith, J. D., 1983. "Influence of the Point Bar on Flow through Curved Channels," *Water Resources Research,* Vol. 19, pp. 1173–1192.

Fisk, H. N., 1944. *Geological Investigation of the Alluvial Valley of the Lower Mississippi River,* U.S. Army Corps of Engineers, Mississippi River Commission, Vicksburg, Mississippi.

Fisk, H. N., 1947. *Fine Grained Alluvial Deposits and Their Effects on the Mississippi River Activity,* U.S. Army Corps of Engineers Waterways Experiment Station, Vicksburg, Mississippi.

Harvey, M. D., 1989. "Meanderbelt Dynamics of the Sacramento River," *Proceedings, California Riparian Systems Conference,* USDA Forest Service General Technical Report PSW-110, pp. 54–61.

Hickin, E. J., and Nanson, G. C., 1975. "The Character of Channel Migration on the Beaton River, Northeast British Columbia, Canada," *Geological Society of America Bulletin,* Vol. 86, pp. 487–494.

Hickin, E. J., and Nanson, G. C., 1984. "Lateral Migration Rates of River Bends," American Society of Civil Engineers, *Journal of Hydraulic Engineering,* Vol. 110, pp. 1557–1567.

Hooke, J. M., 1977. "The Distribution and Nature of Changes in River Channel Patterns: The Example of Devon," in Gregory, K. J. (ed.), *River Channel Changes,* John Wiley & Sons, Chichester, UK, pp. 265–280.

Hooke, J. M., 1984. "Changes in River Meanders: A Review of Techniques and Results of Analysis," *Progress in Physical Geography,* Vol. 8, pp. 473–508.

Hooke, J. M., 1987. "Changes in Meander Morphology," in Gardiner, V. (ed.), *International Geomorphology, 1986: Proceedings of the First International Conference on Geomorphology,* John Wiley & Sons, Chichester, UK, pp. 591–609.

Hooke, J. M., 1991. "Non-Linearity in River Meander Development: Chaos Theory and Its Implications," Working Paper No. 19, Department of Geography, University of Portsmouth, Hampshire, UK, 22 p.

Hooke, J. M., 1997. "Styles of Channel Change," in Thorne, C. R., Hey, R. D., and Newsom, M. D. (eds.), *Applied Fluvial Geomorphology for River Engineering and Management,* John Wiley & Sons, Chichester, UK, pp. 237–268.

Klingeman, P. C., Beschta, R. L., Komar, P. D., and Bradley, J. B. (eds.), 1998. *Gravel-Bed Rivers in the Environment,* Water Resources Publications, LLC, Highlands Ranch, Colorado, 832 p.

Knighton, D., 1998. *Fluvial Forms and Processes—A New Perspective,* John Wiley & Sons, New York, 383 p.

Lagasse, P. F., Schall, J. D., Richardson, E. V., 2001. *Stream Stability at Highway Structures,* Third Edition, Report No. FHWA NHI 01-002, Federal Highway Administration, Hydraulic Engineering Circular No. 20, U.S. Department of Transportation, Washington, D.C.

Lagasse, P. F., Zevenbergen, L. W., Spitz, W. J., and Thorne, C. R., 2003. "Methodology for Predicting Channel Migration," Final Report for NCHRP Project 24-16, prepared by Ayres Associates, Transportation Research Board of the National Academies, Washington, D.C.

Langbein, W. B., and Leopold, L. B., 1966. *River Meanders—Theory of Minimum Variance,* U.S. Geological Survey Professional Paper 422-H.

Leopold, L. B., and Wolman, M. G., 1957. *River Channel Patterns—Braided, Meandering, and Straight,* U.S. Geological Survey Professional Paper 282-B, pp. 39–85.

Leopold, L. B., and Wolman, M. G., 1960. "River Meanders," *Geological Society of America Bulletin,* Vol. 71.

Lohnes, R., and Handy, R. L., 1968. "Slope Angles in Friable Loess," *Journal of Geology,* Vol. 76, pp. 247–258.

Markham, A. J., and Thorne, C. R., 1992. "Geomorphology of Gravel-Bed River Bends," in Billi, P., Hey, R. D., Thorne, C. R., and Tacconi, P. (eds.), *Dynamics of Gravel-Bed Rivers,* John Wiley & Sons, Chichester, UK, pp. 433–450.

Miall, A. D., 1977. "A Review of the Braided-River Depositional Environment," *Earth-Science Reviews,* Vol. 13, pp. 1–60.

Montgomery, D. R., and Buffington, J. M., 1997. "Channel-Reach Morphology in Mountain Drainage Basins," *Geological Society of America Bulletin,* Vol. 109, No. 5, pp. 596–611.

Nanson, G. C., and Hickin, E. J., 1986. "A Statistical Analysis of Bank Erosion and Channel Migration in Western Canada," *Geological Society of America Bulletin,* Vol. 97, pp. 497–504.

National Transportation Safety Board (NTSB), 1990. *Collapse of the Northbound U.S. Route 51 Bridge Spans over the Hatchie River near Covington, TN, April 1, 1989,* Highway Accident Report No. NTSB/HAR-90/01, Washington, D.C.

Neil, C. R. (ed.), 1973. *Guide to Bridge Hydraulics,* University of Toronto Press.

Rosgen, D. L., 1994. "A Classification of Natural Rivers," *Catena,* Vol. 22, pp. 169–199.

Ruhe, R. V., 1975. *Geomorphology,* Houghton Mifflin, Boston.

Schumm, S. A., 1968. *River Adjustment to Altered Hydrologic Regime—Murrumbidgee River and Paleochannels, Australia,* U.S. Geological Survey Professional Paper 598.

Schumm, S. A., 1977. *The Fluvial System,* John Wiley & Sons, New York, 338 p.

Schumm, S. A., 1981. "Evolution and Response of the Fluvial System, Sedimentologic Implications," *SEPM Special Publication 31,* pp. 19–29.

Schumm, S. A., and Meyer, D. F., 1979. "Morphology of Alluvial Rivers of the Great Plains," *Great Plains Agricultural Council Publication 91,* pp. 9–14.

Smith, S. A., and Smith, N. D., 1980. "Sedimentation in Anastomosed River Systems: Examples from Alluvial Valleys near Banff, Alberta," *Journal of Sedimentary Petrology,* Vol. 50, pp. 157–164.

Thompson, A., 1986. "Secondary Flows and the Pool-Riffle Unit: A Case Study of the Processes of Meander Development," *Earth Surface Processes and Landforms,* Vol. 11, pp. 631–641.

Thorne, C. R., 1981. "Field Measurements of Rates of Bank Erosion and Bank Material Strength," in *Erosion and Sediment Transport Measurement, IAHS Publication No. 133,* pp. 503–512.

Thorne, C. R., 1992. "Bend Scour and Bank Erosion on the Meandering Red River, Louisiana," in Carling, P. A., and Petts, G. E. (eds.), *Lowland Floodplain Rivers—Geomorphological Perspectives,* John Wiley & Sons, Chichester, UK, pp. 95–115.

Thorne, C. R., 1997. *Channel Types and Morphological Classification* (Chapter 7), in Thorne, C. R., Hey, R. D., and Newsom, M. D. (eds.), *Applied Fluvial Geomorphology for River Engineering and Management,* John Wiley & Sons, Chichester, UK, pp. 175–222.

U.S. Bureau of the Budget, 1941, 1943, 1947. *United States Map Accuracy Standards.* National Mapping Program Standards, U.S. Geological Survey. Available at http://geography.usgs.gov/standards/.

Water Engineering and Technology, Inc. (WET), 1988. *Geomorphic Analysis of Sacramento River, Phase I Report: Geomorphic Analysis of Butte Basin Reach, River Mile 174 to River Mile 194,* Prepared for U.S. Army Corps of Engineers, Sacramento District, Contract No. DACW05-87-C-0094.

Water Engineering and Technology, Inc. (WET), 1990. *Geomorphic Analysis of Sacramento River, Phase II Report: Geomorphic Analysis of Reach from Colusa to Red Bluff Diversion Dam, River Mile 143 to River Mile 243,* Prepared for U.S. Army Corps of Engineers, Sacramento District, Contract No. DACW05-87-C-0094.

Williams, G. P., 1978. *The Case of the Shrinking Channels—the North Platte and Platte Rivers in Nebraska,* United States Geological Survey Circular 781.

Wolf, P. R., and Dewitt, B. A., 2000. *Elements of Photogrammetry with Applications in GIS* (3rd ed.), McGraw-Hill, Boston, 608 p.

APPENDIX A

DOWNLOADING MICROSOFT TERRASERVER IMAGES FROM THE INTERNET

One of the most useful sources of contemporary aerial photography and topographic maps is the Microsoft TerraServer Web site (http://terraserver.homeadvisor.msn.com/). Figure A.1 shows the homepage of the TerraServer Web site. Information about navigating the Web site is available under the "About" tab, but the basic steps to downloading imagery from this site are provided here.

There are several ways of locating imagery at the TerraServer Web site. The primary method is to type the name of a town or geographic feature near the area of interest in the box labeled "Search TerraServer" shown in Figure A.1. One can also left-click the mouse pointer on a spot on one of the green areas of the world map. If the geographic coordinates of a specific site are known, the user can left-click on the "Advanced Find" tab, which will send the user to the "Advanced Find" page shown in Figure A.2a. The user can search for a specific address, place, or stream gauge, or the user can search using geographic coordinates, as shown in Figure A.2b.

When the user types in the name of the place of interest, a page may appear that has multiple listings with the same name from which the user can choose (see Figure A.3). This "Find Results" page lists available aerial photography and topographic maps for the various sites with the same place name. Once the user has chosen a particular location, left-clicking the mouse button on the image of choice brings up the image page. Figure A.4 shows the image page with a portion of a topographic map for an area near Judson, Minnesota, and Figure A.5 shows the page with an aerial photograph for the same area. The toolbar at the top of the map or photo image page contains several tabs that allow the user to adjust the size of the image viewed, to zoom the image, to view the scale and coordinate details of the image, and to download the image. A zoom bar allows the user to zoom the image, and the arrows around the image are used to move the image laterally.

The types of topographic map images shown are dependent on the resolution chosen. For example, map images with resolutions of 4 m or greater are from 7.5-minute series topographic quadrangle maps (scale 1:24,000). Map images with resolutions between 16 m and 4 m are 15-minute topographic quadrangle maps (scale 1:62,500), and images with map resolutions less than 16 m are 1 degree × 2 degree topographic maps (scale 1:250,000). TerraServer images of aerial photographs are also based on the image resolution chosen.

Each image of a map or aerial photograph has a resolution based on the number of pixels that make up the image. For example, the images shown in Figures A.4 and A.5 have resolutions of 16 m, meaning that each image pixel covers 16 m. To determine the number of pixels in each image, as well as the coordinates of the image, the user selects the "Info" tab at the top of screen as shown in Figures A.4 and A.5. The "Image Info" page (see Figure A.6) provides the image size in pixels, the size of each pixel, the coordinates of the image, the date the image was photographed, and the Universal Transverse Mercator Zone on which the image is projected.

The images can be downloaded and saved in JPEG format. In addition, World Files containing the image coordinates and other information in ASCII format can be downloaded or printed out for use with GIS applications. The "Download" tab at the top of the screen (as shown in Figures A.4 and A.5) is selected for downloading the image shown. The image can be downloaded free of charge (see Figure A.7).

The number of images that will need to be downloaded is dependent on the resolution required and the area of coverage. The more the image is zoomed in, the greater the resolution and the greater the amount of visible detail. However, the user will need to download and splice together a greater number of the high-resolution images to cover a specified area. This is easily done using the World Files in GIS and CAD software, but it can also be done easily using most graphics-editing software.
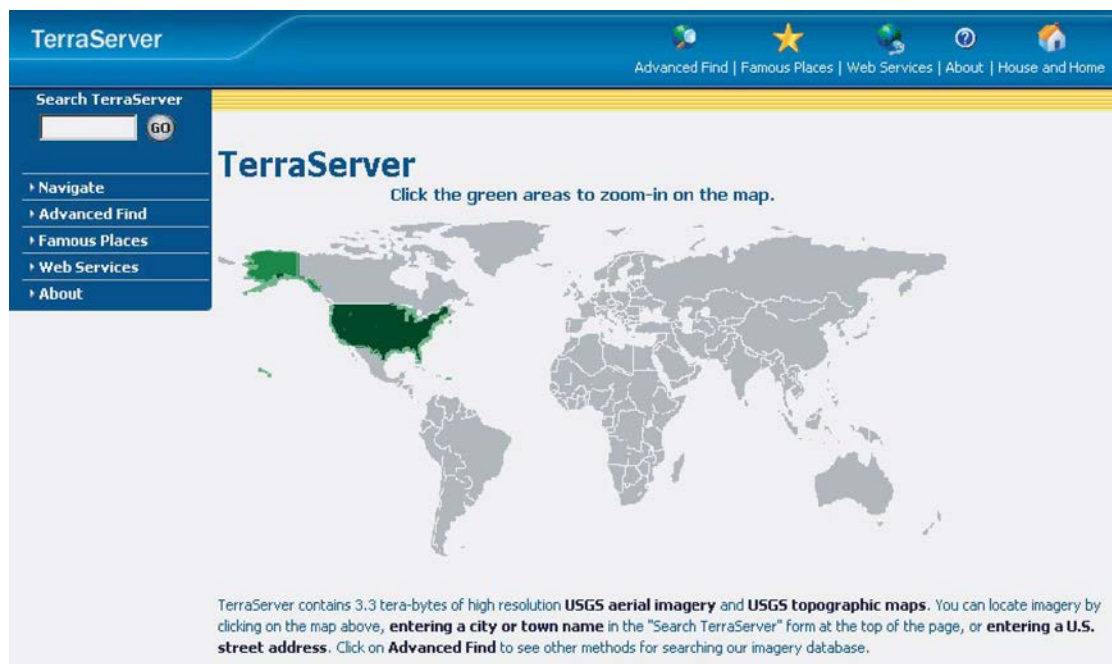
Figure A.1.   Home page for Microsoft's TerraServer Web site.

Figure A.2.   Two TerraServer pages: (a) the "Advanced Find" page, which allows for searches to be conducted using addresses, place names, stream gauges, and geographic coordinates and (b) the "Geographic Coordinate Search" page.

Figure A.3. TerraServer "Find Results" page with multiple map and aerial photo listings for sites with the same place name (Judson).
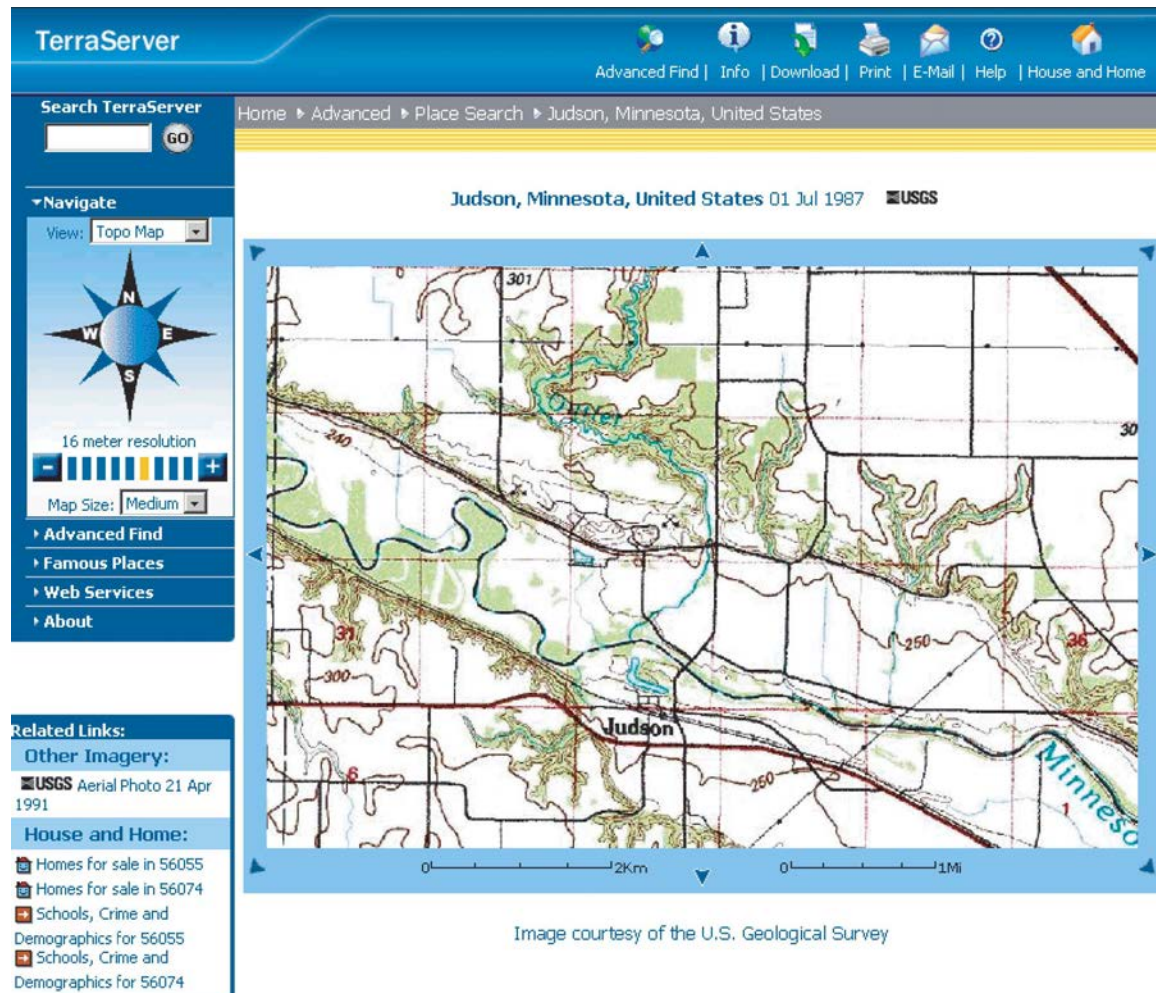
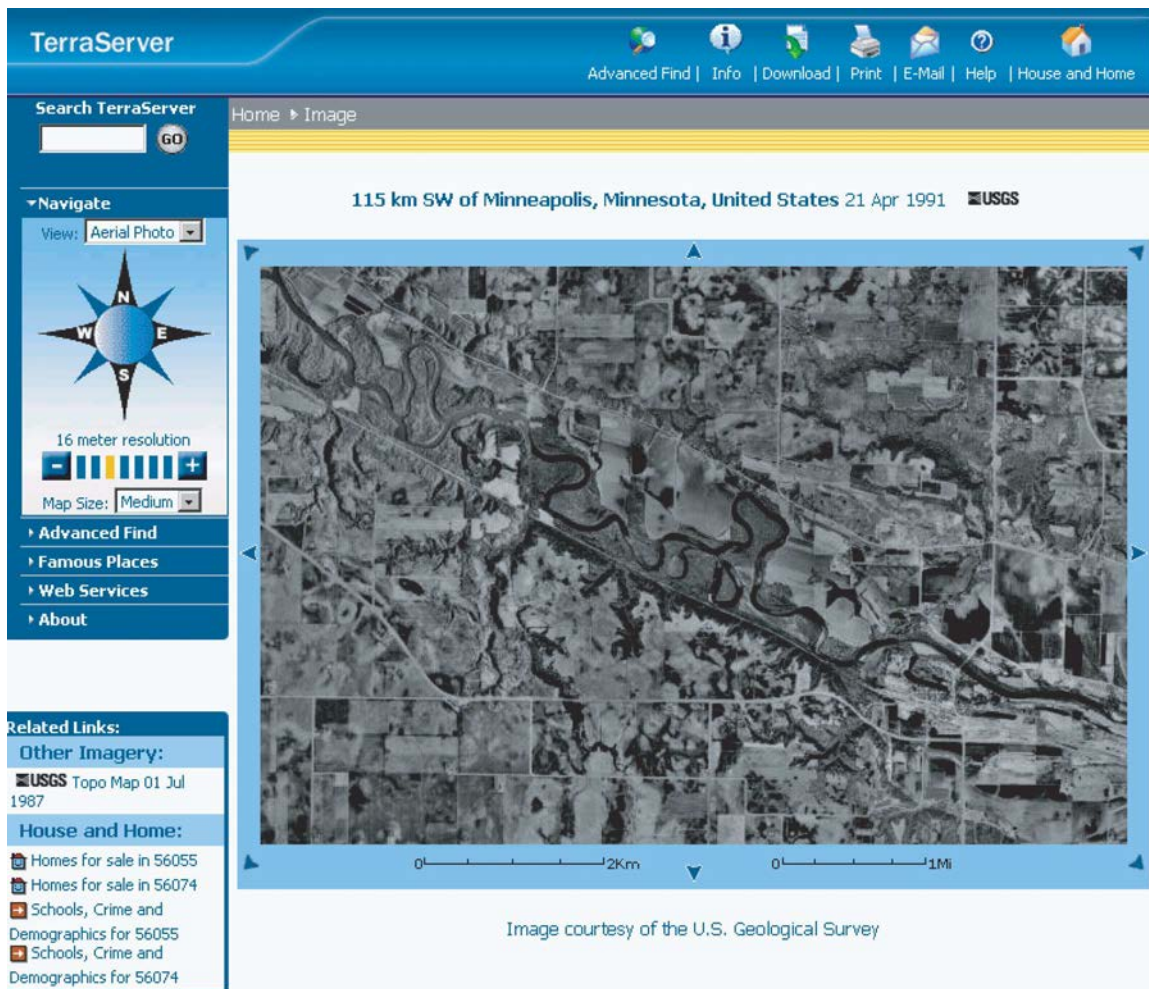*Figure A.4.   TerraServer topographic map page for Judson, Minnesota.*

Figure A.5.   TerraServer aerial photograph page for Judson, Minnesota.

Image Info

Info: Digital Ortho-Quadrangles (digitized and othro-rectified aerial photographs

Provider: U.S. Geological Survey. To find out more about this image, visit the USGS's **Digital Backyard**.

Image Size: 600 pixels wide by 400 pixels high.

Resolution: Each pixel represents 16 meter resolution by 16 meter resolution of earth.

Date: Photographed on 21 Apr 1991 digitized on 27 Jun 1994

Projection: The data below is projected in the Universal Transverse Mercator (UTM) Zone 15 projection using the North American datum of 1983. The decimal latitude and longitude in degrees and the UTM coordinates in meters are shown for each image tile.

Source File: J.judson_MN.ver_1.O4409455.NWS received on tape/group 079

Load Date: 3/29/1999 1:29:27 PM via job DOQ-079

Back to TerraServer

Figure A.6. TerraServer "Image Info" page with detailed information about the aerial photograph taken of an area near Judson, Minnesota.

Figure A.7.   TerraServer "Downloading USGS Aerial Image" page for an area near Judson, Minnesota.

APPENDIX B

DELINEATING BANKLINES AND BENDS

Identifying and delineating banklines is often dependent on the physical scale of the channel, the scale of the aerial photo on which the bankline is being delineated, the resolution and sharpness of the photo, and the density of the vegetation along the bankline. On good quality aerial photos, bankline features are more easily identified on large channels than on small channels. When focusing on a particular location, the optical resolution is generally poorer and the details are less discernable on aerial photos taken at higher altitudes than on those taken at lower altitudes. Sharp, high-resolution aerial photos allow the user to zoom in or focus closely on a particular location to more easily identify bankline features.

Vegetation types and density play a critical role in accurately delineating a bankline, especially when sun angles create significant shadow effects. In addition, the top of a bank on a color aerial photo is easily identified by the differences in color among the bank, the vegetation, and the water, whereas the top of a bank on a black and white aerial photo can be much more difficult to identify.

Because of the difficulty that can be encountered when delineating a bankline and determining the radius of a bend, the following guidelines are provided using a variety of examples for a number of common natural conditions.

BANKLINE DELINEATION

Banks that are naturally devoid of significant vegetation generally occur in arid or semi-arid climates, such as the desert Southwest and the high plains of the western United States, or in areas where riparian forests are nonexistent or poorly developed. Agricultural activities and urban development tend to remove vegetation along a river corridor, often close to or right up to the edge of the channel. In these cases, the bankline is easily delineated. On a black and white aerial photo, the top of the bank along an unvegetated bankline stands out in contrast to the bank slope and the channel bed or water. The bank slope, when lit by the sun, appears much lighter than the top of the bank, and water in the channel can either be darker or lighter than the top of the bank, depending on lighting conditions and the sediment load of the flow in the channel. When the bank slope is shaded, the shadows provide a sharp contrast among the top of the bank and the bank slope, water, or channel bed (see Figure B.1). Even during near-bankfull flows, the break between the top of bank and the water surface is defined by a sharp change in contrast (see Figure B.2).

However, along many rivers and streams, vegetation often partially or completely obscures the banklines, and, depending on the time of year that the aerial photography mission was flown, the vegetation can make delineation of the banklines difficult at best. Aerial photographs obtained in late fall and winter are generally better for delineating banklines because leaf-off conditions exist over much of the country. Photos obtained during the spring and summer months are difficult to use because bank features are obscured by dense leafy vegetation that overhangs and obscures the bankline. When the bankline is only partially visible, the bankline can be delineated by connecting the observable portions of the bank as shown in Figure B.3.

Because not all aerial photography is flown in the fall and winter when leaf-off conditions exist, in some photos dense vegetation can make bankline identification difficult and bankline delineation less accurate. In these cases, exposed sections of the bank should be identified where possible for use in delineating the bankline. It will then be necessary to examine the banklines over the entire photo to determine the general extent of vegetation overhang. In places where the vegetation ends and exposes the bankline, the approximate amount of overhang can be determined. The bank along obscured sections of the channel edge can be delineated by drawing a line at a distance from the edge of the vegetation equivalent to the approximate amount of the overhang. These concepts are shown in Figure B.4.

If the sun is not directly overhead at the time the photo is acquired, the crown of the vegetation at the edge of the bank can be used to locate the bankline approximately (see Figure B.4). At different sun angles, one half of the crown of a tree appears shaded while the other half is in direct sun. The contrast can be used to approximate the center of the tree, which can be used to approximately locate the bankline, assuming that the tree is located directly on top of and at the edge of the bank and is not leaning out over the channel an appreciable amount. The channel width in obscured reaches should be compared to widths in unobscured reaches to ensure that the obscured reach widths are generally consistent with unobscured reach widths.

In some cases, high flows or overbank flooding in combination with overhanging vegetation can also obscure the bankline and make delineation of the bankline difficult. In these cases, the vegetation may aid in identifying the general location of the bankline by changes in contrast as shown in Figure B.5.

Where a channel is small compared with the size of the vegetation crown, the banklines and a significant portion of the channel may be completely obscured by overhanging vegetation, as shown in Figure B.6. In these cases, delineating the banklines may be nearly impossible, and it may be necessary to define the channel and conduct a meander migration analysis using the channel centerline (see Figure
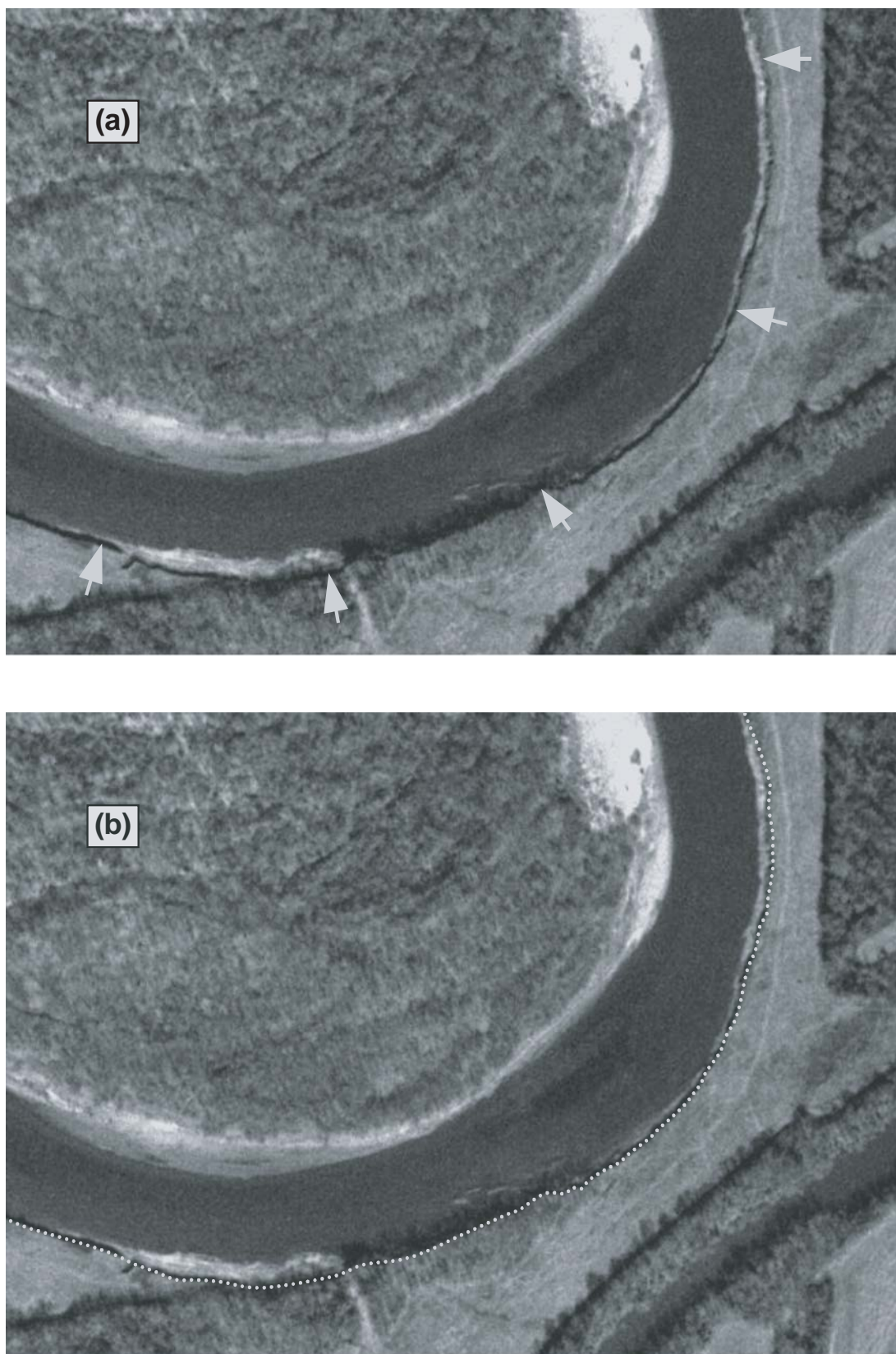
Figure B.1.   The Ouachita River during low flow near Arkadelphia, Arkansas: (a) arrows show the top of the bank; (b) the top of the bank is delineated by a dotted line.
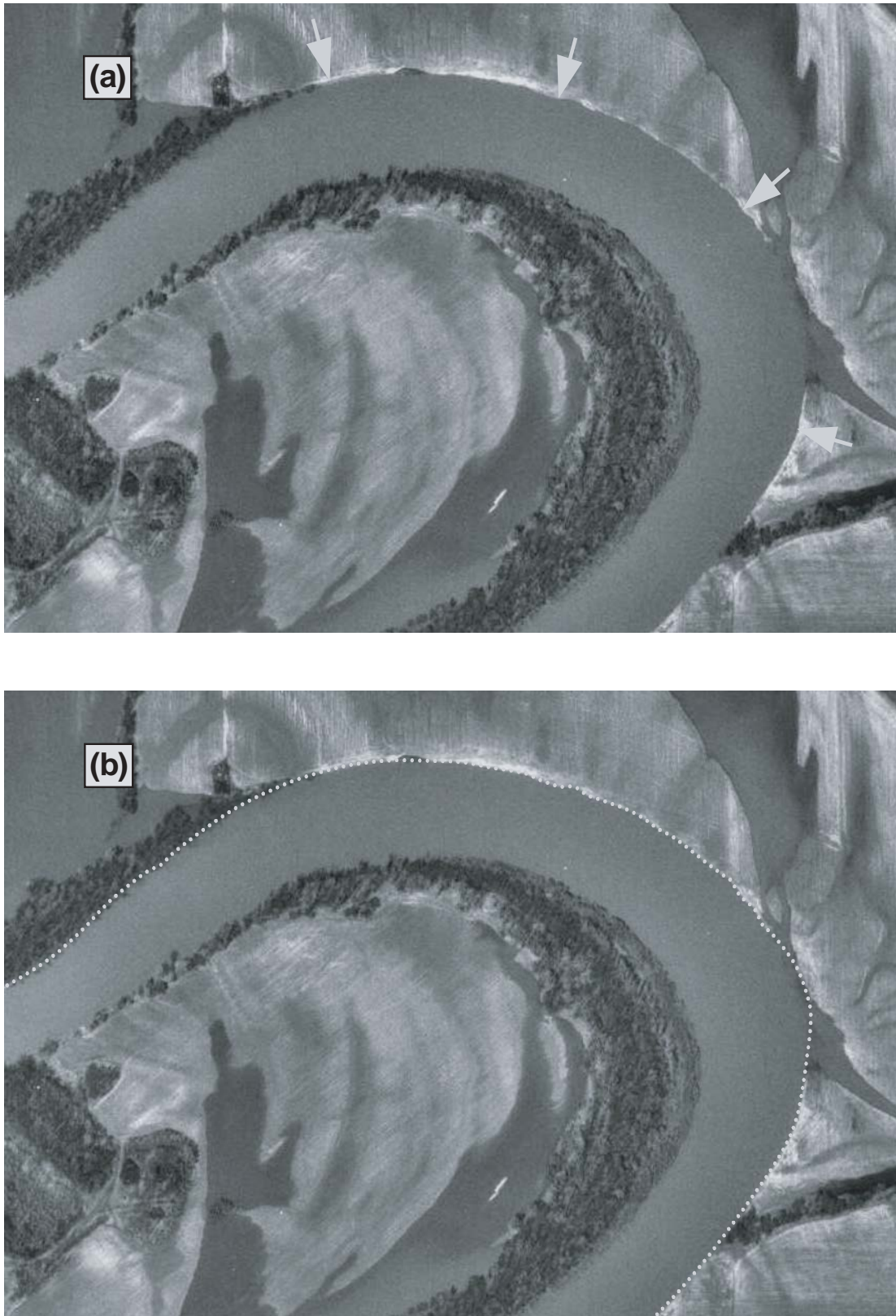
Figure B.2.   The Wabash River during high flow near Newport, Indiana: (a) arrows show the top of the bank; (b) the top of the bank is delineated by a dotted line.
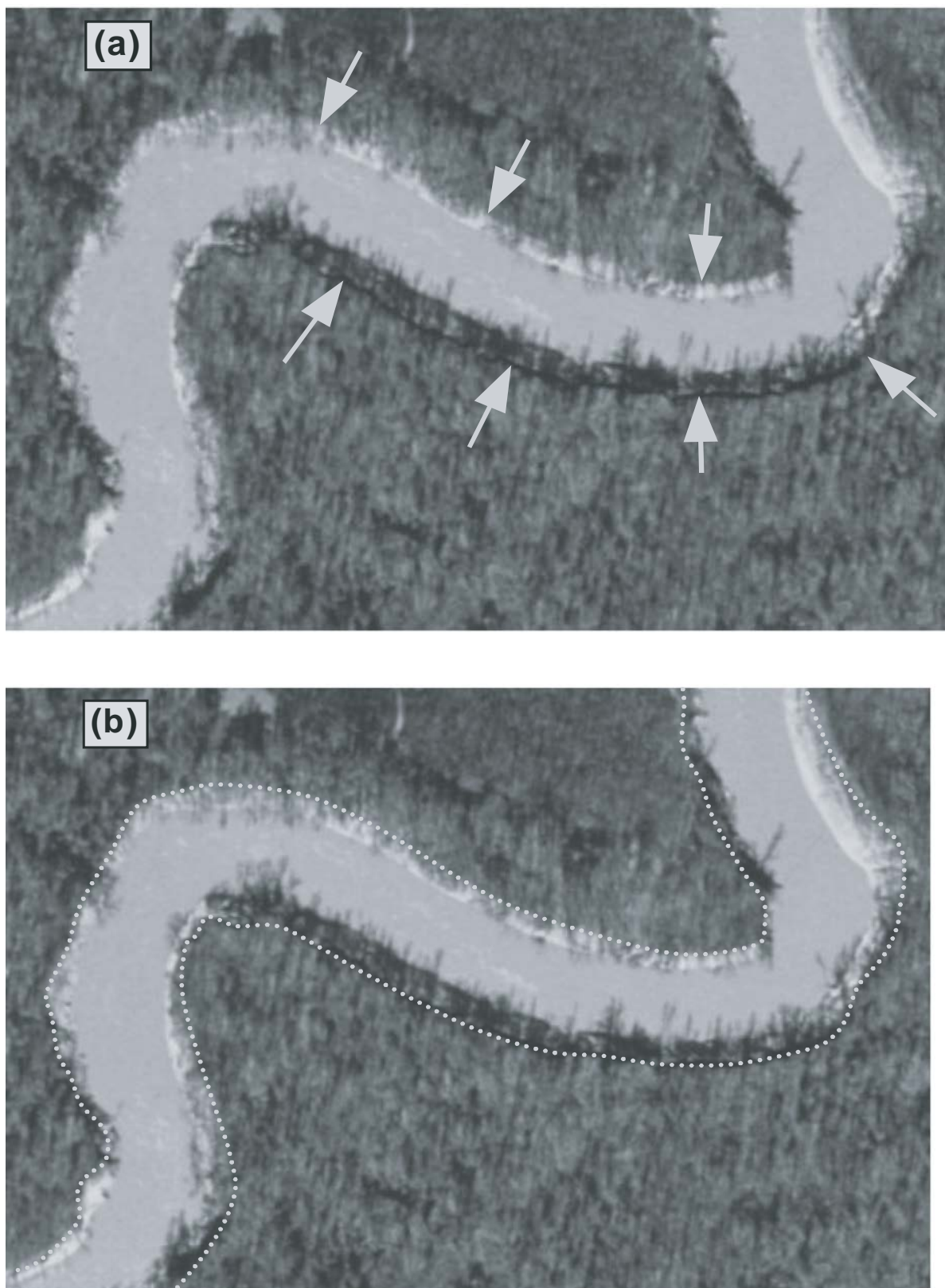
Figure B.3.   The Big Black River during low flow near Bovina, Mississippi: (a) arrows show the top of the bank; (b) the top of the bank is delineated by a dotted line.
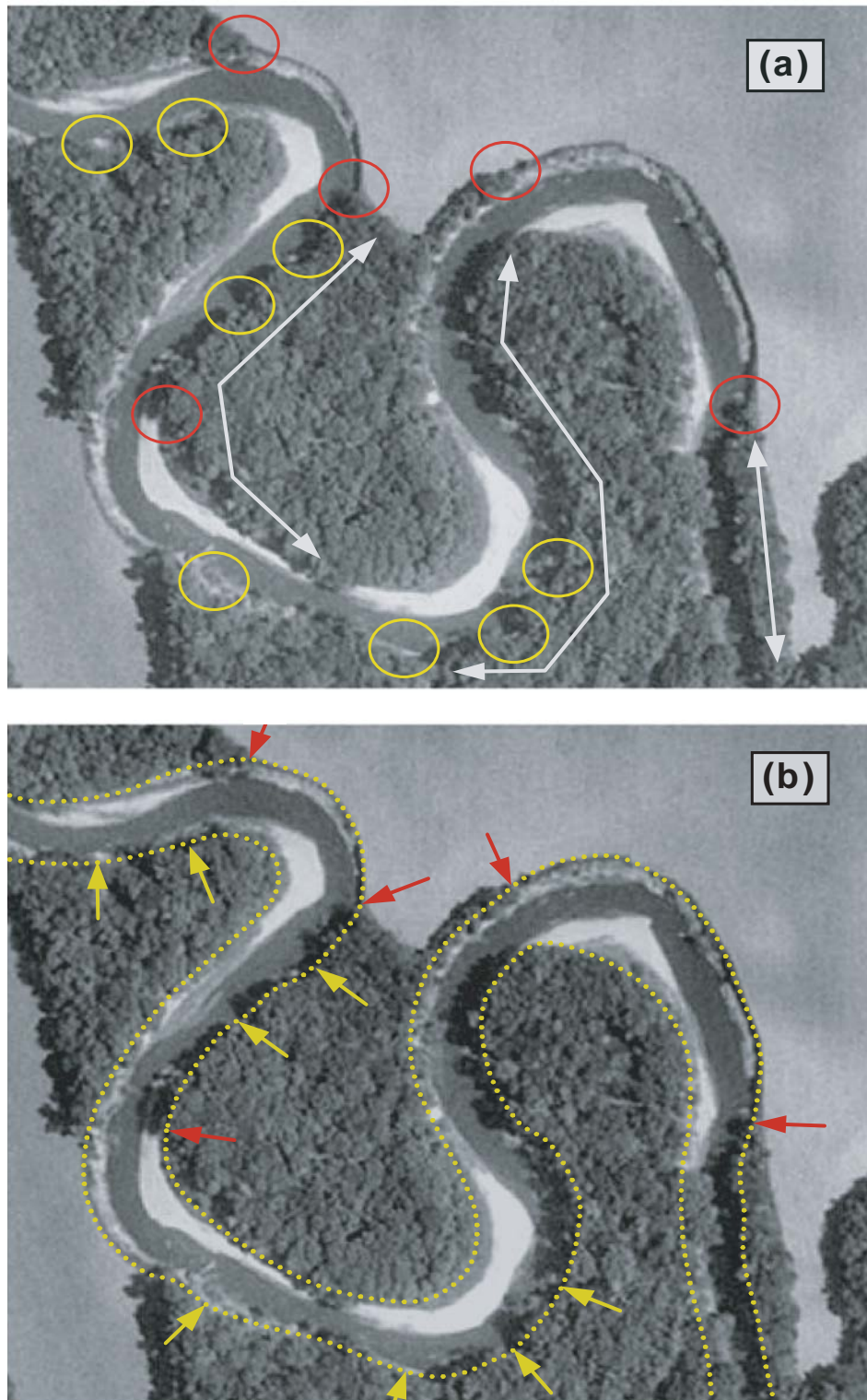
Figure B.4.   The English River near Kalona, Iowa. Yellow ovals in (a) and yellow arrows in (b) identify exposed bankline sites, and red ovals in (a) and red arrows in (b) identify overhanging vegetation sites. White arrows in (a) identify reaches where banklines are delineated using contrasts and shading of vegetation crown. The delineated banklines are shown as dotted yellow lines in (b).
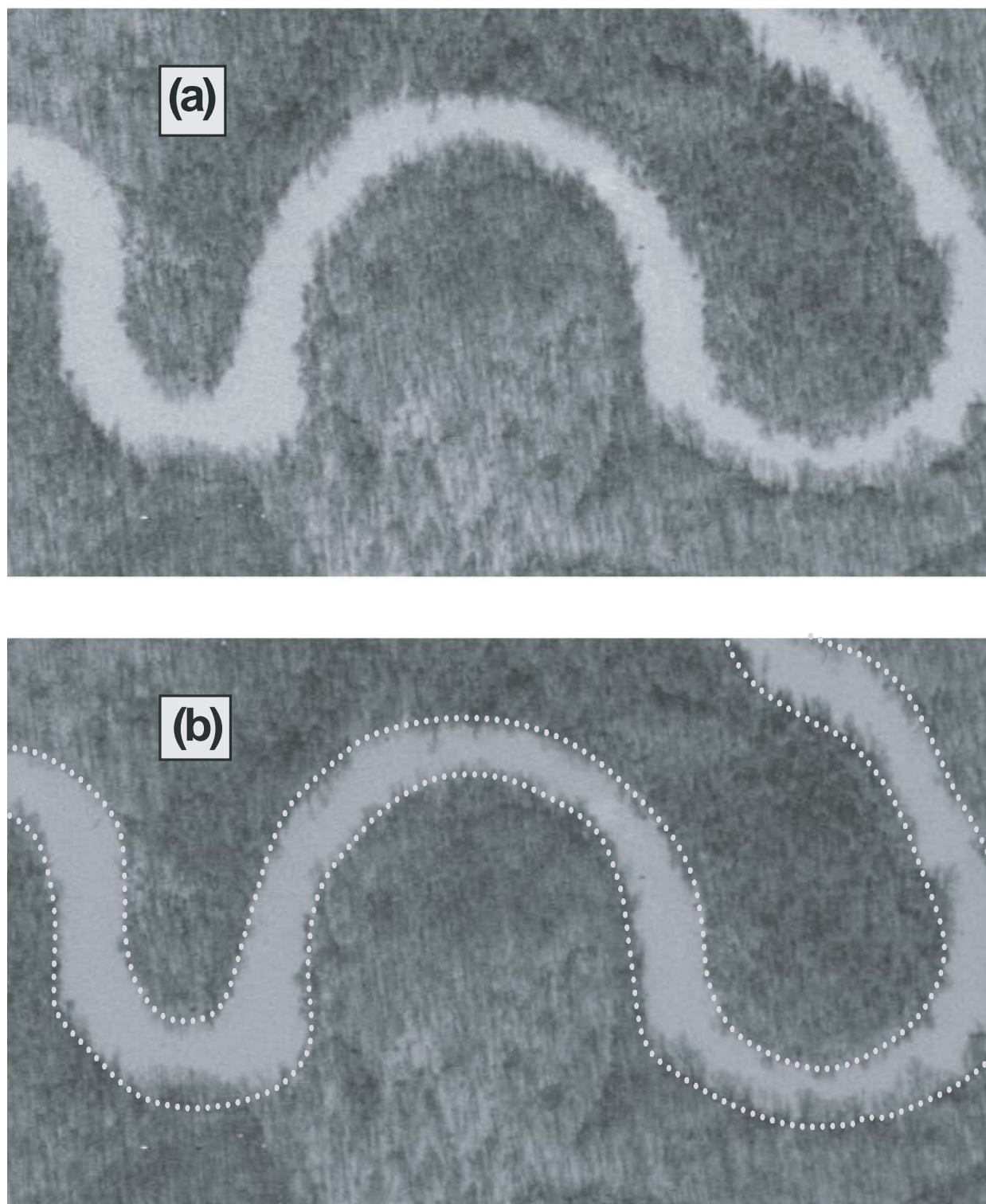
Figure B.5.   The Hatchie River near Sunnyhill, Tennessee, during high flow: (a) overbank flow in some areas obscures the bankline; (b) the approximate banklines are shown as dotted lines.

Figure B.6. The Canoochee River near Claxton, Georgia. The dense vegetation completely obscures the banklines and much of the channel. The approximate channel centerline is shown as the dotted line.

B.6). It should be noted, however, that this condition may be indicative of a relatively stable channel or a channel that is sufficiently small that it does not pose a significant threat from migration.

Finally, in some cases where channel migration is rapid, sloughs, oxbow lakes, and chutes across point bars may make identification of a continuous bankline difficult. It will be necessary in these cases to identify as much of the bankline as possible and then connect the breaks while maintaining a relatively constant channel shape. For example, Figure B.7 shows several bends with sloughs intersecting the outer bank, well-developed chutes on the point bars, and the manner in which banklines would be delineated along the bends.

BEND RADIUS DELINEATION

Bends come in all shapes, as indicated by the Brice meander loop classification diagram shown in Figure 7.4. Bends consist of four main categories of bend loop configuration: (1) simple symmetrical, (2) simple asymmetrical, (3) compound symmetrical, and (4) compound asymmetrical. For simple symmetrical and asymmetrical bends, the bend radius is generally easy to define by fitting a single circle to the outer bankline. For complex or oddly shaped bends, the delineation of the bend radius is more difficult and will depend on both the present and past shape of the bend and the portion of the bend that may be posing a hazard.

For comparative purposes, the shape of a bend in the past will determine evaluation of the shape of the bend in the present or future (see Figure B.8). For example, if the bend has been defined by a single loop in the past, it should be evaluated, if possible, as a single-loop bend in the present and the future (see the yellow circles in Figure B.9). If the bend has been defined by two distinct loops in the past, it should be evaluated, if possible, as a double-loop bend in the present and the future (see the red and blue circles in Figure B.9). If the most recent bend configuration cannot be defined by a double loop, then it may be necessary to redefine the historic bend configuration as a single loop.

As bends migrate or cut off, they may leave behind old chutes, sloughs, or oxbows that may be intersected by other bends, as shown in Figure B.10. When this occurs, delineation of the outer bank of the bend should be conducted as if the slough, chute, or oxbow were not there.
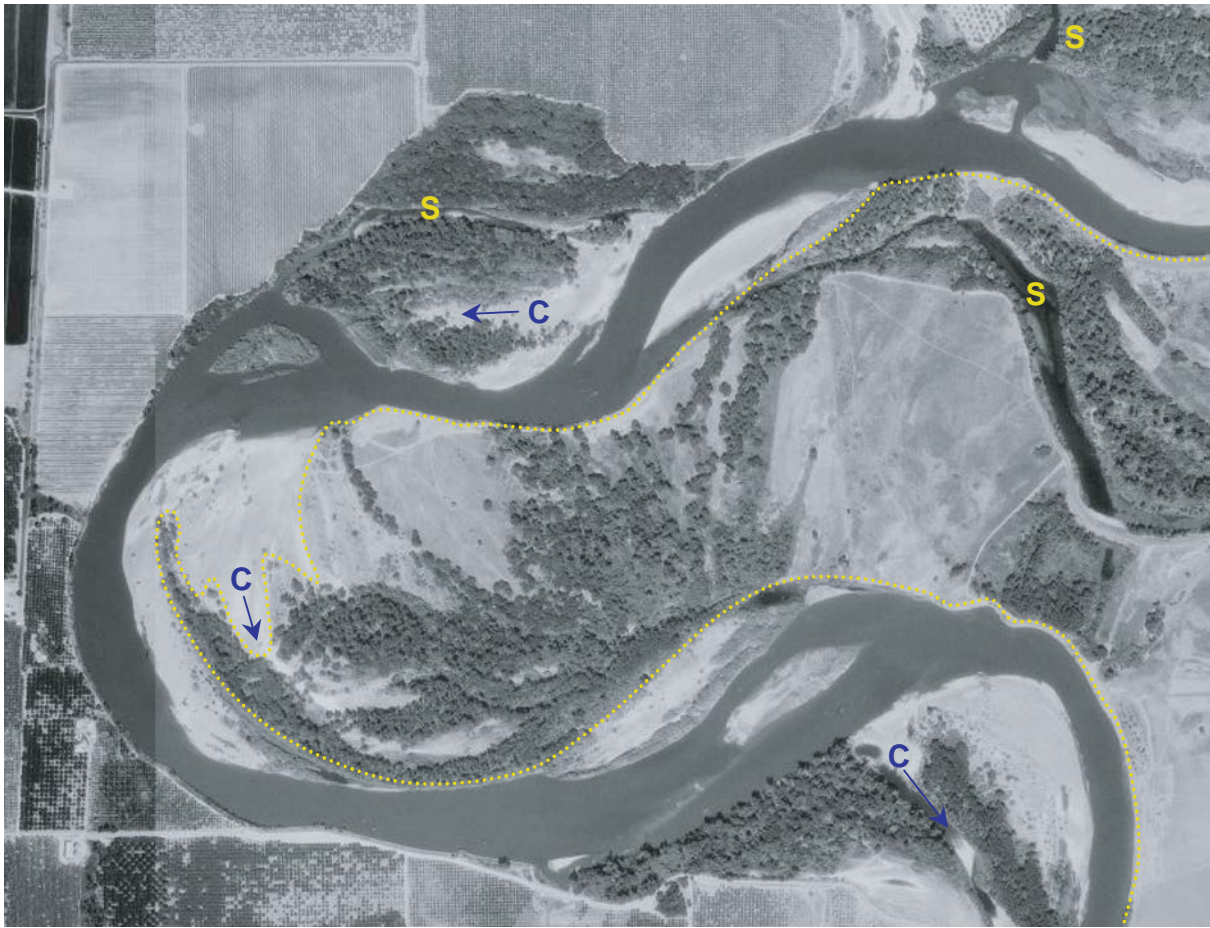
Figure B.7.   The Monroeville Bend on the Sacramento River near Ord Ferry, California, showing delineated banklines, sloughs (S), and chutes (C).
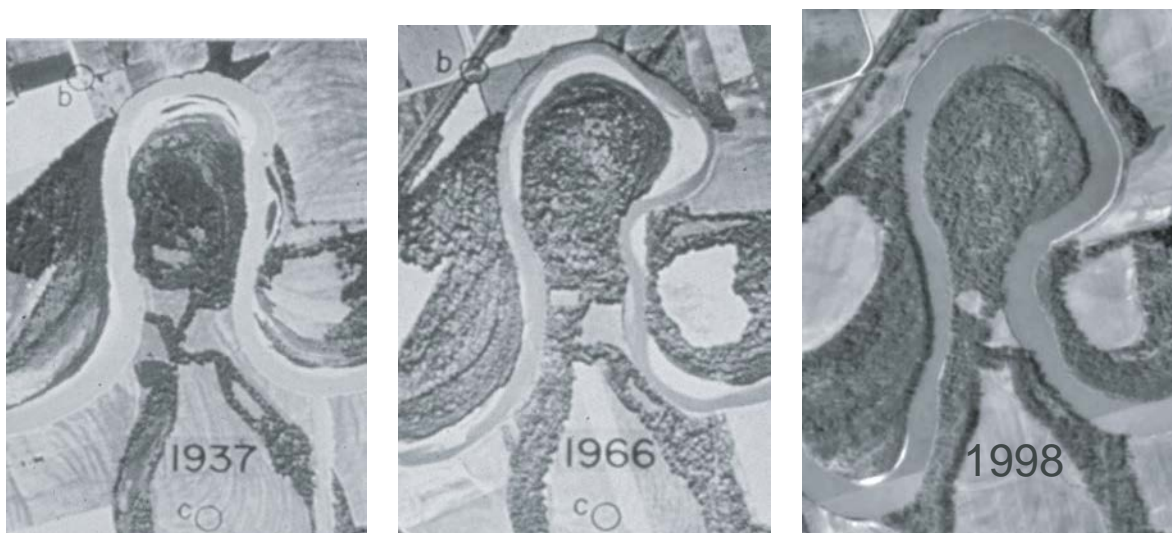

Figure B.8.   The White River site in Indiana showing the development of a simple symmetrical bend in 1937 into a compound asymmetrical bend in 1966 and 1998.
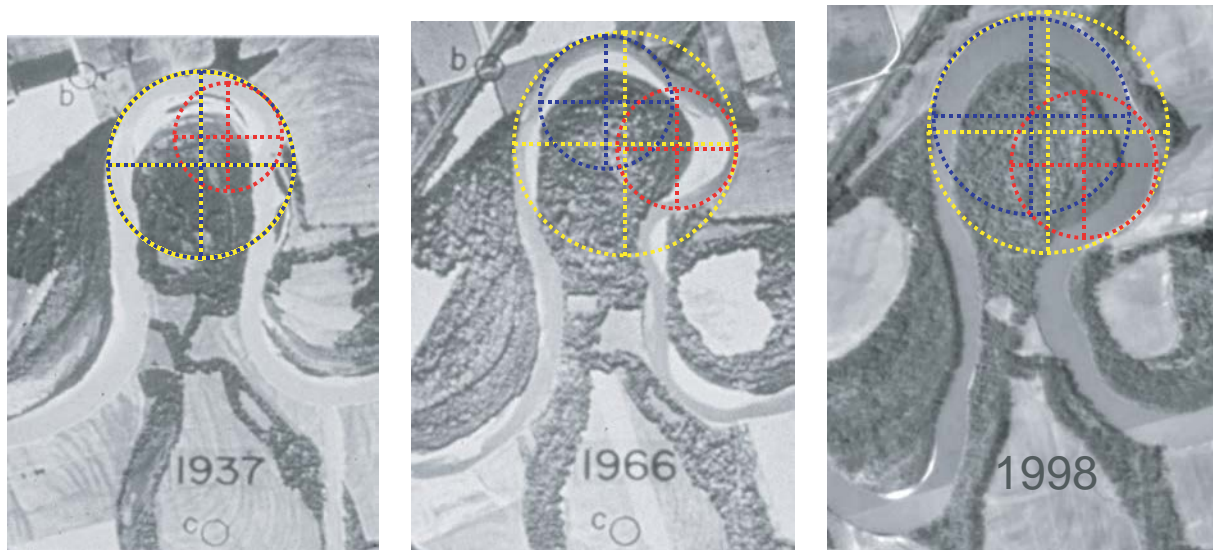
Figure B.9. The White River site in Indiana showing how the bend could be delineated by a single loop (yellow) or by two loops (red and blue).

In addition, the outer bank may be very irregular because of massive geotechnical failures or rapid retreat in areas where there are highly variable bank sediments. When this occurs, the bankline should be delineated as accurately as possible, but a circle that best describes the entire bankline should be used to identify the outer bank radius (Figure B.10).

IDENTIFYING CROSSINGS AND RIFFLES

Crossings and riffles often occupy the same general location on a river—the point where the thalweg or main flow thread crosses from one side of the channel to the other. The riffle or crossing is located approximately midway between two bends, often in the area of overlap between point bars on opposite sides of the channel. In general, the spacing between riffles or crossings is about five to seven channel widths measured along the channel centerline. Figure B.11 shows the position of riffles (or crossings) of an idealized meandering channel. If a long straight reach is present between bends, there may be more than one riffle or crossing separated by alternate bars. The difference between a crossing and a riffle is in the size of the sediment that the channel transports. Riffles are found predominantly in coarse-grained (gravel- and cobble-bed) channels; they rarely occur in sand-bed channels.

Riffles and crossings can be identified by changes in the brightness or contrast of the water on an aerial photograph. The riffle will appear as a bright area in the water because of reflection off of the turbulent water created by the riffle. Where riffles are present, flows may be low enough that an exposed or shallowly submerged bar (shoal) can be identified (see Figure B.12).

The crossing on a sand-bed channel (see Figure B.13) may be more difficult to identify, especially during higher flows when bars may be inundated. In most instances, the crossing can be identified on aerial photos by changes in the contrast or brightness of flow in the channel, but, in some cases, it may be necessary to locate the crossing by locating the midpoint between two bends or measuring five to seven channel widths from a known crossing location.
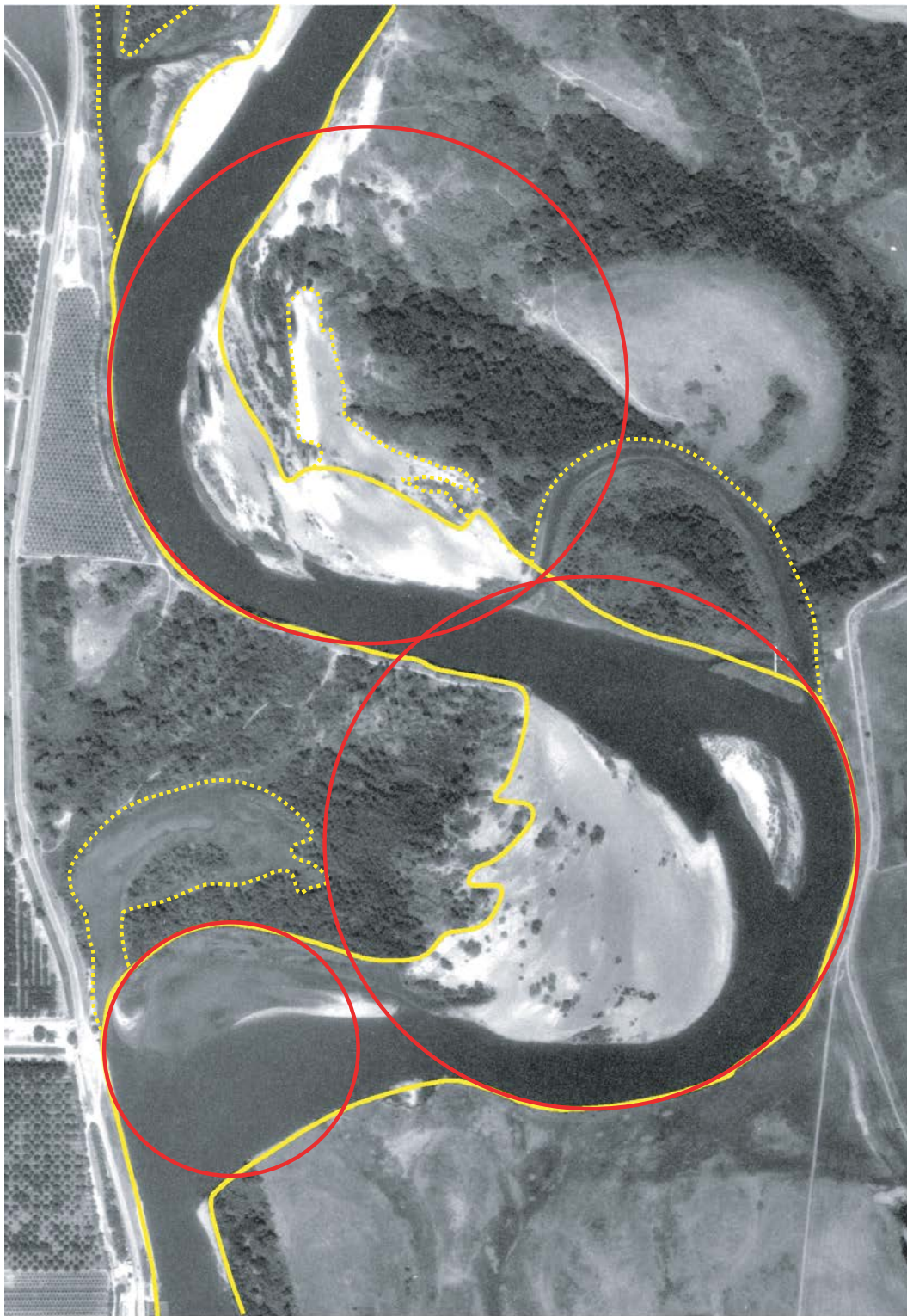
Figure B.10.   Aerial photo of the Sacramento River in California showing the location of the delineated bankline (solid yellow line), the probable top of the bank (dotted yellow line), and the circles that best define the outer bank radius (red circles).
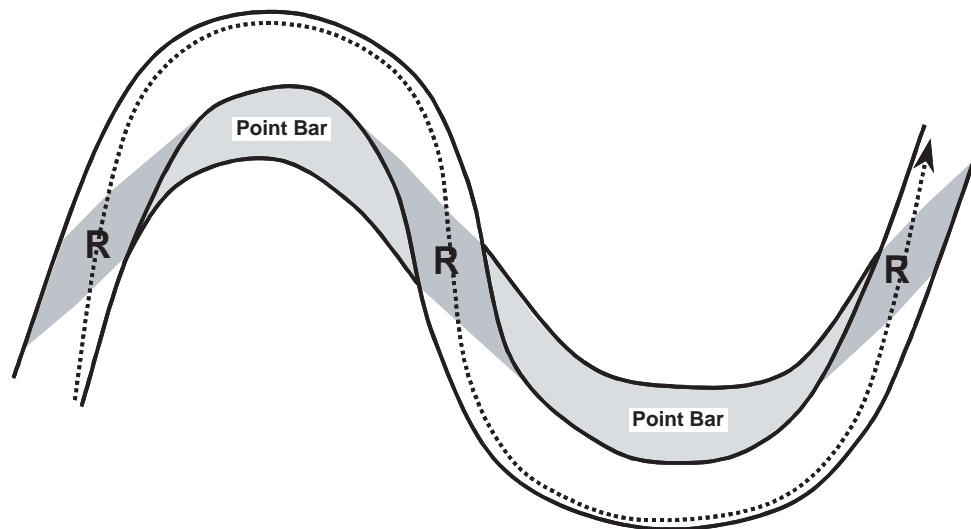
Figure B.11.   Idealized meandering channel showing the hypothetical position of riffles (R) and the thalweg (dotted line).

Figure B.12.   Aerial photo of the gravel-bed Sun River in Montana showing the locations of several riffles identified by circles.
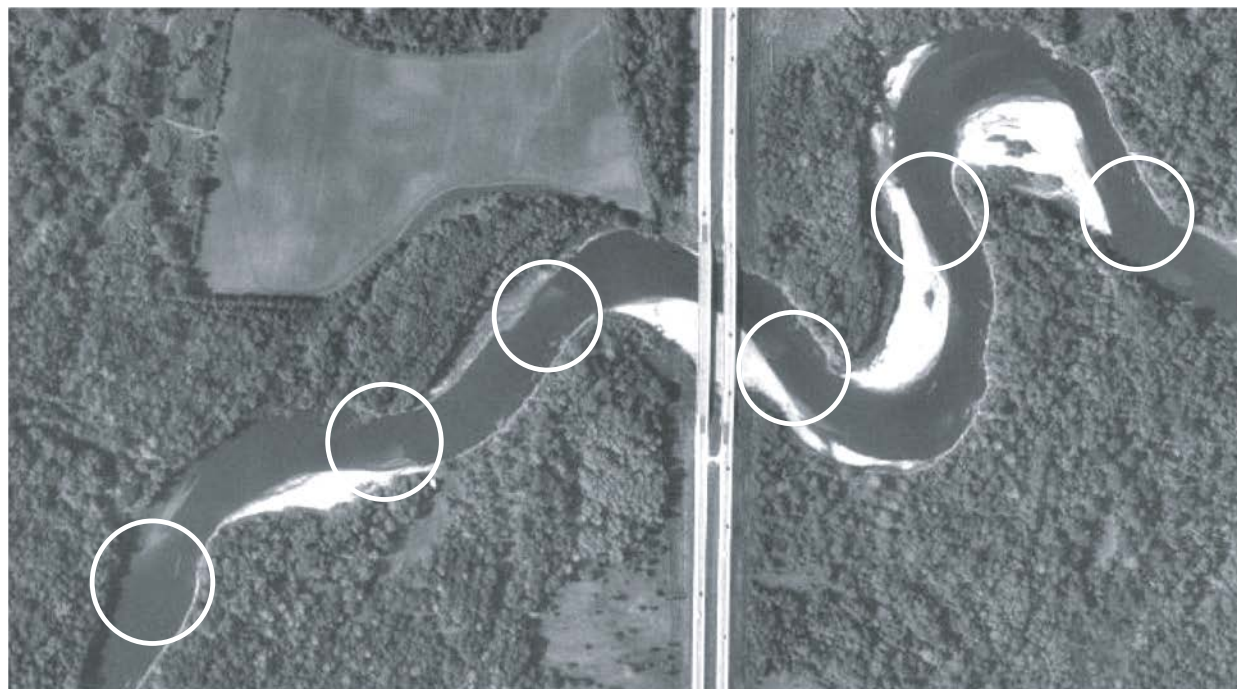
Figure B.13.   Aerial photo of the sand-bed Wapsipinicon River in Iowa showing the locations of several crossings identified by the circles.

APPENDIX C

INSTRUCTIONS FOR INSTALLING DATA LOGGER AND CHANNEL MIGRATION PREDICTOR AND DESCRIPTION OF THE CIRCLE-FITTING ALGORITHM

INSTRUCTIONS FOR INSTALLING DATA LOGGER AND CHANNEL MIGRATION PREDICTOR

The following instructions assume that the user has ArcView 3.x installed. The Avenue scripts for the Data Logger and Channel Migration Predictor are not supported by ArcGIS 8.x. The procedures for installation of the Data Logger extension are as follows:

1. Find the folder named ext32 within the folder in which ArcView is installed. For example, C:\Esri\Arcview\ext32 would be a fully qualified path name to the folder ext32. Copy the file "DataLogger.avx" from *CRP-CD-48* to the folder ext32. On Unix systems, replace the folder ext32 with the directory named ext.
2. Open an ArcView project and select "Extensions . . ." under the "File" menu.
3. Drag the mouse over the check box to the left of the extension named "Data Logger." Notice the cursor turns into a check mark.
4. Click on the check box for the "Data Logger" extension. When the user clicks on the check box, a check mark will appear.
5. Repeat Steps 3 and 4 for the "CAD Reader" extension.
6. Hit OK and the extension will be loaded. (On the ArcView Extensions Dialog, if the box "Make Default" is checked at this point, then the "Data Logger" will be loaded when any new project is created.)

The Channel Migration Predictor is installed using the same procedures. After installing the Channel Migration Predictor extension, make sure the file "frequency.dbf" is in your working directory. (The file "frequency.dbf" is produced by the Data Logger.)

CIRCLE-FITTING ALGORITHM

The equation for a circle with center at $(x, y) = (a,b)$ and radius R is given by:

$$(x - a)^2 + (y - b)^2 = R^2$$

Let (x_i, y_i), $i = 1, 2, \ldots n$, be a set of data points in the xy-plane. To determine values of a, b and R, which provide a best least squares fit of a circle to the data points, we seek to minimize:

$$F(a, b, R) = \sum_{i=1}^{N} \left[(x_i - a)^2 + (y_i - b)^2 - R^2 \right]^2$$

The standard approach to minimizing F calls for setting the partial derivatives of F with respect to a, b, and R equal to zero. Because F is a fourth-degree polynomial in a, b, and R, setting these partial derivatives to zero would lead to a system of three nonlinear equations in a, b, and R. Rather than dealing with a difficult nonlinear system we take the following approach.

From:

$$(x_i - a)^2 + (y_i - b)^2 - R^2 = x_i^2 - 2x_i a + a^2 + y_i^2 - 2y_i b + b^2 - R^2$$

it follows that F can be written as:

$$F(a, b, R) = \sum_{i=1}^{N} \left[x_i^2 - 2x_i a + a^2 + y_i^2 - 2y_i b + b^2 - R^2 \right]^2$$

Next, let $c = a^2 + b^2 - R^2$ and define a new least squares objective function to be:

$$G(a, b, c) = \sum_{i=1}^{N} \left[x_i^2 + y_i^2 - 2x_i a - 2y_i b + c \right]^2$$

The values of a, b, and c that minimize G can be found by setting to zero the partial derivatives of G with respect to a, b, and c. This leads to the following system of linear equations:

$$\begin{bmatrix} n_{11} & n_{12} & n_{13} \\ n_{21} & n_{22} & n_{23} \\ n_{31} & n_{32} & n_{33} \end{bmatrix} \begin{bmatrix} a \\ b \\ c \end{bmatrix} = \begin{bmatrix} d_1 \\ d_2 \\ d_3 \end{bmatrix}$$

The coefficient matrix for the above system of equations is symmetric ($n_{ij} = n_{ji}$), so the system is completely defined by:

$$n_{13} = \sum_{i=1}^{N} 4x_i^2 \qquad n_{12} = \sum_{i=1}^{N} 4x_i y_i \qquad n_{13} = \sum_{i=1}^{N} 2x_i$$

$$n_{23} = \sum_{i=1}^{N} 2y_i \qquad n_{22} = \sum_{i=1}^{N} 4y_i^2 \qquad n_{33} = -N$$

$$d_3 = \sum_{i=1}^{N} \left[x_i^2 + y_i^2 \right] \qquad d_2 = \sum_{i=1}^{N} \left[x_i^2 + y_i^2 \right] 2y_i$$

$$d_1 = \sum_{i=1}^{N} \left[x_i^2 + y_i^2 \right] 2x_i$$

Gaussian elimination can be used to solve for a, b, and c, and then R can be recovered from $R = \sqrt{a^2 + b^2 - c}$.

APPENDIX D

TIPS FOR DELINEATING BANKLINES FROM HISTORIC AERIAL PHOTOS FOR USE WITH THE CHANNEL MIGRATION PREDICTOR

In order to use the Channel Migration Predictor, it is necessary to have banklines in Shapefile format (*.shp) for at least two historical conditions. This information may already be available in some other format that is compatible for use with the GIS software, such as CAD file formats (DWG, DXF, DGN, etc). However, it is more likely that a collection of historical aerial photographs is available in a variety of formats. Some may be digital and georeferenced, some may be digital but not georeferenced, and others may be paper copies. Once these various photo sources have been assembled, the main task becomes extracting banklines, transferring them into a common reference system, and finally bringing them into the ArcView Shapefile format.

There are multiple ways to accomplish this task. One way is to manipulate the aerial images digitally so that they are all rotated, stretched, and aligned to a common coordinate system. Once they have been manipulated, they can simply be brought into ArcView, and the banklines can be traced directly into Shapefiles. This method requires some fairly expensive software that is probably not readily available to the average user. Examples of such software include the Image Analysis extension for ArcView, Descartes Image Manager for MicroStation, and AutoDesk Land Development Desktop.

There is another method that can be accomplished with more readily available software tools. This method is illustrated below. In this example, Microsoft PowerPoint and Jasc Paint Shop Pro are used in addition to ArcView. Paint Shop Pro is one of many affordable image-manipulation software packages.

The following example uses the two images shown in Figure D.1. Both images show a reach of the Minnesota River that has a history of active migration. One photo is from 1991 and was downloaded from TerraServer (see Appendix A). It has a World File defining its geospatial reference (e.g., Universal Transverse Mercator (UTM) coordinates, Zone, NAD83, and meters). The other photo is a scan from a paper copy showing conditions for the year 1968. Notice that the scanned image has no orientation and is at a different scale than the image obtained from TerraServer.

STEP 1—GETTING PHOTOS IN DIGITAL FORMAT

The first step is to get both photos into digital format. As mentioned previously, the 1991 photo came from TerraServer and has a World File associated with it. This image was created by stitching together multiple smaller files. Because the World File references the upper left corner of the overall image, only the World File for the upper-left-most image was used. This file can be brought directly into ArcView using the "Add Data" button, selecting "Image Data Source" as the file type, and browsing for the image. This image will be added as a new theme, and the banklines can be directly traced into a new Shapefile. The other photo (1968 photo) is a scanned image acquired from a paper copy and saved as a TIFF or "Tagged Image File Format" (*.tif) file.

STEP 2—TRANSFERRING BANKLINES TO THE REFERENCE PHOTO

Both images were brought into PowerPoint either on separate pages or side by side on the same page, as shown in Figure D.1. The banklines for a selected bend on the scanned image were traced using the drawing tools in the PowerPoint software. Three registration points common to both photographs were also marked using a simple graphic such as a circle, as shown in Figure D.2. After the banklines and registration features for the 1968 photo were drawn, they were grouped together using the "group" tool and copied to the 1991 image. The 1991 image is the reference image because its coordinate system and orientation are known.

Before proceeding, the aspect ratio for the grouped set of 1968 features was locked. This was accomplished by right-clicking on the graphic set and selecting "Format Object." In the form that appears, there is a "Lock Aspect Ratio" check box on the "Size" tab.

With the aspect ratio locked, the 1968 features may now be resized and rotated so that the registration points are aligned on the 1991 reference photo as shown in Figure D.3. Next, a box is drawn around the exact limits of the 1991 reference photo. This "georeference" box will be used to help create an image file of the 1968 banklines that will be georeferenced to the same coordinates as the georeferenced 1991 image.

STEP 3—BRINGING THE BANKLINES INTO ARCVIEW

Next, the 1991 photo was removed from the newly aligned bankline data, registration points, and the georeference box as shown in Figure D.4. This page was turned into a TIFF file by selecting "Save As" under the "File" pull-down menu in PowerPoint and selecting TIFF as the file type. Only the page that is being viewed will need to be saved as a TIFF file.

The new TIFF file is then opened in Paint Shop Pro and cropped to the limits of the georeference box. A file with the 1968 banklines is created that covers the same area as the
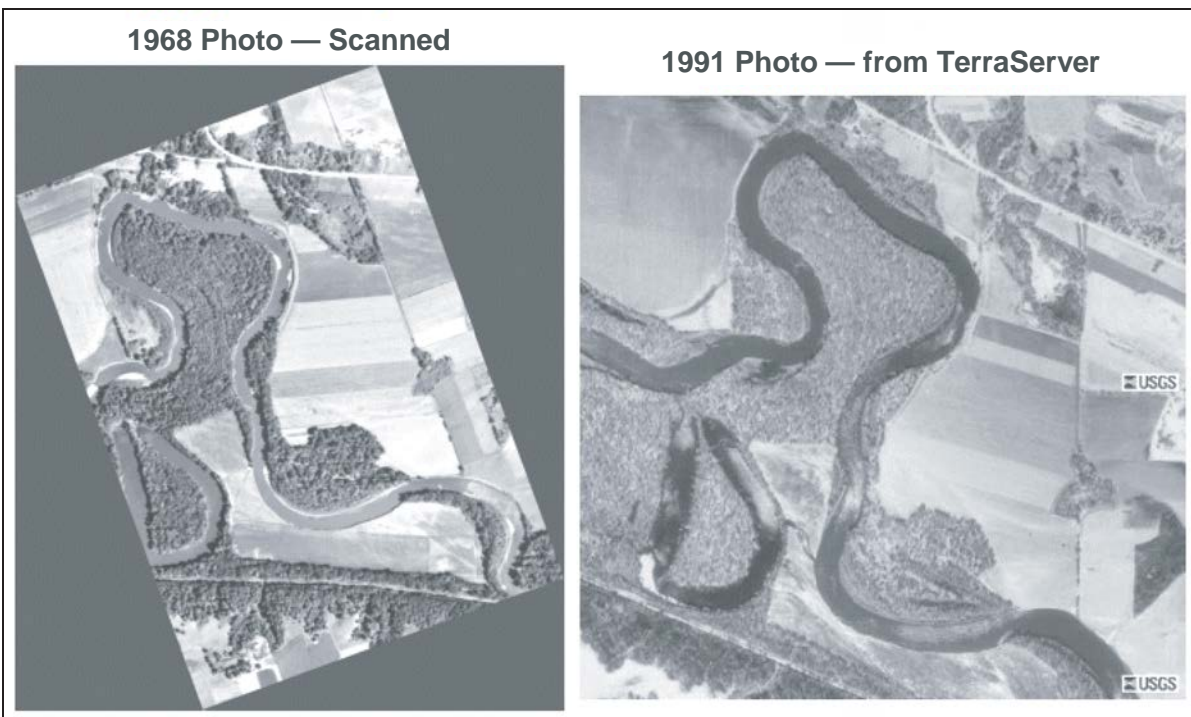
Figure D.1.   Two historical photos used in the meander migration analysis.

1991 reference photo. In order to bring this new image file into ArcView, the TIFF has to be the same size in number of pixels as the 1991 reference photo. The 1991 reference photo is 400 by 400 pixels, so the 1968 bankline image file is converted to the same size. Once the 1968 bankline image file is the same size, the World File (*.tfw) for the 1991 photo can be used to locate it in ArcView. This is done by simply copying the World File to a file with the same name as the new bankline image file.

The 1968 bankline image file can then be brought into ArcView as described in Step 1 above, using the "Add Data" button. The file should open in the same location as the 1991 reference photo that is already loaded. Using the 1968 bankline image as a reference, a second set of 1968 banklines can be traced into a new Shapefile. After the second set of 1968 banklines have been digitized, the 1968 image can be deleted, leaving the 1991 reference aerial photo and the 1968 bankline set as shown in Figure D.5.

This procedure can be repeated for any additional historic photographs that need to be brought into ArcView. Once the banklines are in Shapefile format, the user is ready to begin using the Data Logger and Channel Migration Predictor tools in ArcView.
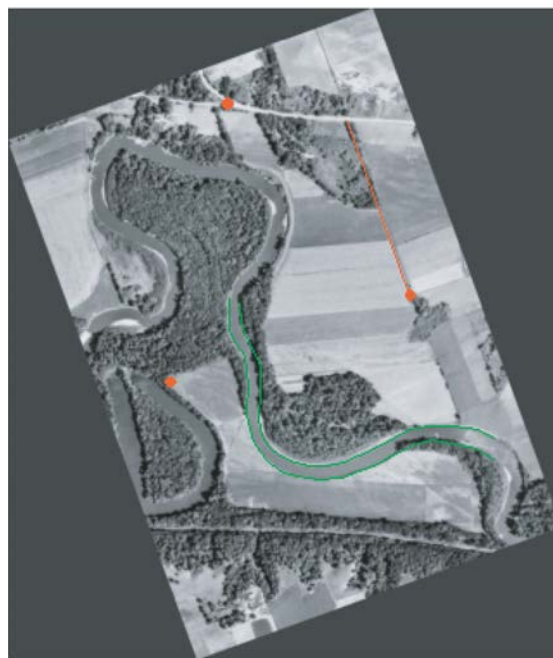
Figure D.2.   Banklines (green) and registration features (red) delineated on the scanned 1968 photo.

Figure D.3.   Banklines (green) and registration features (red) from the 1968 photo rotated and stretched to match the 1991 reference photo.

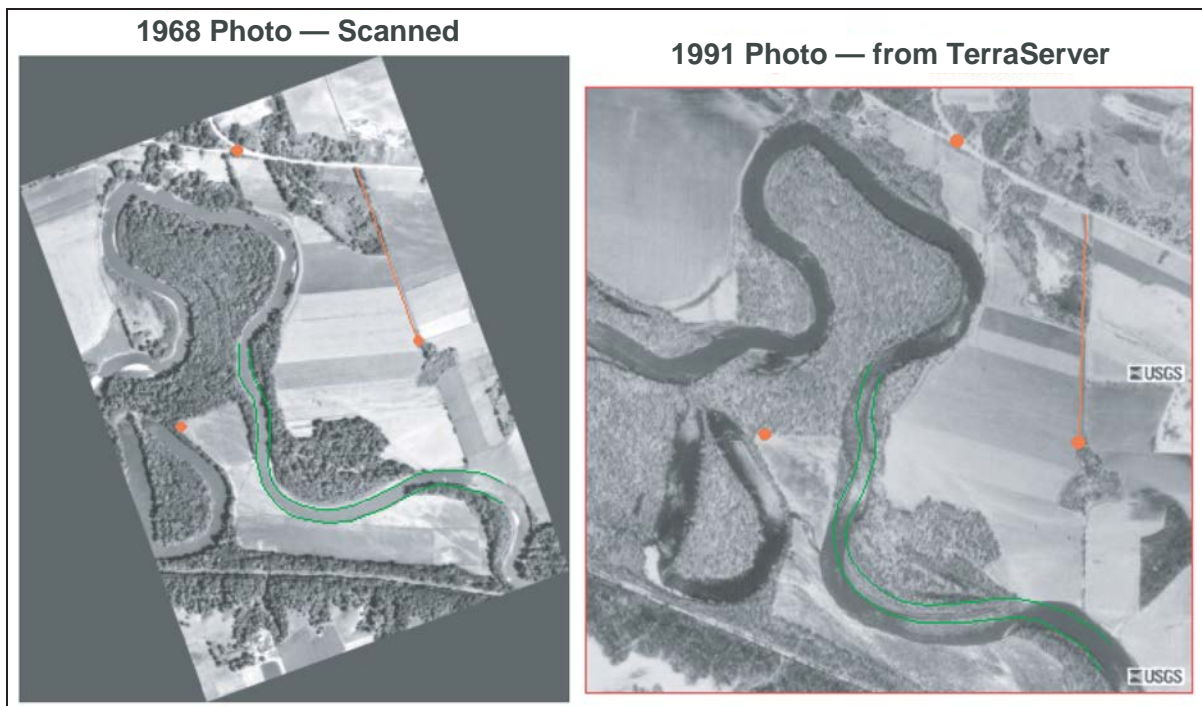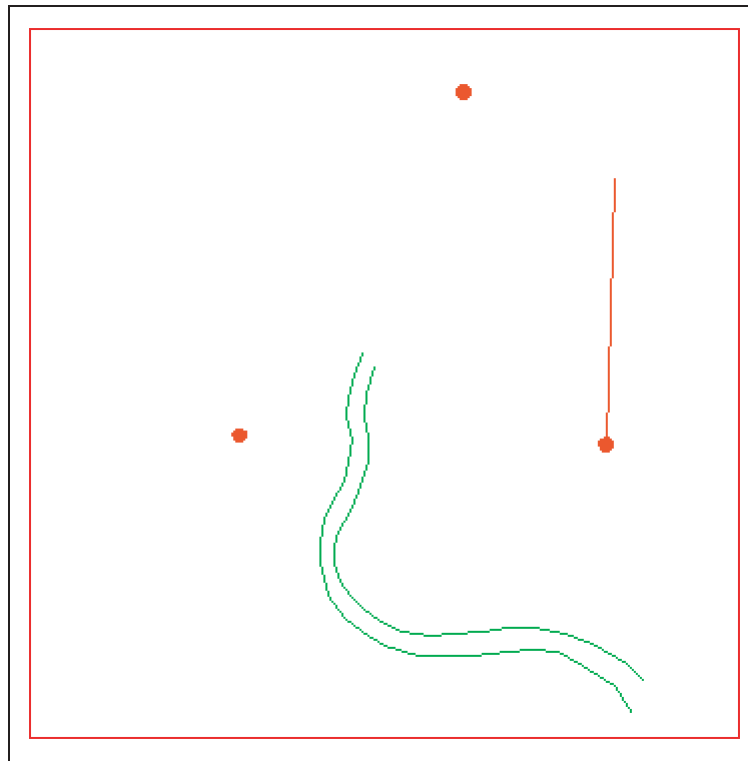*Figure D.4.   Banklines (green), registration features (red), and georeference box (red) to be exported as a TIFF file.*

Figure D.5.   1968 banklines after being turned into a Shapefile and superimposed on the 1991 reference photo.

APPENDIX E

PREDICTING CHANGE IN MIGRATION DIRECTION

As discussed in Chapter 7, there are two methods of defining the angle (θ) of bend migration for a given period based on the migration of the bend centroid in previous periods. The first and simplest method is to use the direction defined by the previous period for the period being predicted. The second method uses the rate of change of the migration angle from the previous period to define the rate of change for the period being predicted (see Equation 7.4). The following is an estimation of the potential change in migration direction, based on the previous angle of bend migration for the example problem presented in Step 7 of Chapter 8.

The migration angle θ_C is plotted relative to the arbitrary line as shown in Figure 8.13. The Period C angle of migration (θ_C) relative to the arbitrary line will be the Period B angle (θ_B) plus the rate of movement of the bend centroid during Period B times the number of years in Period C (Y_C).

The direction of the movement of the bend centroid during Period C, derived using Equation 7.4, is the following:

$$\theta_C = \left[\left(\frac{(\theta_B - \theta_A)}{Y_B} \right) (Y_C) \right] + \theta_B$$

$$= \left[\left(\frac{(46° - 13.5°)}{26 \text{ yr}} \right) (30 \text{ yr}) \right] + 46° = 83.5°$$

As noted, if only one period is available, then one can assume that the migration direction does not change ($\theta_c = \theta_B$) or, using judgment, once can allow the future direction to deviate from θ_B. It would generally be assumed that the bend migration direction would tend more down valley with time. Comparison of Figures 8.13 and 8.14 with Figures E.1 and E.2 shows the difference in the predictions based on the two approaches.
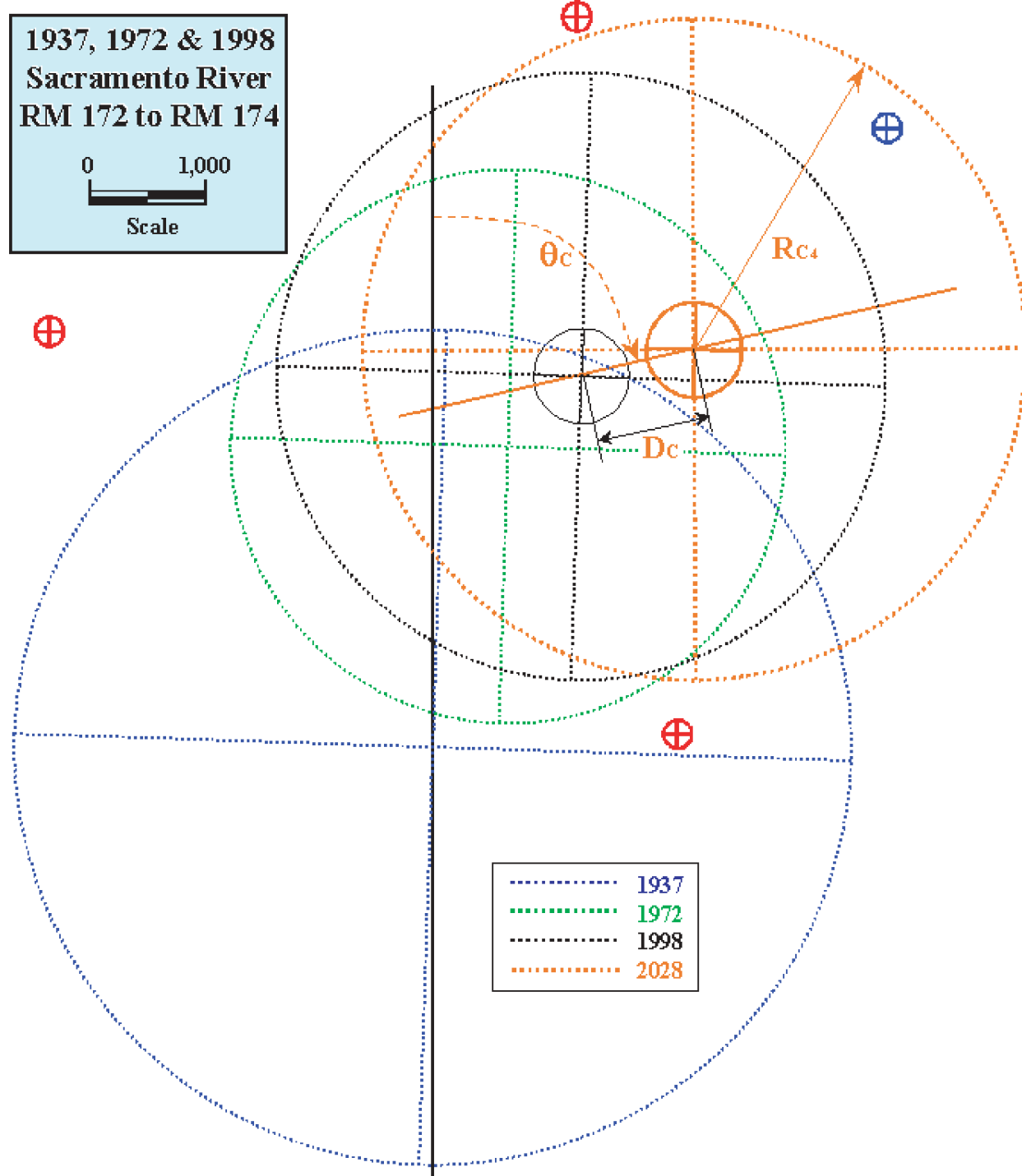
Figure E.1.   Prediction of change in migration direction for the period from 1998 to 2028 and the predicted position of the outer bank of the bend in 2028.

Levee

1998
Sacramento River
RM 172 to RM 174

0   1,000

Scale
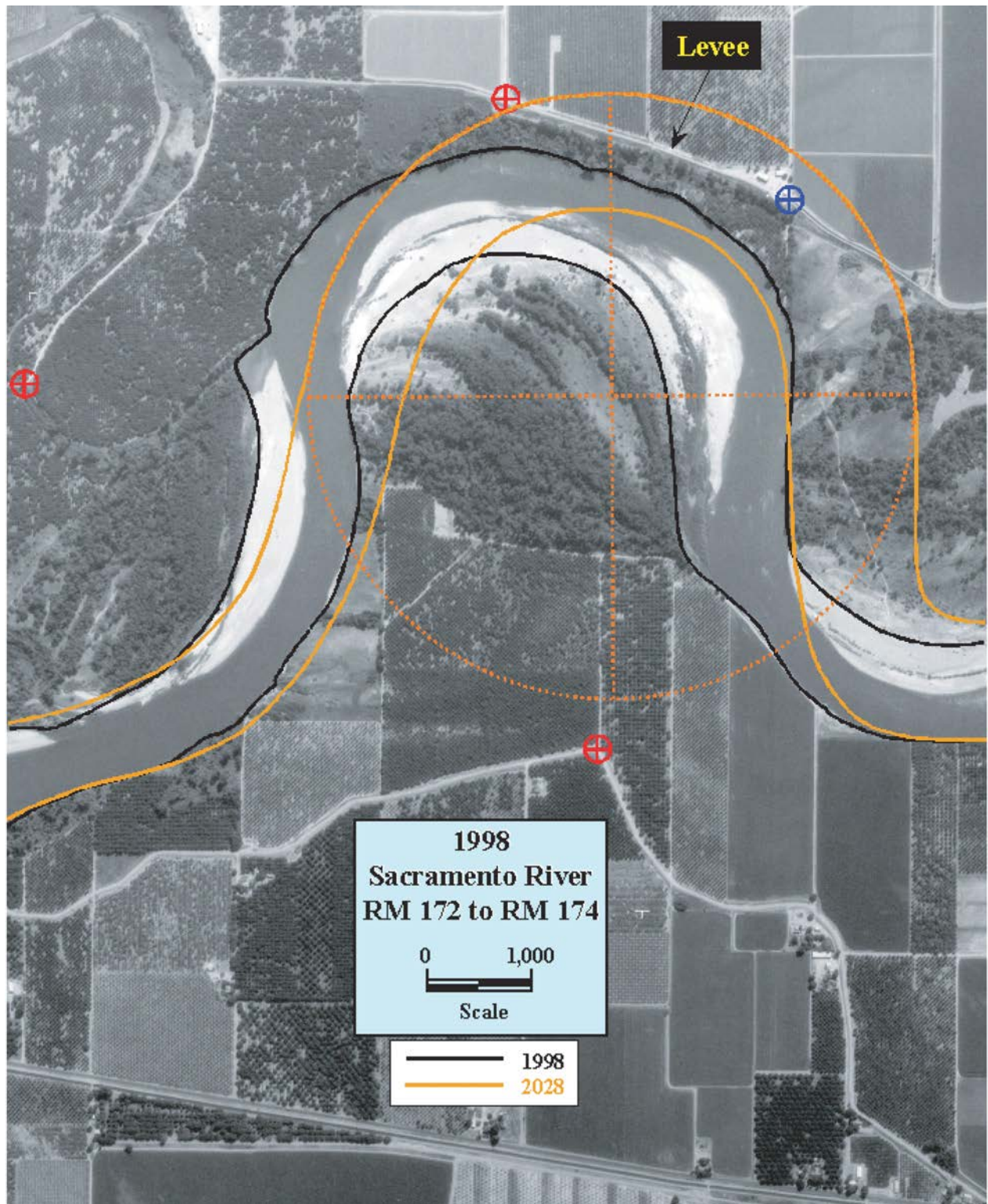
—— 1998
—— 2028

Figure E.2.   Overlay of the predicted channel position in 2028 on the 1998 aerial photograph of the Sacramento River near Butte City, California, considering change in migration direction. Note the threat to the local levee.

APPENDIX F

GLOSSARY

Aerial photograph A vertical or oblique photograph taken from an airplane.

Aggradation General and progressive buildup of the longitudinal profile of a channel bed because of sediment deposition.

Alluvial channel Channel wholly in alluvium; no bedrock is exposed in channel at low flow or likely to be exposed by erosion.

Alluvial stream A stream that has formed its channel in cohesive or noncohesive materials that have been and can be transported by the stream.

Alluvium Unconsolidated material deposited by a stream in a channel, floodplain, alluvial fan, or delta.

Alternate bars Elongated deposits found alternately near the right and left banks of a channel.

Amplitude The distance between points of maximum curvature of successive meanders of opposite phase in a direction normal to the general course of the meander belt, measured between centerlines of channels.

Anabranch Individual channel of a braided or anastomosing stream.

Anastomosing stream A stream whose flow is divided at most stages by vegetated islands that have elevations equivalent to the floodplain. Individual islands are wider than about three times water width, and the channels are more widely and distinctly separated than in a braided stream.

**Apex (of a bend)** The tip, point, or location of maximum outward extension of a meander bend.

ArcView A GIS and software package developed by Environmental Systems Research Institute, Inc. (ESRI).

Avenue A programming language and development environment used to create specialized graphical user interfaces and to run scripts that customize the functionality of ArcView.

Avulsion A sudden change in the channel course that usually occurs when a stream breaks through its banks; it is usually associated with a flood or a catastrophic event.

Bank The sides of a channel between which the flow is normally confined.

Bankline A line defining the top edge of a bank along a channel.

Bank protection Engineering works for the purpose of protecting streambanks from erosion.

Bank revetment Erosion-resistant materials placed directly on a streambank to protect the bank from erosion.

Bar An alluvial deposit forming a topographically distinct feature on the channel bed, not permanently vegetated.

Bed The bottom of a channel bounded by banks.

Bed form A recognizable relief feature on the bed of a channel, such as a ripple, dune, plane bed, antidune, or bar. Bed forms are a consequence of the interaction between hydraulic forces (boundary shear stress) and the bed sediment.

Bed material Material found in and on the bed of a stream (may be transported as bed load or in suspension).

Bedrock The solid rock exposed at the surface of the earth or overlaid with soils and unconsolidated material.

Bend apex The point on the outer bank of a meander bend as defined by the intersection of the bank and a line that passes through the bend centroid and bisects the bend.

Bend centroid The center point of a best-fit circle used to define a meander bend.

Braided stream A stream whose flow is divided at normal stage by small mid-channel bars; the width of the individual bars is less than about three times water width. A braided stream has the aspect of a single large channel within which there are subordinate channels (anabranches).

Channel The bed and banks that confine the surface flow of a stream.

Channel pattern The aspect of a stream channel in plan view, with particular reference to the degree of sinuosity, braiding, and anabranching.

Clay (mineral) A particle whose diameter is in the range of 0.00024 to 0.004 mm.

Clay plug An abandoned meander bend filled with fine-grained cohesive sediments.

Cobble A fragment of rock whose diameter is in the range of 64 to 250 mm.

Confluence The junction of two or more streams.

Countermeasure A measure intended to prevent, delay, or reduce the severity of hydraulic problems.

Crossing The relatively short and shallow reach of a stream between bends where the main thread of flow shifts from one side of the channel to the other, also called a crossover or riffle.

Cross section A section normal to the trend of a channel or flow.

Cutbank The concave wall of a meandering stream, often found along the outer bank of a meander bend, formed as a result of erosion at the base of the bank.

Cutoff (1) A direct channel, either natural or artificial, connecting two points on a stream, thereby shortening the original length of the channel and increasing its slope, and (2) a natural or artificial channel that develops across the neck of a meander loop (neck cutoff) or across a point bar (chute cutoff).

Debris   Floating or submerged material, such as logs, vegetation, or trash, transported by a stream.

Degradation (bed)   A general and progressive (long-term) lowering of the channel bed because of erosion over a relatively long channel length.

Discharge   Volume of water passing through a channel during a given time.

Drainage basin   An area confined by drainage divides, often having only one outlet for discharge (also catchment, watershed).

Erosion   Displacement of soil particles because of water or wind action.

Floodplain   A nearly flat, alluvial lowland bordering a stream that is subject to frequent inundation by floods.

Fluvial geomorphology   The science dealing with the morphology (form) and dynamics of streams and rivers.

Fluvial system   The natural river system consisting of (1) the drainage basin, watershed, or sediment source area; (2) the tributary and mainstem river channels or sediment transfer zone; and (3) alluvial fans, valley fills and deltas, or the sediment deposition zone.

Geographic information system (GIS)   A computer-based system that enables storing, integrating, manipulating, analyzing, and displaying spatially related information.

Geomorphology/morphology   That science that deals with the form of the earth, the general configuration of its surface, and the changes that take place because of erosion and deposition.

Georeference   Aligned with north and east in a ground coordinate system.

Gravel   A rock fragment whose diameter ranges from 2 to 64 mm.

Hard point   A streambank protection structure whereby "soft" or erodible materials are removed from a bank and replaced by stone or compacted clay. Some hard points protrude a short distance into the channel to direct erosive currents away from the bank. Hard points also occur naturally along streambanks as passing currents remove erodible materials, leaving nonerodible materials exposed.

Helicoidal (helical) flow   Three-dimensional movement of water particles along a spiral path in the general direction of flow. These secondary-type currents are of most significance as flow passes through a bend; their net effect is to remove soil particles from the cutbank and deposit this material on a point bar.

Hydraulics   The applied science concerned with the behavior and flow of liquids, especially in pipes, channels, structures, and the ground.

Hydrology   The science concerned with the occurrence, distribution, and circulation of water on the earth.

Incised stream   A stream that has deepened its channel through the bottom of the valley floor, so that the floodplain is left as a terrace.

Island   A permanently vegetated area, emergent at normal stage, which divides the flow of a stream. Islands originate by establishment of vegetation on a bar, by channel avulsion or flow splits, or at the junction of a minor tributary with a larger stream.

Lateral erosion   Erosion in which the removal of material is extended horizontally, as contrasted with degradation and scour in which erosion occurs in a vertical direction.

Levee   An embankment, generally landward of the top bank, which confines flow during high-water periods, thus preventing overflow into adjoining lowlands.

Meander   A meander in a river consists of two consecutive loops—one flowing clockwise relative to the meanderbelt alignment and the other flowing counterclockwise.

Meanderbelt   The distance between lines drawn tangent to the extreme limits of successive, fully developed meanders.

Meander loop   An individual loop of a meandering or sinuous stream lying between inflection points with adjoining loops.

Meander width   The amplitude of a fully developed meander measured from midstream to midstream.

Meandering stream   A stream having a sinuosity greater than some arbitrary value. The term also implies a moderate degree of pattern symmetry, imparted by regularity of size and repetition of meander loops. The channel generally exhibits a characteristic process of bank erosion and point bar deposition associated with systematically shifting meanders.

Migration   The change in position of a channel by lateral erosion of one bank and simultaneous accretion of the opposite bank.

Outcrop   The exposure of bedrock projecting through the overlying soil.

Overbank flow   Water movement that overtops the bank either because of stream stage or overland surface water runoff.

Oxbow   The abandoned former meander loop that remains after a stream cuts a new, shorter channel across the narrow neck of a meander (often bow-shaped or horseshoe-shaped).

Photogrammetry   The art, science, and technology of obtaining reliable information about physical objects and the environment through processes of recording, measuring, and interpreting photographic images and patterns phenomena.

Point bar   An alluvial deposit of sand or gravel lacking permanent vegetal cover occurring in a channel at the inside of a meander loop, usually somewhat downstream from the apex of the loop.

Radius of curvature   The radius of a circle inscribed on the centerline or outer bankline of a meander loop that best defines the meander bend.

Reach   A segment of stream length that is arbitrarily bounded for purposes of study.

Rectify The removal of the effects of tilt or edge distortion from an aerial photograph.

Revetment Rigid or flexible armor placed to inhibit scour and lateral erosion (see bank revetment).

Riffle A natural, shallow flow area extending across a streambed in which the surface of flowing water is broken by waves or ripples. Typically, riffles alternate with pools along the length of a stream channel.

Riparian Pertaining to anything connected with or adjacent to the banks of a stream (corridor, vegetation, zone, etc.).

Runoff That part of precipitation that appears in surface streams of either perennial or intermittent form.

Sand A rock fragment whose diameter is in the range of 0.062 to 2.0 mm.

Scour Erosion of streambed or bank material because of flowing water, often considered as being localized (see local scour, contraction scour, and total scour).

Script In an ArcView project, the component that contains the Avenue code used to automate tasks and add new capabilities to ArcView.

Sediment/fluvial sediment Fragmental material transported, suspended, or deposited by water.

Shear stress The force or drag developed at the channel bed by flowing water. For uniform flow, this force is equal to a component of the gravity force acting in a direction parallel to the channel bed on a unit wetted area (usually in units of stress, Pa $[N/m^2]$ or $[lb/ft^2]$).

Shoal A relatively shallow submerged bank or bar in a body of water.

Silt A particle whose diameter is in the range of 0.004 to 0.062 mm.

Sinuosity The ratio between the channel centerline length and the length of the valley as measured between two points on the channel or valley floor.

Slope (or gradient) Fall per unit length along the channel centerline or thalweg.

Stability A condition of a channel when, though it may change slightly at different times of the year as the result of varying conditions of flow and sediment charge, there is no appreciable change from year to year; that is, accretion balances erosion over the years.

Stream A body of water that may range in size from a large river to a small rill flowing in a channel. By extension, the term is sometimes applied to a natural channel or drainage course formed by flowing water whether it is occupied by water or not.

Streambank erosion Removal of soil particles or a mass of particles from a bank surface primarily because of water action. Other factors, such as weathering, ice and debris abrasion, chemical reactions, and land use changes, may also directly or indirectly lead to bank erosion.

Streambank failure Sudden collapse of a bank because of an unstable condition, such as removal of material at the toe of the bank by scour.

Streambank protection Any technique used to prevent erosion or failure of a streambank.

Terrace An abandoned floodplain that was formed when the channel flowed at a higher level.

Thalweg The line joining the deepest points of a stream channel.

Theme In an ArcView project, a set of geographic features in a view.

Upper bank The portion of a streambank having an elevation greater than the average water level of the stream.

View In an ArcView project, an interactive map that allows the user to display, explore, query, and analyze geographic data.

Wandering channel A channel exhibiting a more or less nonsystematic process of channel shifting, erosion, and deposition with no definite meanders or braided pattern.

Watershed See drainage basin.

Wavelength The straight-line distance between corresponding points of successive meanders.

World File An ASCII file containing coordinate information about an image that is needed by ArcView to perform an "image-to-world" transformation.

Abbreviations used without definitions in TRB publications:

AASHO	American Association of State Highway Officials
AASHTO	American Association of State Highway and Transportation Officials
APTA	American Public Transportation Association
ASCE	American Society of Civil Engineers
ASME	American Society of Mechanical Engineers
ASTM	American Society for Testing and Materials
ATA	American Trucking Associations
CTAA	Community Transportation Association of America
CTBSSP	Commercial Truck and Bus Safety Synthesis Program
FAA	Federal Aviation Administration
FHWA	Federal Highway Administration
FMCSA	Federal Motor Carrier Safety Administration
FRA	Federal Railroad Administration
FTA	Federal Transit Administration
IEEE	Institute of Electrical and Electronics Engineers
ITE	Institute of Transportation Engineers
NCHRP	National Cooperative Highway Research Program
NCTRP	National Cooperative Transit Research and Development Program
NHTSA	National Highway Traffic Safety Administration
NTSB	National Transportation Safety Board
SAE	Society of Automotive Engineers
TCRP	Transit Cooperative Research Program
TRB	Transportation Research Board
U.S.DOT	United States Department of Transportation